Anatomical and physiological characterization of the optic lobe and associated pathways involved in visual processing in *Hieroglyphus banian*

A thesis submitted during 2023 to the University of Hyderabad in partial fulfilment of the requirements for the award

of

Doctor of Philosophy

in

Cognitive Sciences

by

Chalavadi Sivaraju

Centre for Neural and Cognitive Sciences

School of Medical Sciences

University of Hyderabad,

(P.O) Central University, Gachibowli,

Hyderabad-500 046

Telangana, India

June 2023

University of Hyderabad

Centre for Neural and Cognitive Sciences, School of Medical Sciences

(P.O) Central University, Gachibowli, Hyderabad-500 046

Telangana, India

DECLARATION

I, **Chalavadi Sivaraju**, hereby declare that this thesis entitled, **"Anatomical and physiological characterization of the optic lobe and associated pathways involved in visual processing in *Hieroglyphus banian*"** submitted by me under the guidance and supervision of **Dr. Joby Joseph** is a bonafide research work. I also declare that it has not been submitted previously in part or in full to this University or any other University or Institution for the award of any degree or diploma. I also declare that this is a bonafide work which is free from plagiarism.

A report on plagiarism statistics from the University Librarian is enclosed.

Date: **Chalavadi Sivaraju**

Hyderabad **Registration no: 15CCHL03**

University of Hyderabad

Centre for Neural and Cognitive Sciences, School of Medical Sciences

(P.O) Central University, Gachibowli, Hyderabad-500 046

Telangana, India

CERTIFICATE

This is to certify that the thesis entitled **'Anatomical and physiological characterization of the optic lobe and associated pathways involved in visual processing in *Hieroglyphus banian*'** submitted by **Mr. Chalavadi Sivaraju** bearing registration no **15CCHL03** in partial fulfilment of the requirements for the award of Doctor of Philosophy in Cognitive Sciences is a bonafide work carried out by him under my supervision and guidance.

The thesis has not been submitted previously in part or in full to this or any other University or Institution for the award of any degree or diploma.

(Dr. Joby Joseph)
Research Supervisor

(Prof. Ramesh K. Mishra)
Head of the Department/Centre

(Prof. Geeta K. Vemuganti)
Dean of the School

CERTIFICATE

This is to certify that the thesis entitled **'Anatomical and physiological characterization of the optic lobe and associated pathways involved in visual processing in *Hieroglyphus banian*'** submitted by **Mr. Chalavadi Sivaraju** bearing registration no **15CCHL03** in partial fulfillment of the requirements for the award of Doctor of Philosophy in Cognitive Sciences is a bonafide work carried out by him under my supervision and guidance.

The thesis has not been submitted previously in part or in full to this or any other University or Institution for the award of any degree or diploma.

Parts of this thesis have been:

A. Submitted for publication in the following journal: Journal of Comparative Neurology (2023, in review process);

B. Presented in the following conferences/workshops:

1. Sivaraju C and Joby Joseph. "Simple and Complex cells of the visual system of an insect" in Annual Conference of Cognitive Science 2019, December 10-12 at BITS,Goa (Talk)

2. Sivaraju C and Joby Joseph. "Simple and Complex cells of the visual system of an insect" in No Garlanding Neuroscience (NGN) 2020 , January 2-4th at IISER PUNE (Poster)

3. Sivaraju C and Joby Joseph. "Detailed architecture of the Hieroglyphus banian (rice grasshopper) optic lobe" in XL Annual meeting of the Indian Academy of Neurosciences (IAN-2022), December 7-10th at North-Eastern Hill University (NEHU), Shillong, Meghalaya (Poster).

Further, the student has passed the following courses towards fulfilment of coursework requirement for PhD.

S.no	Course code	Course name	Credits	Pass/Fail
1	CO701	Statistics and Research Methodology	4.00	Pass
2	CO702	Foundation of Neuroscience	4.00	Pass
3	CO703	Foundation of Cognitive Science	4.00	Pass
4	CO704	Lab Course for Three Theory Course	4.00	Pass
5	CO705	Research Proposal	2.00	Pass
6	CO706	Behavioural Neurobiology	4.00	Pass

(Dr. Joby Joseph)

Research Supervisor

(Prof. Ramesh K. Mishra)
Head of the Department/Centre

(Prof. Geeta K. Vemuganti)
Dean of the School

Dedicated to

All those grasshoppers and other insects which I have to sacrifice during my experiments.

And

To My father, mother and all other family members.

And

To Joby, for not giving up on me and without him the thesis would not have taken this shape.

And

To all my friends and well wishers whose constant support helped me during my hard times.

And

To Dr. B. R . Ambedkar , without whose forethought I would not have come this far.

Acknowledgements

In this 8 years of long journey My PhD is a learning experience which can not be compared to anything. In those 8 years, 2 years of the Pandemic is one of the toughest phases I have ever experienced. In spite of all these ups and downs, it is a defining part of my life because of the people who have been with me in this journey.

I would like to thank my supervisor Dr. Joby Joseph for not giving up on me. Supporting me emotionally whenever I'm in bad shape either because of experiments or because of my personal issues. And for supporting me economically whenever I'm in need of it. My association with you gave me an eye to look into this world of wonders, either it is bird watching or observing nature. Now it's hard for me to walk from hostel to the department without noticing a trail of ants and their chores, birds and their behaviour. My association with you made me understand that "This world is full of wonders, there exists a secret at every nook and corner, all you need is an eye to look at it". Whenever we are stuck at something, you will sit and work with us. And whenever we are down due to experiment failures you always say that "It's ok, every day you improve by delta change". Happy to know that constant push brought me this far.

I would like to thank my doctoral committee members Dr. Sudiptha Saraswati and Dr. Akash Gautam for their valuable suggestions.

I thank Dr. Ramesh Kumar Mishra, HoD of CNCS.

I thank all my lab mates for being such a big support. You guys are like my family. I spent and shared part of my life with you guys. Dr. Shilpi singh, being the senior most in the lab,you taught me dissections and intracellular recordings, you are such a perfectionist, you are always there whenever I need something. And thanks for helping me during my hard times. Shalini, thanks for being there. Whenever I lose myself and nothing works out, your pep talks helped me. Dr. Sandya garu, you are always like a mother, constantly taking care and suggesting things to me. Bhavana, dude you are always helpful and informative. I always remember you, me and shilpi's cake baking and chicken making experiments in the lab. Such memorable days. Dr. Meenakshi, you are such a wonder woman, if it has to be done means, you will finish it in no time. Hats off to you. Pranay and Deepak, you both are amazing. You guys are always there for me. Thanks for pushing me to ride the scooty. It was Joby who first taught me how to ride a scooty. I just did it. But never had enough courage to take it onto the road. You guys gave that little push, which changed everything. You guys in no time became soo close. I wonder how I would have managed stressful days during writing without you guys. A big thanks to both of you. Samuel (samu,sam), my little brother. Those treks, cycle rides and bonfires soo many memories. Though we are a decade apart, I got connected soo much man. Thanks for teaching some basics of football. Sam, you gave me two more good friends Emil and Naneshawar. Thanks to all three of you for leaving such memories. Dileep ji (Dr. D, Mr. Cool and so on), your love and peace always spreads positive vibes wherever you are. And Pallavi is another replica of you. Always calm and hard working. Thanks to both of you.

Thanks Andrea, Anuradha, Bhavi, Depro, Irtisha and Soumili. Largest number of people in the lab during my stay. All of you gave me soo many memories.

Pridvi, friend, extended lab member. Thanks for such love and care, you and Joby gave it to me. We went on many trips and you people hosted many parties. Thanks for all those memories.

I thank all my family members waiting patiently and supporting me in this journey.

I thank my colleagues Sanjay, Jayasri, Kamala and Abhilash.

I thank Dr. Prathap for always being there for me. Those treks, bonfires, cooking sessions, photography sessions, trips, movie nights, what not. You are part of everything I do. Thanks to Sagar and all your family members for hosting me during lockdown.

I thank Darmapuri Srinu and Kavya for such a lovable care and support you guys give.

I thank Sqn. Ldr Ruthvik Chowla and Dr. Deepa (Sqn. Ldr) for their constant support.

I thank G. Srinivas, Asithakeshakambal,Dr. Thandu Vamshi, Bhanu Prakash, Raghavaram, Naresh Shyga, Chaitanya, Nabaneetha Barman, Sudheer. You guys helped me during my tough days, you guys are always there for me. I thank Dr. Ashok gurram anna and Gopi anna.

I thank Dr. Leela, Dr. Avishek and Dr. Manasa. We had lots of cooking sessions, Tea sessions and treks. Thanks for making all those memories.

I thank my post graduate mentor Prof. Krishnaveni Mishra, Summer internship guide Prof. K. Veluthambi.I thank my post graduate lab members Dr. Guranaa, Dr. Hita, Dr. Neethu, Kathir, Dr. Abdul, Dr. Imil, Abhirami, Dr. Pallavi, Annapurna and Shahid.I thank my summer internship lab members Rajgopalan, Dr. Karthikeyan, Dr. Kannan, Muthuganesh, Prakash, Dr. Bhagya, Dr. Shanmugha for the love and care you have shown on me.

I thank U. Rajesh (Mr. Cool) for always being there for me. I thank K. Hemanth, we miss you man. I thank C. Sandeep, Raghuveera, Balaankaiah Naik, Venkatesh Naik, Dr. Karun Kumar, Dr. J. Sandeep, Praveen Kumar and all other JNV family members who are there in this journey with me all along.

I thank Ramesh anna for helping in maintaining the insect room. I thank Deepthi and Nalini for helping in Confocal imaging. I thank former and current CNCS office staff Keerthi, Sharada and Jayanth.

Contents

Abbreviations

AFP: Anterior fiber plexus
AL: Antennal Lobe
ALO: Anterior Lobula
ALO-D: Anterior Lobula Dorsal
ALO-V: Anterior Lobula Ventral
aMe: Accessory Medulla
AOC: Anterior optic commissure
AOT: Anterior Optic Tract
AOTu: Anterior Optic Tubercle
AOTu-LU: AOTu Lower Units
AOTu-UU: AOTu Upper Units
AOTu-UU-IL: AOTu-UU Inner Layer
AOTu-UU-OL: AOTu-UU Outer Layer
aPDFMes: Anterior Medulla Neurons
AVLP: Anterior Ventro Lateral Protocerebrum
Ca: Calyx
CBL: Central Body Lower
CBU: Central Body Upper
CRE: Crepine
CS: Conditioned Stimulus
DCMD: Descending Contralateral Movement Detector
DLO: Dorsal Lobula
DRA: Dorsal Rim Area
DSGC: Direction selective ganglion cells
EEG: Electroencephalogram

ERG: Electroretinogram
FPS: Frames per second
GABA: Gamma Amino butyric acid
HB: Hieroglyphus banian
HS: Horizontal Sensitive
ILO: Inner Lobula
ISI: Inter Spike Interval
ITI: Inter Trail Interval
ITT: Inter Tubercle Tract
KC: Keynon cells
L1-L5: Laminar Monopolar Neurons
LAL: Lateral Accessory Lobe
LBU: Lateral Bulb
LFP: Local Field POtentials
LGMD: Lobula Gaint Movement Detection
LGN: Lateral geniculate nucleus
LN: Local Neuron
Lob: Lobula
Lom-TK II: Locust Tachykinin II
LPi: Lobula Plate Intrinsic Neurons
LPTC’s: Lobula Plate Tangential Cells
LT: Lateral Triangle
LVT: Lobula Valley Tract
LX: Lateral Complex
MBU: Medial Bulb
Med: Medulla (Med)
Mi: Medulla Intrinsic

Mi1: Medulla Interneuron
mITT: Medial inter-tubercle tract
MO: Median Olive
Nc82: Bruchpilot Brp Antibody
ND: Null Direction
OLO: Outer Lobula
ORN: Olfactory Receptor Neuron
PB: Protocerebral Bridge
PBS: Phosphate buffer saline
PCA: Principle Component Analysis
PD: Preferred Direction
PDF: Pigment Dispersing Factor
PDF-ir: Pigment Dispersing Factor-Immuno Reactive
PED - Peduncle
PER: Probosis Extension Reflex
PFA: Paraformaldehyde
PLP: Posterior Lateral Protocerebrum
PLP: Posterior Lateral Protocerebrum
PN: Projection Neurons
POC: Posterior optic commissure
POT: Posterior Optic Tract
POTu: Posterior Optic Tubercle
pPDFMes: Posterior Medulla Neurons
PSTH: Peri stimulus time histogram
PTX: Picrotoxin
PVLP: Posterior Ventro Lateral Protocerebrum
R1-R8: Retinular cells

ROI: Region of Interest
SAC: Starburst amacrine cells
SIP: Superior Intermediate Protocerebrum
SLO: Stalk Lobe
SMP: Superior Median Protocerebrum
STA: Spike triggered average
STMD: Small Target Motion Detectors
SVD: Single Value Decomposition
TALT: Tubercle accessory lobe tract
Tm: Tangential Medulla
TMR: Tetra methyl rhodamine
ULAL: Upper lateral accessory lobe
US: Unconditioned stimulus
Vam: Vacuolar medulla
vITT: Ventral inter-tubercle tract
VNC: Ventral Nerve Cord
vPDFLas: Ventral Lamina Neurons
VPN: Visual projection neurons
VPN-MB: Visual projection neuron-mushroom body
VS: Vertical Sensitive
WN: White noise stimulus

List of Tables

List of figures

Chapter 1

Introduction

1.1 Vision

During the Early Cambrian period around 541 million years ago (mya) first time eyes appeared in marine arthropods, Trilobites (Clarkson et al., 2006; Honkanen et al., 2019; Martinsson, 1975). Later on, parallel evolution led to the complexity of eyes. A wide range of organisms, ranging from insects to higher vertebrates like birds and mammals have to resolve several visual problems to sustain their life. These include motion, depth and distance estimation for escaping from a predator or to avoid colliding objects. Polarisation vision for navigation, keeping track of the day and night for entraining the circadian clock and colour vision for resolving the identity and characters of an object.

Insects are good model organisms for studying visual systems and some of the most well studied are Drosophila, Blowfly, Ants, Locust, Honeybee, Dung beetle, Cockroach and Mantis. Many insights have been garnered about visual processes using these model systems. Insects have fixed compound eyes. Compound eyes of all the insects have following functional components in common: cornea, cone, rhabdom and screening pigment. Compound eyes contain hundreds or thousands of hexagonal structures called ommatidia/facets. Each of the ommatidia have photoreceptors called retinula cells. Number of ommatidia and retinula cells varies from insect to insect. Retinula cells microvillar structures give rise to photosensitive structures called rhabdomeres, rhabdomeres collectively form rhabdom. Rhabdoms are also called light guides which help in directing the photons over the microvilli of the retinula cells. Adjacent ommatidia and rhabdoms are separated from each other by screening pigment.

Based on optical properties, compound eyes are divided into apposition eyes and superposition eyes. In apposition eyes, light from the corneal facets go to rhabdoms directly adjacent to it in the column (fused rhabdom) i.e., ommatidia acts as an optically isolated unit whereas in superposition eyes,

ommatidia are not optically isolated (open rhabdom, screening pigment is not present). That is, each facet projects light from it over many rhabdoms.

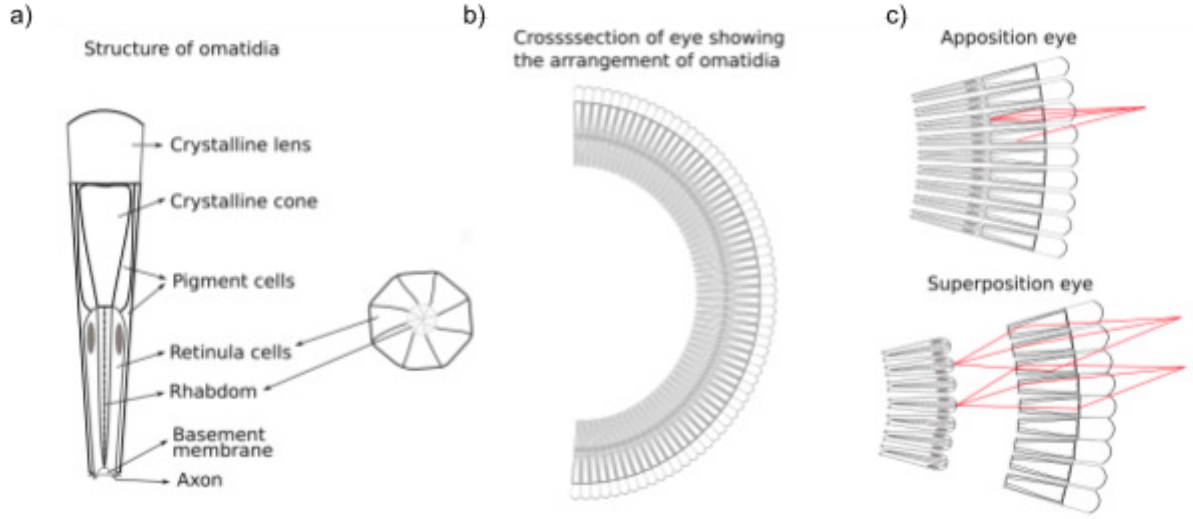

Figure 1.1: Compound eye. a). Structure of ommatidium b). Cross section of the eye c). Optical properties of apposition eye (upper) and superposition eye (bottom)

Apposition eyes further classified as simple apposition/focal apposition, afocal apposition and transparent apposition eyes. Whereas, superposition eyes are classified as reflecting superposition, refracting superposition and parabolic superposition eyes. Among all these types, simple apposition eyes are very common in insects like bees, mantids, locusts, cockroaches, dragonflies.

1.2 Flertebrate

Vision is well studied in the order diptera, which includes flies. Flies have focal apposition with open rhabdom eyes, which show neural superposition. In 1914, Alexei Alexseevich Zavarzin studied Dragonfly optic lobes, based on cell types involved in initial visual processing, he showed that there are corresponding elements in the optic lobes of mammals and cephalopods also (Zawarzin, A. A., 1925). In 1915, Cajal and Sanchez studied fly visual systems, by rearranging in the drawing, the cell bodies of the neuron types of initial visual processing to a vertebrate like position without altering the neuropil (later called as Flertebrate arrangement), they showed that lamina monopolar neurons, amacrine cells and trans medullary cells of fly appeared as bipolar neurons, horizontal cells and retinal ganglion cells of vertebrates (Ramón y Cajal, S., & Sanchez, D., 1915) (Fig 1.2). Based on further

studies on vertebrate and Drosophila visual systems, anatomists have claimed that, lamina, medulla and lobula of insects may corresponds to the retina, LGN and visual cortex of vertebrates (Millard & Pecot, 2018; (Sanes & Zipursky, 2010).

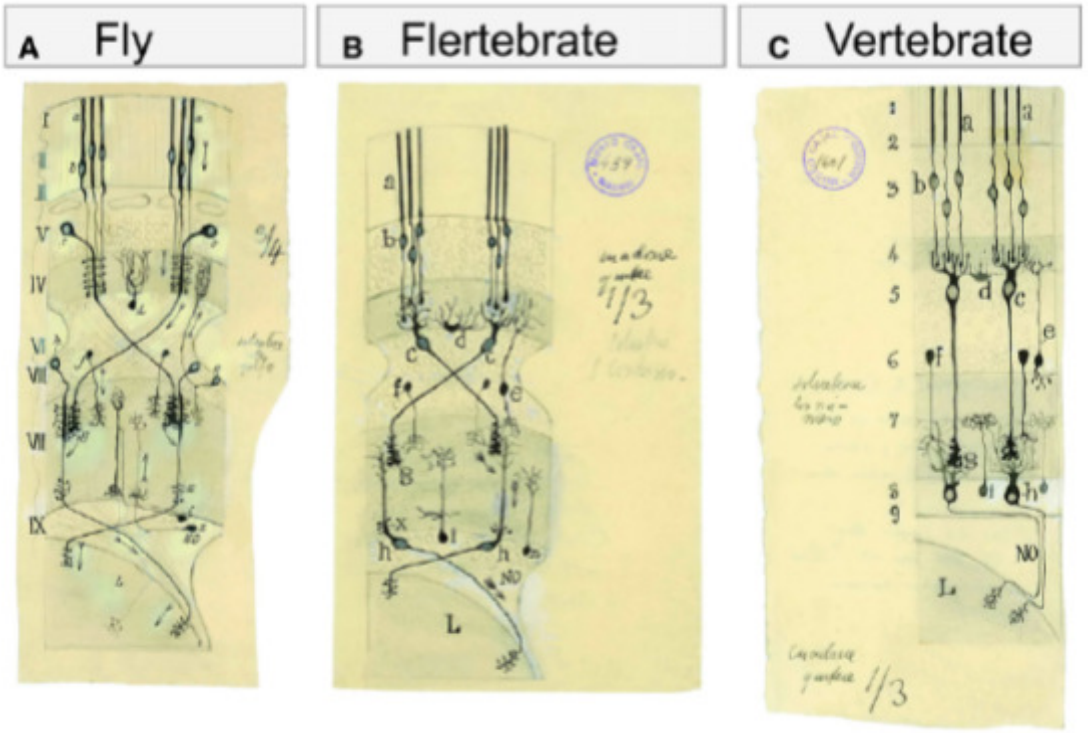

Figure 1.2: Similarities in the initial visual processing pathway of vertebrate and fly. A). Cell types involved in visual processing in Drosophila optic lobe. B). Cell bodies of the Drosophila optic lobe neuron types moved in position according to the neuronal cell types of the vertebrate retina (Flertebrate). C). Types of neurons involved in initial visual processing in vertebrates. (Source: Ramón y Cajal, S., & Sanchez, D., 1915).

1.3 Similar circuit design in motion vision of insects and mammals

Motion detection circuit is well studied in both mammals and Drosophila. In the motion detection processing mechanism in Drosophila, brightness level in an area of the visual field is detected by photoreceptors (retinula cells). The retinula cells synapse onto the lamina monopolar neurons. These neurons primarily respond to transients in the brightness. They synapse on to the medullary neurons. In medulla, this pathway is divided into ON and OFF pathways made up of T4 and T5 cell types respectively. T4 and T5 cells have four subtypes (T4a-d, T5a-d), each subtype is sensitive to one cardinal direction. These subtypes synapse onto the widefield lobula plate tangential cells (LPTC,

Horizontal System (HS) and Vertical System (VS) cells) in one of the four layers of the lobula plate which are sensitive to one cardinal direction for detecting preferred direction (PD) and onto the Lobula plate interneurons (LPi). LPi further have inhibitory synapse with the LPTCs of the neighbouring layers of lobula plate for inhibiting the LPTCs for null direction (ND) motion. Thus, forming the motion detection circuit (Fig 1.3).

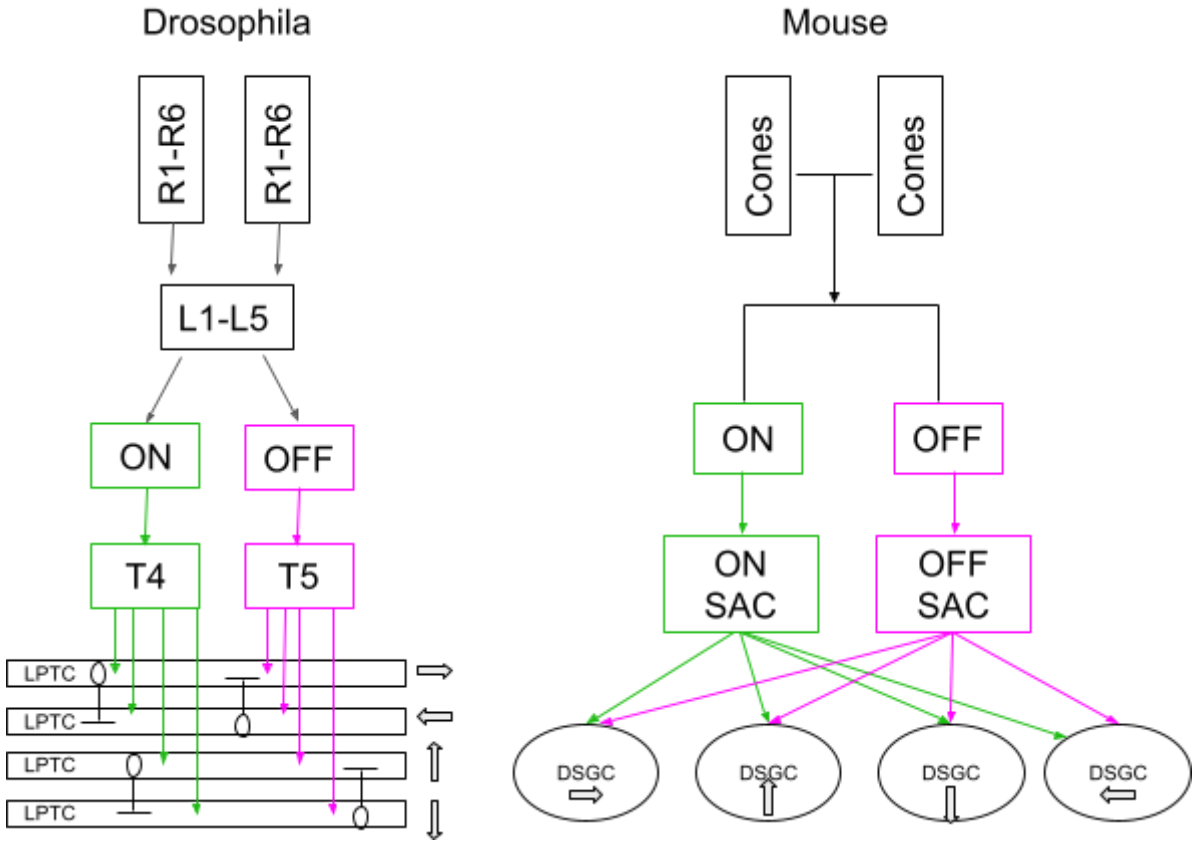

Figure 1.3: Comparison of motion detection circuits of Drosophila and Mouse (Adapted from Borst, A., & Helmstaedter, M. (2015))

If we see the motion detection circuit in the mouse, brightness changes are detected by photoreceptors which further convey it to the bipolar cells. Here, at the bipolar cell level (the second neuron analogous to lamina monopolar cells) itself, the motion detection pathway is divided into ON and OFF pathways. Bipolar cells further synapse onto starburst amacrine cells (SAC), which have inhibitory synapse onto the direction selective ganglion cells (DSGC). This forms the motion detection circuit (Fig 2). Thus, there are commonalities and differences between fly and mouse motion detection circuits.

1.3.1 Commonalities

Splitting of motion detection pathway into ON and OFF pathway in early stage itself in mouse retina and fly optic lobe. This splitting occurs at photoreceptors level in mice whereas in fly it occurs one synapse ahead of the photoreceptors. Luminance representation is similar in both the systems. Upon illumination, photoreceptors in the mouse retina and lamina monopolar neurons of the fly optic lobe are hyperpolarized. Motion detection is represented in four cardinal directions in both the systems.

1.3.2 Differences

Direction tuning curves are narrower for fly motion vision than mouse. In mice, ON and OFF motion information is fused at DSGC, local cells whose visual field covers a few degrees. Whereas in Drosophila, the ON and OFF pathway is fused on the wide field LPTC dendrites, whose visual field covers almost 180°. LPTC's show motion opponency whereas this feature is not seen in retinal ganglion cells.

The common ancestor of insects and mammals lived around 550 mya . Despite this evolutionary distance, the motion detection circuit processing is similar for insects (Drosophila) and mammals (Mouse) due to convergent evolution.

In the Drosophila visual pathway, posterior to the cornea hexagonal structures (Ommatidia/facets) are visible. Ommatidia contain eight photosensitive cells (R1-R8 retinula cells). R1-R6 retinula cells are arranged in a circle and R7 is present at the centre of the circle and posterior to it R8 is present. R1-R6 expresses a single type of opsin (Zuker et al.,1985; O'Tousa et al., 1985) which conveys achromatic information, and responds to a broad band of the spectrum (Hardie, 1979). R7 expresses UV sensitive opsins while R8 expresses blue-green sensitive opsins (Zuker et al.,1987;Montell et al., 1987; Fryxell and Meyerowitz, 1987; Papatsenko et al., 1997; Chou et al., 1996) and conveys chromatic information (Heisenberg and Buchner,1977; Yarnaguchi et al., 2008). With respect to the vertebrate (Zuker et al.,1987; Montell et al., 1987; Fryxell and Meyerowitz, 1987; Papatsenko et al., 1997; Chou et al., 1996) visual system, we can consider R1-R6 as rods and R7-R8 as cones. Proximal to the retinula cells, rhabdom is present. Photo signal from a single source is received by multiple

ommatidia in the neighbourhood. Fibers of the retinula cells from these ommatidia are 180° twisted and pooled together in the lamina (first neuropil, Fischbah and Hiesinger 2008).

There are four neuropils which all together make the optic lobe of the Drosophila. They are lamina, medulla, lobula and lobula plate. The lamina contains lamina monopolar neurons arranged in columns called cartridges. Each cartridge contains five lamina monopolar neurons (L1-L5) (Meinertzhagen and Oneil, 1991; Meinerzhagen and Hanson, 1993; Meinerzhagen and Sorra, 2001), of which L1 and L2 are necessary for motion vision (Riester et al., 2007).

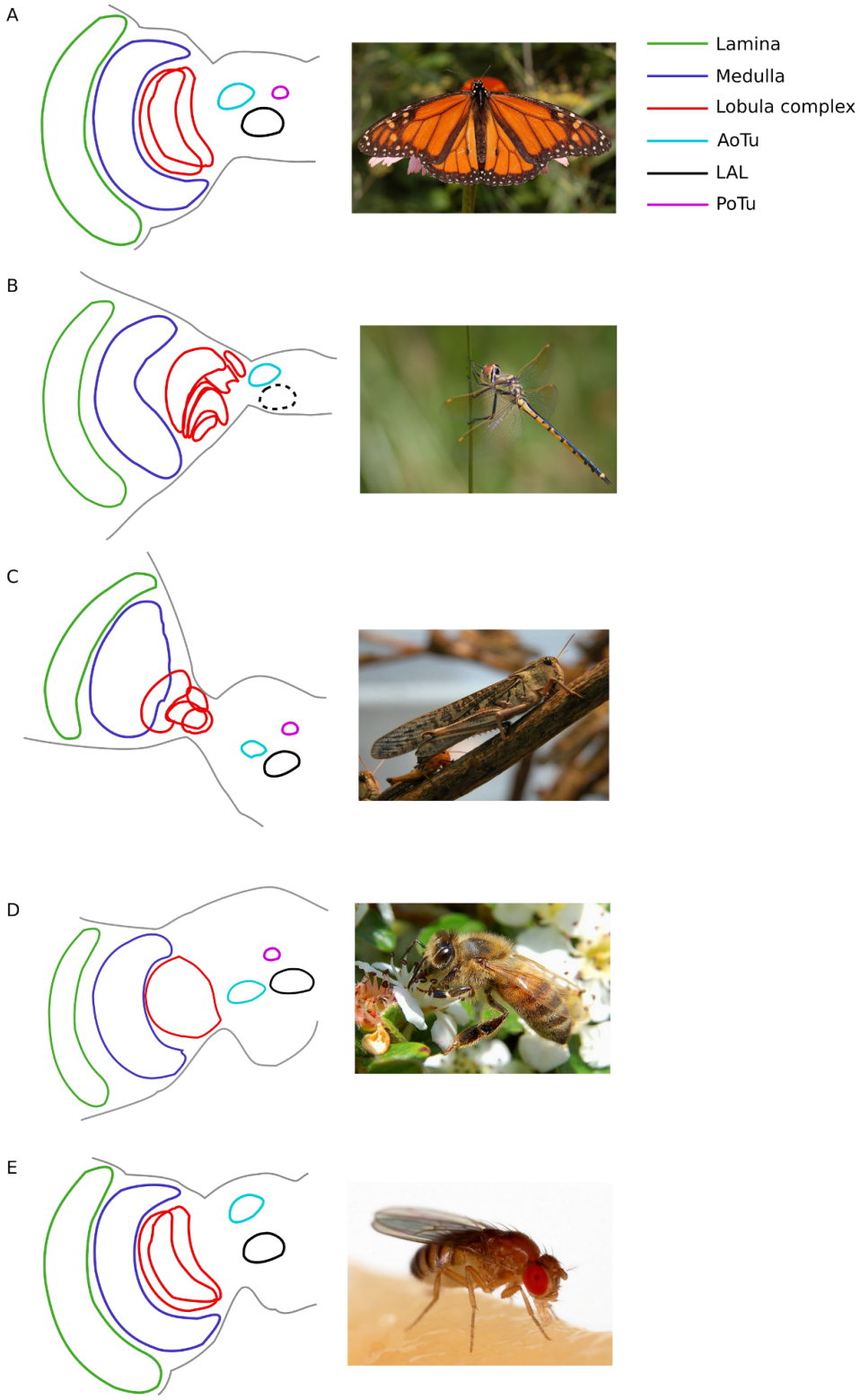

Figure 1.4: Comparing the neuropils in the optic lobe and their known output regions drawn based on combined information from the literature. A) Monarch butterfly (*Danaus plexippus)* B) Dragonfly tau emerald (*Hemicordulia tau*) C) Locust D) Honeybee (*Apis mellifera*) E) *Drosophila melanogastor*. Notice that the lobula complex (red) is strikingly different between these species. (Insect images from Wikipedia)

1.4 Insect optic lobes

The number of neuropils and their structures varies from species to species. For anti-synapsin staining, Drosophila lamina showed a single layer with multiple columnar structures called cartridges, Monarch butterfly's (*Danaus plexippus*) lamina was characterised with single layer and a synapsin rich inner rim (Heinze. S.et al., 2012) and lamina of diurnal beetle (*Scarabaeus lamarcki*) showed 4 layers whereas nocturnal beetle (*Scarabaeus satyrus*) showed 7 layer structure (Immonen et.al., 2017). African desert ant (Cataglyphis nodus) lamina showed single layer structure (Habenstein J et.al., 2020). *Apis mellifera* and *Musca domestica* also showed single layer structure in lamina upon nc82 staining (presynaptic marker, similar to anti-synapsin) whereas *Schistocerca gregaria* showed single layered structure.

Medulla is the second optic neuropil,which showed 10-12 layered structures across the species. In Drosophila, golgi stained preparations showed that medulla is a 10 layered structure, it can be divided 1-6 layers as outer (distal) and 8-10 as inner (proximal) medulla separated by a 7th layer called serpentine layer (Fischbach, K. F., & Dittrich, A. P. M., 1989). In monarch butterflies, synapsin immunoreactivity showed 10 layered structures, divided as outer and inner medulla, separated by serpentine layer (Heinze, S., & Reppert, S. M., 2012). In honey bee (*Apis mellifera*) based on ethyl gallate staining, medulla is divided as outer and inner medulla separated by serpentine layer (Ehmer, B., & Gronenberg, W.,2002). Based on GABA staining, praying mantis (*Hierodula membranacea*) medulla showed 10 layered structures, cockroaches showed 6 layered structures and desert locust (*S. gregaria*) showed 10 layered structures (Rosner, R., von Hadeln, J., Salden, T., & Homberg, U.,2017). Anti-synapsin and anti-5-HT stainings of both the nocturnal and diurnal dung beetles showed 11 layered structure medulla (Immonen et.al., 2017). African desert ant medulla is divided as outer and inner medulla separated by serpentine layer (Habenstein J et.al., 2020).

Lobula complex is very diverse in species (Fig 1.4). A set of insects have only two distinct structures making up lobula complex, lobula and lobula plate. Lobula is present as a single neuropil or a number of sub-neuropils. Golgi staining in Drosophila showed lobula is a single neuropil with six horizontal layers (Fischbach, K. F., & Dittrich, A. P. M.,1989). Anti-synapsin immunoreactivity in Monarch

butterfly (Heinze, S., & Reppert, S. M., 2012) and in dung beetles (Immonen et.al., 2017) showed that lobula is divided as inner and outer lobula. In Praying mantis, lobula has 5 sub neuropils called outer lobula (OLO), dorsal lobula (DLO), anterior lobula-ventral and anterior lobula dorsal (ALO-V & ALO-D) and stalk lobe (SLO), GABA staining revealed cockroach lobula has 3 sub-neuropils called dorsal lobula(DLO), outer lobula (OLO) and anterior lobula (ALO) (Rosner, R., von Hadeln, J., Salden, T., & Homberg, U.,2017). Anti-synapsin staining in desert locust showed that lobula has 4 sub neuropils called outer lobula (OLO) which showed 3 layered structure whereas GABA staining showed 4 layers, inner lobula (ILO), dorsal lobula (DLO) is GABA positive and anterior lobula (ALO) showed 4 layered structure (Rosner, R., von Hadeln, J., Salden, T., & Homberg, U., 2017).

Lobula plate is another neuropil thought to be exclusively present in holometabolous insects (Strausfeld, N. J.,2021) (There are exceptions like hymenoptera where this arrangement is not clear though they are holometabolous). In Drosophila, the lobula plate is the centre for direction detection. It is a 4 layered structure, each layer has T4 and T5 neurons innervations which are specific to one cardinal direction (Maisak et al., 2013). Neurons specific to vertical motion (up or down)/ horizontal motion (left or right) are present in adjacent layers and lobula plate interneurons in those layers help in detecting null direction by inhibiting the neurons in the adjacent layer which detect opposing motion (Mauss et al., 2015).

According to the studies of SR Shaw 1978, *Locusta migratoria* has approximately 3mmX2mm compound eyes, each eye having ~8500 ommatidia. Each ommatidia has eight retinula cells. In distal half of the ommatidium, 6 long retinular cells and two short retinular cells in proximal ommatidium are present, whose photosensitive microvilli extensions together form a 350-500µ long cylindrical structure called rhabdom. Light is focused onto the rhabdom by a corneal lens through crystalline cones. Each cone is 30µ at widest diameter and 60-90µ in length and it is divided into four segments. At the end of the cone tip, each segment has ~100 hollow tubules of diameter 20 mµ. These tubules give mechanical support for retinula cells and hold them just beneath the crystalline cone. Around the crystalline cone, there are two primary pigment cells and also 16 secondary pigment cells (Horridge, G. A.,1966).

In Schistocerca, Meinertzhagen 1976 showed that the cyclic order of the retinula cells is 1, 2, 3, 4, 8, 5, 6, 7 or occasionally cell 8 moving between cell 5 and 6. Wide range of arthropods contain compound eyes (Land and Nilsson, 2002).

Table 1.1: Optic lobes organisation in different insects.

	Eye	**Lamina**	**Medulla**	**Lobula complex**
Drosophila melanogaster	~800	Columnar structure	10 layered structure (Golgi staining), Outer medulla(1-6) and inner medulla (8-10) are separated by serpentine layer (7th)	Lobula complex consists of lobula (6 layered structure) and lobula plate (4 layered structure).
Danaus plexippus		Lamina with inner rim, synapsin immuno reactive.	10 layered structure (Anti-synapsin staining)	Lobula is divided as outer and inner lobula. Lobula plate divided into 3 layered structure.
Cockroach			6 layered structure (Anti-GABA staining)	Three sub neuropils. OLO, DLO ALO
Mantis	~9000 ommatidia		10 layered structure (Anti-GABA)	Five sub-neuropils, OLO,DLO,ILO,ALO and SLO
Apis mellifera	Drone: ~10000 Queen: ~4000 Worker: ~5000-6000		Multi layered structure, divided as outer and inner medulla separated by serpentine layer.	Lobula as a single neuropil.
Dragonfly	~24000		21 layers, outer medulla (MEO1-MEO7) separated from inner medulla (MEI1-MEI10) by serpentine layer (S1-S4) (Anti-synapsin & anti-seratonin staining)	Lobula complex consists of primary lobula (PLO), medial lobula (MLO), inner lobula (ILO), sub lobula (SLO) and lobula plate (Lop)
Dung beetle	*Onthophagus posticus* ~ dorsal eye: 100; ventral eye: 500.	3 layered structure in diurnal beetle and 7 layered in nocturnal beetle (Anti-synapsin staining)	11 layered structure, outer medulla (OMe,1-7) separated from inner medulla (IMe,9-11) by serpentine layer (8th).	Lobula is divided into outer lobula (OLO) and inner lobula (ILO). Lobula plate is present.

Table 1.2: Visual processing areas in the protocerebrum of different insects

Species	AOTu	POTu	LAL
Drosophila melanogaster	AOTu is constituted of three distinguishable neuropils. They are the medial compartment (AOTUm), intermediate AOTU [AOTUin] and lateral AOTU [AOTUl]..		Lateral complex consists of gall (GA), bulb (BU,lateral triangle). LAL has ventral body and crepine (CRE).
Danaus plexippus	AOTu is divided as the upper unit which is large in size and nodular unit (3 compartments), lower unit, and the strap, the last two being smaller in size.	POTu is present	
Apis mellifera	AOTu is divided into 4 compartments, major unit (MU) (dorsal lobe (MU-DL) and ventral lobe(MU-VL) & Lateral unit and ventro-lateral unit (LU and VLU). VLU is similar to the lower unit of the locust AOTu. AOTu is connected to the other parts of the brain through., 1. Anterior optic tract (AOT): connected to the Optic lobe (OL). 2. ventral inter-tubercle tract (vITT) 3. medial inter-tubercle tract (mITT) bot (2)& (3) connect two AOTu's. 4.Tubercle accessory lobe tract (TALT): AOTu to LAL(lateral accessory lobe) And AOTu is connected to the vertical lobe of the mushroom bodies by A5-2 neuron.	POTu is present	Lateral complex (LX) consists of two bulbs (BU) medial bulb (MBU) & lateral bulb (LBU).
Dung beetle	AOTu is divided as upper unit (UU) and lower unit complex (LUC), LUC is further divided into 6 sub-neuropils. LUC- polarisation vision UU-unpolarized and chromatic vision.		

1.5 Computational models of motion detection

Integrating the local motion is necessary for survival as well as to integrate the global motion. Every motion detector requires luminance changing inputs from adjacent locations in the space. These inputs had to be processed asymmetrically and a non-linear interaction between them (Borst & Egelhaaf, 1989; Buchner et al., 1984; Poggio & Reichardt, 1973).

Motion detection can occur by 1) comparing luminance change in a particular location at a given point of time to the luminance change in the adjacent location after a time point and 2) Brightness changes in the temporal domain at a given location is related to the brightness change in the spatial domain of the same location. Based on these, there are two classes of models which account for local motion detection (Fig 1.5) . They are

1) Gradient detector models

2) Correlation detector models.

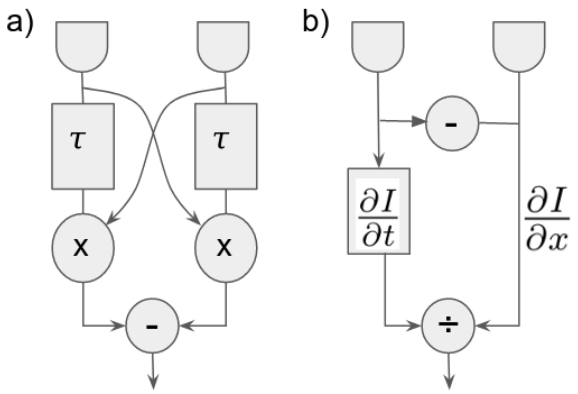

Figure 1.5: a) Reichardt detector made of two delay elements, multipliers and a difference operator. b) Gradient detector made up of time differential operator, spatial differential operator and a divider.

Of these, the Reichardt model satisfies the experimental observations in fly better, namely fitting at different luminance levels and matching the observed automatic gain control (Barlow & Levick, 1965; Borst, 2007; Borst & Egelhaaf, 1989; Egelhaaf et al., 1989; Haag et al., 2004; Single & Borst, 1998).

1.5.1 Gradient detector models

These detectors receive brightness change inputs from two adjacent subunits. Both the inputs are high pass filtered and approximate the temporal brightness change (dI/dt) and then added together. The resulting temporal brightness change (dI/dt) is divided by spatial brightness change (dI/dx) (Srinivasan, M. V.,1990), giving rise to the image velocity. Spatial brightness change is computed from brightness difference between two adjacent points in the visual space separated by a distance dx (Fig 1.5b). These detectors suit best for high frequency signal to noise ratio (SNR) systems (Potters, M., & Bialek, W. (1994)).

1.5.2 Correlation detector models

1.5.2.1 Hassenstein–Reichardt detector (HR detector)

This model is derived from the quantitative analysis of Chlorophanus beetle walking behaviour (Hassenstein, B., & Reichardt, W.,1956). This model works on delay and comparison mechanisms. HR detector (Fig 1.5a) has two mirror subunits, each receiving input of changes in light intensities from adjacent locations. One of the inputs in each of the subunits is delayed by a delay time corresponding to the possible motion related delay. The inputs from two subunits are multiplied in each subunit and at the end of the operation product from one operation is subtracted from the other. Any object moves in the visual field of the motion detector, activating the subunits in sequence. For preferred direction(PD), delayed input signal is time compensated and at particular velocity, inputs from both the subunits coincide and maximise the output signal (Fig 1.6a-b). Whereas for null direction(ND), temporal signals from both the inputs are reversed, because of this output signal is minimised (Fig 1.6c-d).

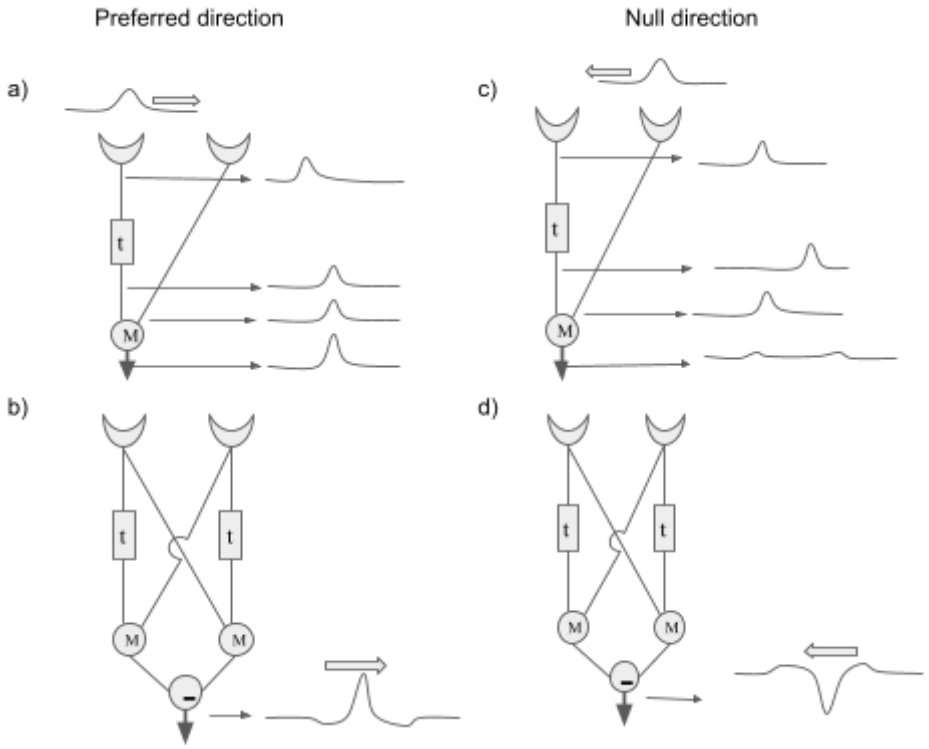

Figure 1.6: Hassenstein–Reichardt detector (HR detector). a) Single subunit detecting PD. b) Mirror symmetrical subunits of detecting PD. c) Single subunit detecting ND. d) Mirror symmetrical subunits of detecting ND.

1.5.2.2 Barlow and Levick model

This model is based on the electrophysiological observations of rabbit retina (Barlow, H. B., & Levick, W. R.,1965). This model is equivalent to the half detector of the HR detector. It has two subunits, brightness signals received from two subunits. Input from one of the subunits is delayed and input from another subunit is passed without any delay. Delayed input is subtracted from non-delayed input. For preferred direction, an excitatory signal arrives at the output gate before the delayed inhibitory signal reaches, resulting in no detection of the motion (Fig 1.7b). Whereas for null direction, inputs from both the subunits reach the output gate at the same time. This results in maximum suppression of the signal (Fig 1.7a).

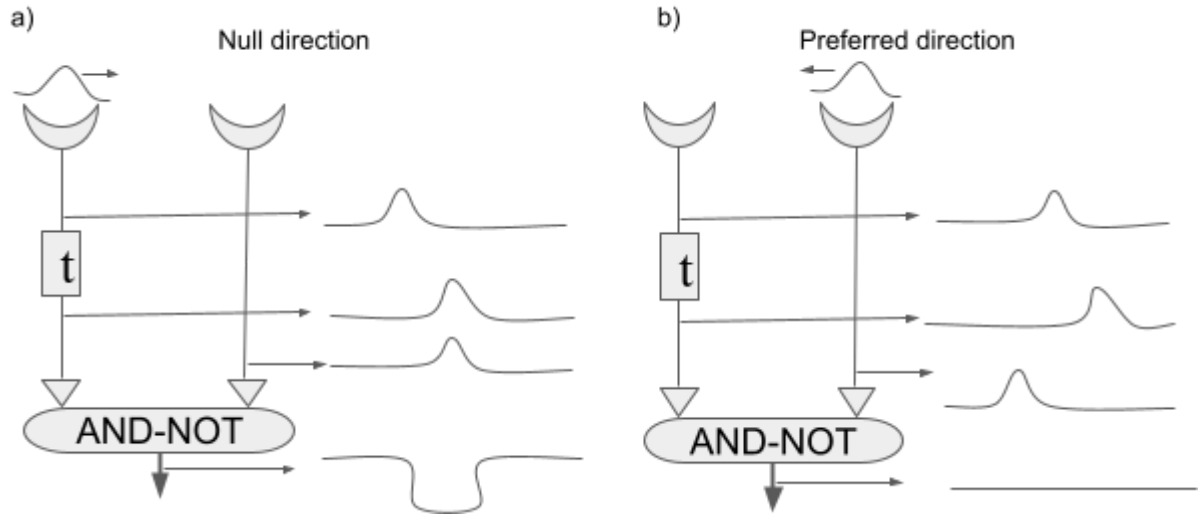

Figure 1.7: Barlow and Levick ND detector. a) BL detector null direction detection. b) BL detector not detecting the preferred direction.

1.6 Different visual pathways in insects

1.6.1 Circuit for detection of motion direction

In Drosophila, it has been shown that motion direction selectivity occurs in lobula plate mediated by lobula plate intrinsic neurons (Maisak et.al 2013, Mauss et.al 2015, Haag et.al 2016). Photoreceptors (R1-R6) in the retina detect changes in light intensity, which convey brightness increase (ON) and brightness decrease (OFF) information to medullary ON (Mi1&Tm3) and OFF (Tm1, Tm2, Tm4, Tm9) pathways through lamina monopolar neurons (L1-L2). L1 and L2 neurons cell bodies are located distal to the lamina, these neurons branch throughout the lamina in a columnar manner and receive inputs from R1-R6 receptor terminals of the cartridge by forming tetrad synapse (Burkhardt, W., & Braitenberg, V., 1976; Nicol, D., & Meinertzhagen, I. A.1982). L1 neuron innervates M1 and M5 medulla layers whereas L2 neuron innervates M2 medulla layer (Fischbach, K. F., & Dittrich, A. P. M.,1989). Medullary ON and OFF pathway neurons cell bodies are present in the first chiasma, distal to the medulla. Medulla interneuron (Mi1) has arborisations in M1 and M5 layers, Trans medulla (Tm) neurons having cell bodies in cell body rind, distal to the medulla (outer chiasma), Tm1 and Tm2 have smooth innervations in M2, M3 and M9 medulla layers and innervate into the first layer of the lobula. Tm3 neurons have innervations in M1, M4 and M5 medulla layers and innervate deep into the lobula upto 4th layer. Tm4 neurons have arborisations in M2, M3, M4 and M8 of the

medulla and innervates deeper into the lobula having minor branches upto 4th layer. Tm9 having innervations in M2, M3 and M4 , in lobula it innervates deep upto 4th layer of the lobula.

Medullary ON & OFF pathways converge on to the 4 sub-types of each of the tangential neurons T4 (T4a-d) and T5 (T5a-d) respectively (Maisak et al., 2013). T4 and T5 cells cell bodies are located in the cell body rind posterior to the lobula plate. T4a-d have fine dendrites in M10 medulla layer, indicating input regions and arborise in lobula plate layers 1, 2, 3 and 4 respectively with punctate structures, indicative of output regions. T5a-d cells have fine dendrites in the 1st layer of the lobula indicating receiving inputs and synapse in lobula plate layers 1, 2, 3 and 4 respectively with punctate structures, indicating output regions. . T4 and T5 neurons synapse onto the lobula plate tangential cells (LPTC's) in the lobula plate. So far there are 60 reported cell types of LPTC's in blowfly. There are mainly two classes of LPTC's based on their preferred orientation. They are horizontal sensitive (HS) and vertical sensitive (VS) cells. T4 and T5 cells synapsing (cholinergic inputs) onto the HS and VS cells detect the preferred direction motion. Subtype which detects the preferred direction also inhibits the neighbouring neuronal circuit which is responsible for detection of null direction through lobula plate interneurons (LPi) (Mauss et al., 2014; Mauss et al., 2015). Another class of neurons, lobula plate/lobula columnar, type II (LPLC2) computes local looming responses (Klapoetke et al., 2017). They receive inputs from small field neurons (T4 and T5) selective to direction of motion and local input that is inhibitory from LPi4-3. In this way motion information of different kinds are computed in the lobula complex of Drosophila.

1.6.2 Polarisation vision circuit

Polarisation vision is the capability of animals to find out the oscillation plane of the electric field vectors (E-vector) of light and to use it for different behaviours of everyday life. Butterflies use E-vectors for finding sites for ovipositing (Kelber 1999; Kelber et al. 2001), marine invertebrates use for intraspecific communications (Marshall et al, 1999; Chiou et al, 2008). Migrating insects such as Monarch butterflies (Rappert et al, 2004; Merlin et al, 2012) and Locusts (Homeberg 2004), insects showing homing behaviour like honey bees and desert ants (Wehner and Labhart 2006) and dung

beetles that needs consistency in its trajectory to escape competition while collecting dung (Dacke et al,2003), use it for navigation.

Circuits underlying polarisation vision are well studied in locusts (Homberg and Peach 2002), Monarch butterfly (Labhart et al. 2009) and crickets (Brunner & Labhart,1987). The Dorsal rim area of the eye of insects is specialised to detect polarised light. In DRA, optical axis of ommatidia directed upwards, shorter and compact rhobdoms with orthogonally arranged microvilli giving larger cross sectional area and screening pigment is either reduced or absent.

In *S. gregaria*, ommatidia have R1-R8 rhobdoms, R7 microvilli of each dorsal rim ommatidia are orthogonal to the R1, R2, R5, R6 & R8. R3 & R4 microvilli are irregularly arranged (Homberg & Paech, 2002). In crickets, it has been shown that axons of R1, R2, R5 & R6 innervate into the dorsal rim of lamina and R7 innervate into the dorsal rim of medulla (Blum & Labhart, 2000). Tract tracings from the dorsal rim area of the eye, dorsal rim of medulla (DRMe), anterior optic tubercle (AOTu) and single neurons of the central body (CB) of locusts have revealed that tangential medulla neurons from medulla dorsal rim have innervated into the lower unit of AOTu (AOTu-LU) through the anterior lobe of lobula via anterior optic tract (Homberg et al., 2003). Neurons from AOTu-LU and lower division of CB (CBL) synapse at median olive (MO) and lateral triangle (LT) of lateral accessory lobe (LAL) (Müller et al., 1997). Physiological studies have also revealed polarisation sensitive neurons from accessory medulla (aMe) which are arborized into posterior optic tubercle (POTu) and intertubercular neurons of the posterior optic tubercle. Information received from AOTu-LU path and POTu path is processed in the central complex. Tangential neurons of CBL TL2/3 receive polarisation information from LAL and transfer to CBL. Columnar neurons CL1 may receive input from TL2/3 and transfer to tangential neurons of the protocerebral bridge (PB) TB1 which has innervations into the posterior optic tubercle. TB1 neurons connect the columns of both left and right hemispheres of PB that are 8 columns apart, this linearly corresponds to its E-vectors tuning angles and create a compass-like representation of zenithal E-vectors covering 180 degrees in each hemisphere (Heinze & Homberg, 2007). Columnar neurons CP1, CP2 & CPU1 receive inputs from PB and give output to LAL. In this way polarisation, vision processing occurs in *s.gregaria*. The

neurons which are involved in this pathway are TIM1, TIM2, TML1, MeMe1, MeMe2 (Jundi et al., 2011). And LoTu1, LoTu2, TuTu1, LALTu1, (TuLAL2-doubt), TuP1, TuP2, (Homberg et al., 2003). Tangential neurons of the optic lobe ,majorly innervated in medulla involved in polarisation vision (Stanley Heinze,2014). Neurons innervating in the dorsal rim area of the lamina,medulla ,4th layer of the medulla, accessory medulla (Tangential medulla lamina neuron TML1,Tangential intrinsic medulla neurons TIM1 & TIM2, inter medulla neurons MeMe1 & MeMe2; (Homberg & Würden, 1997; Jundi et al., 2011) and anterior lobula (LoTu1) (Homberg et al., 2003) in locust.

In crickets, neurons innervating dorsal rim area of medulla, accessory medulla (Polarisation sensitive POL1 neurons) (Labhart & Petzold, 1993) and anterior lobula are involved in processing the polarisation vision in the optic lobe. With the inputs from the two optic lobes, polarisation vision is further processed in the central brain.

1.6.3 Network in the visual pathway involved in circadian function

Circadian rhythms and mechanisms in insects have been studied in Drosophila (Allada & Chung, 2010), crickets (Yukizane et al., 2002) and cockroaches (Nishiitsutsuji-Uwo & Pittendrigh, 1968). Circadian rhythms are maintained by a master clock in the brain which receives inputs from a number of peripheral clocks. There are number of photopigments which entrain peripheral clocks which further entrain the master clock (Photoentrainment). In insects, accessory medulla (AME) is the circadian rhythmic centre, circadian rhythms are well studied in Drosophila genetically. In Drosophila, timeless (tim), period (per), cycle (cyc) and clock (Clk) are the genes involved and photopigment cryptochrome (CRY) photoentrains the circadian clock (Emery et al., 2000). Cockroach (*Leucophaea maderae*) is also another well established model organism for circadian rhythms. Through ablation studies, people have confirmed that AME is the circadian pacemaker in *maderae* cockroach (26).

Special network of neurons expressing pigment-dispersing factor (PDF) are involved in keeping track of the day and night to entrain the circadian clock. Most of the characterised AME neurons are pigment dispersing factor-immuno reactive (PDF-ir) (Reischig & Stengl, 1996); (Reischig & Stengl,

2003), neuropeptide PDF is responsible for coupling of circadian pacemakers, controls locomotive behavioural rhythmicity and possibly involved in photoentrainment of circadian clock (Helfrich-Förster, 2014; Lee et al., 2009; Reischig et al., 2004; Shafer & Yao, 2014). PDF function in insects is similar to that of the neuropeptide vasoactive intestinal peptide (VIP) in the mammalian circadian system (An et al., 2011; Helfrich-Förster, 1995; Homberg et al., 1991; Vosko et al., 2007; Wei et al., 2014). PDF is also expressed in accessory lamina (ALA) neurons. Immunohistochemical studies on PDF-ir neurons have revealed the following neuronal circuit. PDF-ir fibres invade the proximal layer of lamina and 1st and 4th layers of the medulla. PDF fibres in the lamina receive light input via long-wavelength sensitive short photoreceptors whereas light may reach indirectly to PDF fibres of medulla through short wavelength sensitive long photoreceptors of the compound eyes that terminate in the 2nd layer of medulla. Based on their cell body location, PDF-ir neurons are classified as anterior & posterior medulla neurons (aPDFMes & pPDFMes) and dorsal & ventral lamina neurons (vPDFLas & dPDFLas) (Petri et al., 1995; Reischig & Stengl, 2003). aPDFMes connect AME to the medulla and lamina in both the optic lobes via anterior fiber fan and median layer system of the medulla. A few aPDFMes from ipsi and contralateral side form a bundle and travel through lobula valley tract (LVT) which further bifurcates between lobula and median protocerebrum, here it forms plexus1 (P1). One branch enters into the posterior optic commissure (POC) and other into the anterior optic commissure (AOC) During this both the branches form small plexus of arborisations. AOC branch forms plexus3-5 (P3-P5) and area1 & area2 (a1 & a2) and connects both the AOCs by passing through superior median protocerebrum (SMP) where as POC branch forms plexus2 (P2) and connects both the posterior optic tubercles (POTu). PDF-ir branches are highly interconnected through plexus1 (P1) and anterior fiber plexus (AFP), AOC and POC are also interconnected by this, which help in exchange of information (Wei et al., 2010). In this way, aPDFMes connect both the AME and couple the circadian pathway.

In cricket (*Gryllus bimaculatus*), medulla bilateral neurons (MBNs) connect two optic lobes and couple the two circadian pacemakers. There are five classes of MBNs, represented as MBN-1, MBN-2, MBN-3, MBN-4 and MBN-5 (Yukizane et al., 2002).

These circadian activities are modulated by several other neurotransmitters like acetylcholine(Ach), glutamate (Glu) , gamma-amino butyric acid (GABA), histamine(HA), octopamine (OA) and Serotonin (5-HT).

1.6.4 Neurons involved in colour vision

Colour vision has been studied in many insects (Song & Lee, 2018). A number of insects gave been used to understand different aspects of color vision, Drosophila (Schnaitmann et al., 2020), *Apis mellifera* (Mota et al., 2016), Butterfly (Chen et al., 2020; Kelber, 1999; Kelber et al., 2001), *S. gregaria* (Schmeling et al., 2014a). Karl von Frisch first showed that bees (*Apis mellifera*) can identify colors (Frisch, 1914). Color vision identifies different spectral wavelengths. It helps in mate selection, intraspecies communication, food source identification and quality judgement. From the above discussions, it's clear that the number of ommatidia and photoreceptors in insects vary from species to species. As we have already seen, the Drosophila eye contains ~800 ommatidia (Ramaekers et al., 2019) and each ommatidia contains R1-R8 photoreceptors. R1-R6 are broad band detectors also called outer photoreceptors containing Rhodopsin Rh1 which helps in contrast and motion detection. R7-R8 are narrowband detectors also called inner photoreceptors containing rhodopsin rh3-rh6 which help in colour vision. Based on the rh content of R7-R8, ommatidia are further classified as yellow (y) discriminates longer wavelengths and pale (p) discriminates shorter wavelengths. Retinula cells pR7, yR7, pR8 and yR8 express rh3, rh4, rh5 and rh6 respectively, R7y/p λmax is 350nm (UV), R8p λmax is 440nm (blue), R8y λmax is 570nm (green) (Feiler et al., 1992; Salcedo et al., 1999).

One of the neural pathways identified for colour vision is as follows. R7-R8 photoreceptors responsible for colour vision arborise in the medulla M6 and M3 layers (Fischbach & Dittrich, 1989a; Gao et al., 2008) respectively onto the trans medullary Tm5a, Tm5b and Tm5c neurons and Tm20 neuron. These neurons have cell bodies in the cell body rind of distal medulla, Tm5a has arborisations in M2-M8, Tm5b has arborisations in M2-M9, Tm5c has arborisations in M1-M7 and Tm20 has arborisations in M1-M3 and in M7. These trans medulla neurons synapse onto the 4th and 5th layer of the lobula. Visual projection neurons (VPN) connect visual processing centres in the optic lobe to the

visual processing centres in the central brain. Lobula tangential 11 (LT11) neuron and medulla columnar 61 (MC61) are two such VPN's. LT11 is a single neuron with cell body in lateral cell body rind of the lobula, dendrites are in Lo3, Lo4, and Lo5 layers of the lobula receiving inputs from Tm5a-c & Tm20 and axon terminals are in the posterior ventro lateral protocerebrum (PVLP) and posterior lateral protocerebrum (PLP) of the central brain. MC61 cell bodies are in the lateral surface of the medulla, dendrites are arborised in M6 and M7 layers of the medulla. LT11 neuron receives inputs from Tm5a-c and Tm20. It sends outputs to the posterior ventro lateral protocerebrum (PVLP) and posterior lateral protocerebrum (PLP).

Katrin Vogt et.al found two direct pathways connecting the optic lobes to the mushroom bodies. They are visual projection neuron-mushroom body 1 (VPN-MB1) and 2 (VPN-MB2) pathways. Blocking the outputs of VPN-MB1 using GAL4 driver lines has impaired the colour discrimination ability whereas blocking the VPN-MB2 outputs did not affect the colour discrimination ability. VPN-MB1 neurons arborize in the M8 layer of the medulla, a region where Tm5 neurons presynaptic terminals are present. From the above discussion and from the literature, it is known that Tm5 neurons are crucial in colour vision processing. VPN-MB2 pathway is shown to be responsible for conveying intensity information (Vogt et al., 2016).

1.7 Field potentials

Field potentials like ERG, LFP and EEG can reflect the population activity of neurons in and around the recording electrode. They are changes in potentials produced at the recording electrodes by transient changes in the charges outside the neurons. These transient changes are caused by membrane currents caused by channel mechanisms involved in sensory transduction, synaptic current generation and spikes.

1.7.1 Electroretinogram (ERG)

Field potentials from the retina are called electroretinograms (ERG). It is largely produced by currents in the retina and lamina. ERG from Drosophila is well studied. By placing probing electrode (+) over the eye and ground electrode (-) electrode in the thorax, for a flash of light we can see ERG response

containing positive ON transient, negative sustained receptor potential and negative OFF transient (Pak et al., 1969). In another experiment, Hiesenberg recorded Drosophila ERG response for a flash of light by placing a probing electrode over the eye and ground electrode in the thorax. ERG shape looked the same as what we saw in Pak et al., experiment with positive ON transient, negative sustained receptor potential and negative OFF transient. When he moved the ground electrode into the basement membrane by keeping the probing electrode over the eye, ERG response had a negative monophasic wave. When he moved the probing electrode over the lamina and ground electrode into the thorax, ERG response had positive ON transient and negative OFF transient. With these observations, he concluded that negative monophasic potential is contributed by photoreceptors and positive ON & negative OFF transients were contributed by lamina currents (Heisenberg, 1971).

Several ablation and genetic studies have been carried out to find out the neurons responsible for the shape of the ERG. Though many people have thought that lamina monopolar neurons are responsible for transients (Goldsmith & Bernard, 1974; Heisenberg, 1971), it was P.E. Coombe who first tried to show experimentally that lamina monopolar neurons are responsible for transients in ERG. Using Vam (Vacuolar medulla, large monopolar neurons L1 and L2 degenerate as they age) and triple mutant rol mnb sol (3 sex-linked mutant genes, reduced optic lobes^{KS221}, mini brain and small optic lobes^{KS58}). In triple mutant, the size of the optic lobes is reduced to 8% of the WT optic lobes (great reduction in the size of medulla, lobula and lobula plate, and number of facets is reduced to ~500, lamina size is also reduced with disorganisation of retinula cells). ERG responses from Vam mutants showed a negative nonlinear relationship between lamina monopolar neurons degeneration and amplitude of the ON transients and OFF transients (Coombe, 1986). ERG response from Vam (0% degeneration) is the same as WT ERG whereas Vam (100% degeneration) ERG is monophasic without the transients. ERG response from triple mutant rol mnb sol showed reduced ON and OFF transients along with reduced sustained potential. Based on the studies on Vam and triple mutant rol mnb sol, Coombe tried to show that L1 and L2 neurons are responsible for ON,OFF transients and less large monopolar cells resulting in reduced transients respectively (Coombe, 1986).

Autrum did ablation studies on Calliphora optic lobes to show that lamina monopolar neurons are responsible for transients. Normal Calliphora ERG has larger ON and OFF transients whereas

sustained receptor potential is less negative. When he repeated the experiment with medulla ablated eyes, the shape of ERG did not affect much. When he repeated the same experiment with lamina and medulla ablated eyes, there were no transients (Autrum & Hoffmann, 1960). This confirms the Autrum hypothesis that "transients of the flies ERG are due to the lamina neurons and retina response alone is monophasic and negative".

1.7.1.1 Slow eye and Fast eye

Autrum, 1958 tried to classify insects as slow eye and fast eye based on their ERG responses. Fast eye category insects are those insects which are fast flyers and diurnals. These include flies, bees and wasps. Fast eye insects ERG contains positive ON transient, negative sustained receptor potential and negative OFF transient. Slow eye insects are those insects which are slow flying/non-flying and nocturnals. These include grasshoppers, beetles and cockroaches. Slow eye insects ERG contains monophasic negative potential without transients (Autrum & Hoffmann, 1960).

Cockroaches are classified under the slow eye category. German cockroach is a slow flyer, it's ERG is negative monophasic wave (Chang & Lee, 2001) whereas *Leucophaea maderae*, another cockroach, it's ERG contains positive ON transient, negative sustained receptor potential and negative OFF transient (Colwell & Page, 1989), which is against Autrum's classification. Chang et.al., explained that though Leucophaea maderae is a slow moving insect, it's a strong flyer. That's why ERG shape is similar to fast eye insects ERG (Chang & Lee, 2001).

Grasshoppers are classified under slow eye, according to this theory grasshopper ERG is a negative monophasic wave (Autrum & Hoffmann, 1960), 1958). Coombe and Bicker also claimed that grasshopper ERG is a negative monophasic wave without the ON and OFF transients (Coombe, 1986; Schmachtenberg & Bicker, 1999). Even in cricket (Gryllus bimaculatus) (belongs to the order orthoptera, in which grasshopper is also included), they have shown that ERG response is a negative monophasic wave without the transients (Saifullah & Tomioka, 2002).

1.7.2 Local field potentials (LFP)

Local field potentials (LFP) are similar to ERG, where a blunt electrode is placed in the region of interest in the brain instead of the eye. Oscillations in the range of 100Hz-200Hz were observed while recording LFP from the optic lobe of the blow fly by illuminating one of the eyes. Amplitude of the oscillations increased upon increasing the illumination area and/or intensity of the light (Kirschfeld, 1992). Gamma oscillations were observed in the visual cortex of the cat, which are one-third of the oscillations frequency observed in the blowfly optic lobe (Kirschfeld, 1992). In the mammalian olfactory system, 40–100 Hz oscillations were observed in the olfactory bulb and piriform cortex during an inspiration (Adrian, 1950; Freeman, 1978). In *Apis mellifera*, 30Hz oscillations were observed upon presenting odour stimuli for 1sec to the antenna while recording LFP from the calyx of the mushroom body (Stopfer et al., 1997). Laurent showed that in *Schistocerca americana* ~ 20Hz oscillations were observed while recording local field potentials from the mushroom body (Laurent & Naraghi, 1994). Stopfer (1999) showed that in Locust (*Schistocerca americana*), LFP oscillatory power around ~20Hz increased maximally from trial 1 to trial 8 while recording from mushroom body, which was unaffected upon further odour stimulation (Stopfer & Laurent, 1999). Singh and Joseph 2019 has recorded LFP from *Hieroglyphus banian* mushroom body calyx. They have observed ~25Hz oscillations, and the power of the high frequency components(15-40Hz) has increased over the trials whereas the power of the low frequency components (1-5Hz) (Singh & Joseph, 2019).

From the above discussions, it is clear that oscillations are present in different sensory systems (Delaney et al., 1994; Gelperin & Tank, 1990) and they arise in response to stimulus presentation but the function of those oscillations is still not clear.

1.8 Neuronal cell types in proximal optic lobe of an insect

In *Hieroglyphus banian*, the olfactory circuit is well studied and it has been shown that cell types through 4th order neurons are similar to that in *S. americana* . No new cell type was found in the olfactory circuit of HB. Visual systems of *S. gregaria* are reasonably well studied. So far 78 cell types with morphology and response to some subset of stimuli have been reported in locusts and closely

related species (locusts, crickets, mantis and cockroach). From the understanding of HB, olfactory studies and 78 cell types reported in locusts and closely related species in the literature we decided to find out 3rd and 4th order neuronal cell types of HB visual systems. For this, we intracellularly recorded from the cells in the proximal optic lobe and attempted filling the cell with intracellular dye after measuring the responses to a set of stimuli, including synthetic patterns, video recorded natural scenes and spatio-temporal white noise sequence.

As Drosophila visual systems are well studied, if we look into the cell types reported in the proximal optic lobe (Medulla and lobula complex), in medulla three types of cell types are reported. They are medulla intrinsic neurons, trans medulla (Tm) and TmY neurons, based on golgi staining 12, 26 and 13 distinct morphological cells reported respectively (Fischbach & Dittrich, 1989b). Advancement of genetic techniques would have added a few more cells. In lobula complex, horizontal sensitive (HS) and vertical sensitive (VS) cells are well studied (Borst, 2009; Raghu et al., 2007, 2009), lobula plate intrinsic neurons (LPi) (Mauss et al., 2015) and tangential cells of lobula and lobula plate (Otsuna & Ito, 2006).

1.9 White noise stimulus as a rescue stimulus for visual neurons

In studying electrophysiology of visual systems, one of the toughest problems is finding out the preferred stimulus of a neuron. Even the 1981 Nobel laureates Torsten N. Wiesel and David H. Hubel accidentally discovered that neurons in the visual cortex of the cat are orientation selective due to the improper placement of the glass slide which they have used to present the stimulus (Licholai, 2021). When we have no clue to what stimulus a neuron responds, presenting white noise stimulus is the best option. White noise spans a wide variety of stimulus sets, it's robust and adaptation does not occur even for multiple presentations. Using white noise stimulus analysis, one can characterise the spatial, temporal and chromatic sensitivity of a neuron.

Even to characterise the function of a neuron by identifying its spatiotemporal receptive fields using linear filter theory, scientists have calculated spike triggered average (STA) of a neuron using its response to the white noise stimuli (Chichilnisky, 2001). Receptive field is an area in the visual field

of a neuron, any change in that area will affect the response of the neuron. Based on response of the neuron, receptive fields are of two types.,

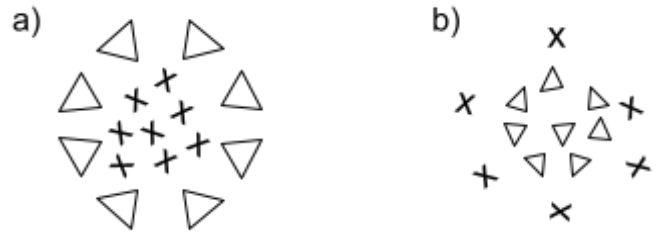

Figure 1.8: Ganglion cell receptive fields. a) ON centre-OFF surround receptive fields b) OFF centre-ON surround receptive field.

ON receptive field: If a flash of light in the receptive field of a neuron depolarises that neuron then that receptive field is called ON receptive field.

OFF receptive field: If a flash of light in the receptive field of a neuron hyperpolarizes that neuron then that receptive field is called OFF receptive field.

Kuffler by flashing ON and OFF of the small spots of the light on a light adapted cat retina showed that ganglion cells are having the ON centre and OFF surround receptive fields (Fig 1.8a) and vice versa (Fig 1.8b) (Kuffler, 1953). Areas of ON and OFF within a receptive field are mutually antagonistic. In an ON centre-OFF surround receptive field, a light spot restricted to the centre is more effective than light spreaded all over the receptive field (Barlow et al., 1957). Based on the properties of receptive fields, Hubel and Weisel classified cells in the primary visual cortex of the cat as simple cells and complex cells.

Simple cells : Narrow receptive fields with antagonistic areas (on centre-off surround or off centre-on surround). These are orientation sensitive. These cell responses can be captured by linear-nonlinear models. Convergence of the receptive fields of lateral geniculate cells aligned in space constructs the simple cells (Fig 1.9).

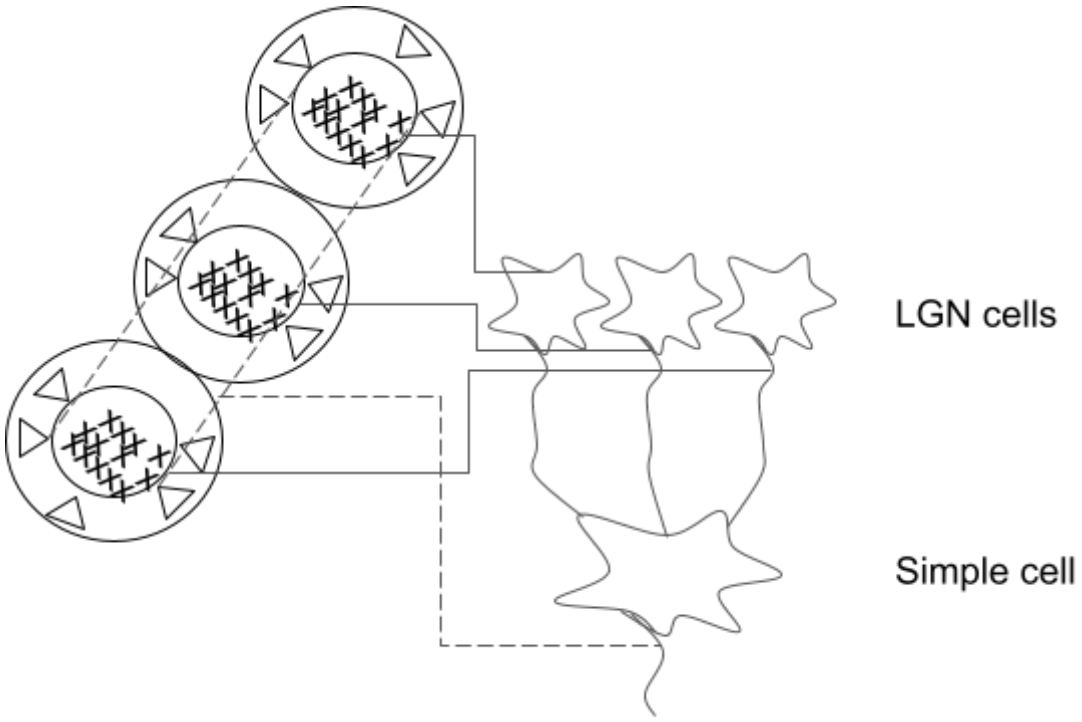

Figure 1.9: Building of the simple cell from the convergence of the receptive fields of LGN cells.

Complex cells : Broad receptive fields,orientation sensitive, show position invariance (These cells are orientation selective but irrespective of the position in the receptive field they respond). Complex cell responses can not be captured by linear-nonlinear models. They require multiple layers of computation. Convergence of the receptive fields of simple cells with similar orientation and different positions constructs the complex cells (Fig 1.10).

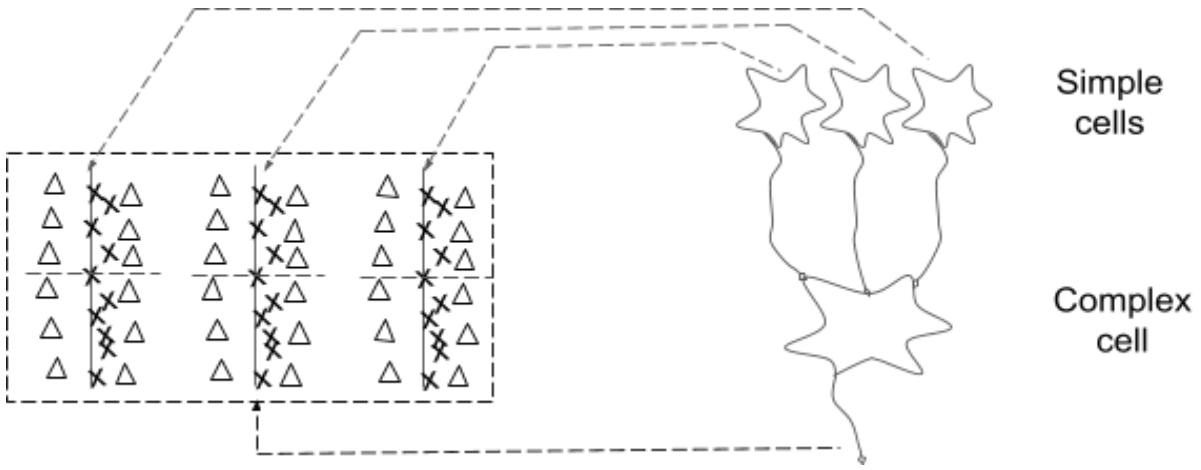

Figure 1.10: Complex cells constructed by converging the receptive fields of similarly oriented and different spatial simple cells.

Table 1.3: Simple cell vs Complex cells

	Simple cells	**Complex cells**
Receptive fields	Narrow receptive fields	Broad receptive fields
Orientation	Orientation sensitive	Orientation sensitive
Position invariance	No	Yes
Construction	By converging the LGN receptive fields aligned in space.	By converging the similarly oriented simple cell's receptive fields varied in position.
Modelling	These cells response can be captured by simple linear-nonlinear modelling	To capture the response of these cells requires multiple layers of higher computation.

It is clear from the above discussion that simple cell responses can be captured by linear-nonlinear modelling. Linear-nonlinear modelling can be performed as follows. Firstly, spike triggered average (STA) is calculated (Fig 1.11a). STA is the sum of all the frames of the stimulus that preceded each spike divided by the total number of spikes. Then the stimulus vector is passed through the linear filter obtained from STA to get the generator signal (ω.s). Non-linear function over this signal generator gives the spike rate R(s) (Fig 1.11b).

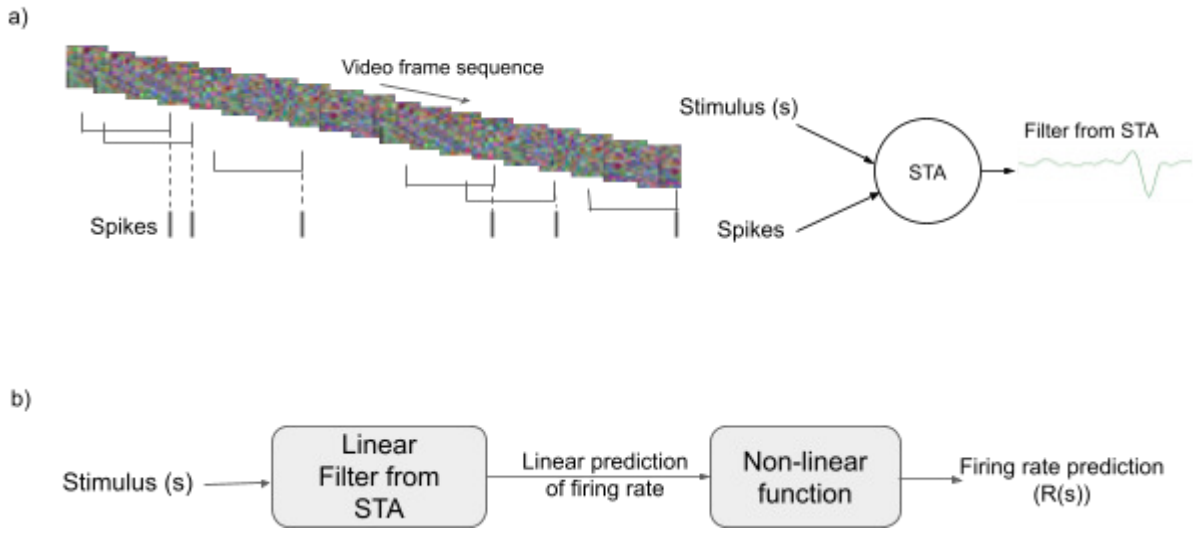

Figure 1.11: Linear-nonlinear modelling flowchart. a) Calculation of STA. b) Firing rate prediction.

Objectives of the study:

1.10 Principal objectives of the research

- To characterise the gross anatomy of the grasshopper *Hieroglyphus banian* optic lobe and major visual processing regions of the brain in terms of neuropils and their connectivity.
- To identify the physiological properties of the eye and major visual processing regions of the brain by performing ERG and LFP recordings.
- To characterise the anatomy and response properties of the neurons recorded from the proximal optic lobe.
- Nature of models that capture the response properties of the cell types in the proximal optic lobe using white noise analysis.

1.11 Layout of the thesis

Chapter 2 deals with the materials and methods used in this study.

Chapter 3 presents the grass anatomy of *Hieroglyphus banian* optic lobe, other major neuropils involved in vision innervated from optic lobe.

Chapter 4 presents the nature of the field potentials along the visual pathway and insights into the mechanism of their generation.

Chapter 5 presents the response properties and classification of the responses of the intracellularly recorded and filled neurons and compares the relationship to morphology.

Chapter 6 presents the nature of linear models that capture the response properties of the cell types in the proximal optic lobe.

Chapter 7 presents the summary.

Chapter 2

Materials and methods :

2.1 Animals

Both the sexs of adult Hieroglyphus banian (Fig 2.1), commonly called rice grasshopper, were used in experiments. Culture is maintained at Centre for Neural and Cognitive Sciences, University of Hyderabad, Hyderabad. Culture room relative humidity and temperature is maintained at 70% and 29℃ respectively and 300 watt bulbs were used to maintain light/dark cycle for14h/10h daily throughout the year. During winter/rainy season a room heater is switched on and during summer window AC is switched on to maintain temperature. And wet mats are used to maintain humidity in the room whenever required.

Nymphs of *Hieroglyphus banian* and the unknown grasshopper nymph were caught in the wild. House fly (*Musca domestica*) caught in the wild, and *Drosophila melanogaster* of the Canton-s strain provided by Sudipta Saraswati lab were used for electroretinogram experiments.

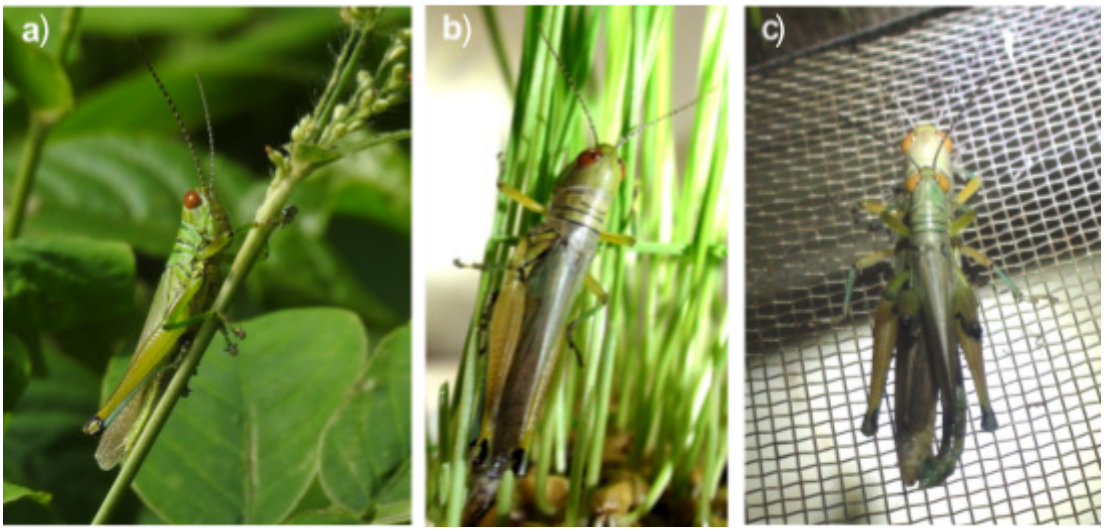

Figure 2.1: *Hieroglyphus banian* (rice grasshopper) a). Male b). Female c). Mating of adult HB male and female.

2.2 Animal preparation for the experiment

Grasshopper legs are cut and left whole night for avoiding hemolymph leakage.The following day grasshopper was placed on to a holder (Used disposable plastic cuvettes were cut in such a way to hold the grasshopper) and taped. A hard plastic sheet attached to the petri dish using epoxy/super glue

and modelling clay was used to adjust the platform. Then the grasshopper is mounted onto the platform in such a way that the head is put onto the platform and the whole animal is pulled gently to lift the head for a proper dissection. After mounting the animal, a wax cup is made around the animal head to hold the saline. The wax cup was such that the left eye of the animal was clear of the saline and viewed the screen at the desired angle. Both the antennae were fixed in wax to avoid the unnecessary movement during dissection and experiment (Fig 2.2). Small incisions made to the cuticle using hand made axes (razor blades are cut into small pieces and fixed onto the toothpick using epoxy). With the help of forceps and micro scissors cuticles are removed to access the brain. Then the fat bodies and trachea are removed, and below the brain muscles attached to the brain are also removed. Then metallic wire is used as a platform to lift the brain a little bit and is pushed from the dorsal side of the head. Once the brain is elevated appropriately, the platform is fixed in wax.After that saline from the wax cup is removed and protease is applied onto the brain and left like that for a minute or two washed off with saline. Using superfine forceps, the protein sheath is removed gently. Then a perfusion tube is attached and kept for continuous perfusion of saline and now the animal is ready for the recording or dye injection.

For the electroretinogram of the adult HB, the animal is prepared the same as above. Where as the grasshopper nymphs, Drosophila and house fly were anaesthetised and fixed onto the gum applied onto the platform (dental wax is fixed onto the 2cm X 1cm rectangular plastic sheet and a thick white paper fixed onto the dental wax, on the paper thin layer of gum is applied) in such a way that eye is faced towards the screen. Animals fixed onto the gum firmly.

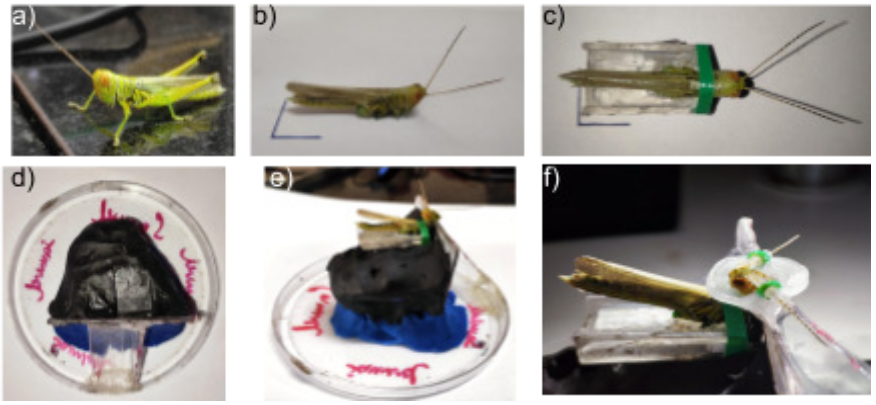

Figure 2.2: Animal preparation. a). Adult male grasshopper. b). Grasshopper legs cut and left overnight. c). Grasshopper wings are scissored and the animal is restrained onto a plastic holder with the help of insulating tape. d-e). Further the animal is mounted onto a dissection platform (clay fixed onto the petri plate). f). Wax cup made around the head of the grasshopper to hold the saline and antennae is tethered to avoid unnecessary movement.

2.3 Ommatidia Counting

Animals are restrained on the platform using adhesive tape and place on moldable clay. Then a layer of nail polish is applied over the eyes and left to dry for 30 min - 1 hour. Once the cast is dried, it is peeled off from the eye carefully and small cuts were made to spread the cast flat on the glass slide. A cover slip is placed on top of the cast and attached with scotch tape. The slide is taken under the Eclipse FN1 Nickon microscope and photographs of the whole cast were taken under 10X using R1 Retiga camera with overlapping regions. Once the photographs were taken, overlapping regions were used to merge the photographs in ImageJ using the pairwise stitching plugin tool. Once the eye cast is recreated (Fig 2.3a), 'multipoint tool' of ImageJ is used to count the number of ommatidia (Fig 2.3b).

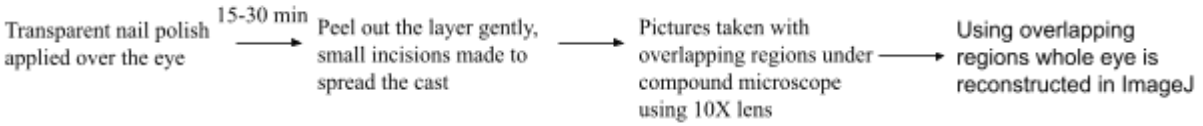

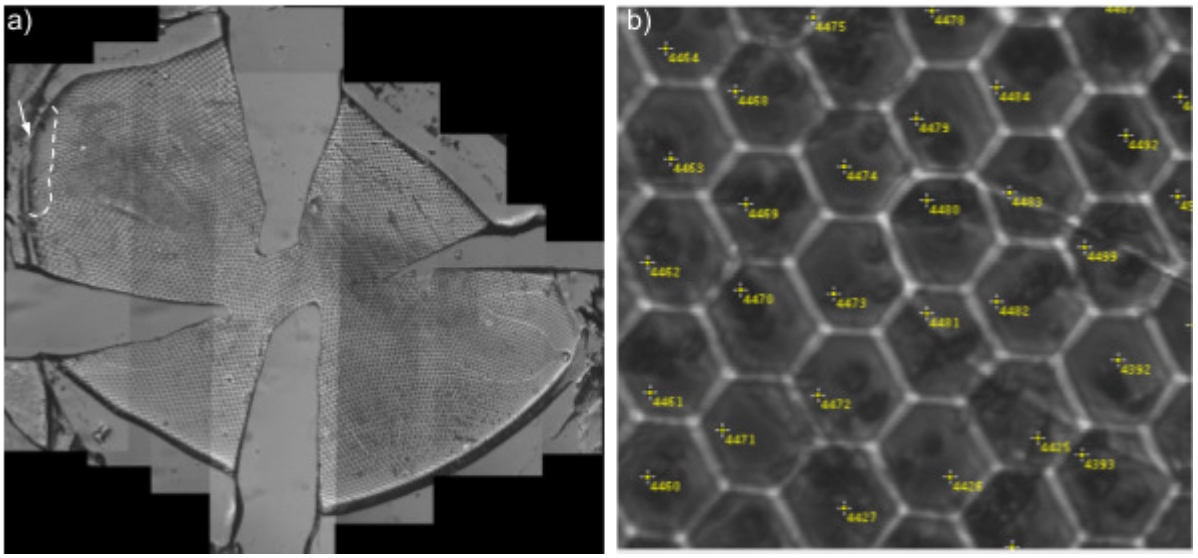

Figure 2.3: Ommatidia counting. a). Replica of an eye casted using nailpolish. White arrow indicates the dorsal rim area (DRA) of the eye. White dashed lines denote the demarcation of the DRA from the rest of the ommatidia. b). Ommatidia counting using multipoint tool in ImageJ.

2.4 Intracellular recording

In our experiments we did blind intracellular recordings. We don't know which neuron we are recording but we targeted a particular region of the brain. Borosilicate sharp electrodes (filamented,10cm in length, inner and outer diameter are 0.5mm and 1mm respectively, catalog no BF-100-50-10, Sutter Instrument, Novato, CA, USA)pulled using a horizontal electrode puller (P-97,Sutter instrument Co., Novato, CA, USA). Electrodes were filled with 200 mM KCl and had an

impedance 80 MΩ - 150 MΩ. Prior to filling with KCl, the electrode tail end is dipped in one of the intracellular dyes (2% Neurobiotin, SP-1120,Vector labs; Alexa Flour™ 633 Hydrazide (Invitrogen, A30634) / Alexa Fluor™ 568 Hydrazide (Invitrogen, A10437) made in 200mM KCl solution, dye gets filled in the sharp end through the capillary action. Chlorided silver wire was used as a ground electrode. The recordings were carried out using (Axoclamp 900A, Molecular Devices). Signals were amplified 100 times low pass Bassel filtered at 4kHz. Data was acquired on Digidata 1440A, Molecular Devices at a sampling rate of 10kHz controlled Clampex 10.3 interface software. Blind recording of the neuron is performed by positioning the electrode at the interested region of the brain using micromanipulators (MP-225, Sutter Instruments). After placing the electrode at a region of interest, the electrode was moved only in the z-axis through fine movement and current buzz is given until we see a cell is impaled which can be observed when membrane potential goes negative. After getting a cell, if it is unstable, a small negative current is sometimes injected to hold the cell. Once the cell is stable, intracellular recordings were performed while presenting the visual stimulus. After the completion of intracellular recording, cells were filled with either of the intracellular dyes iontophoretically by injecting 1-4nA current at 2Hz pulse for 30-45minutes. Positive currents for neurobiotin and negative current for hydrazide dyes. After dye injection the animal is perfused with saline for 2-4hours then the brain is dissected out and fixed in 4% PFA.

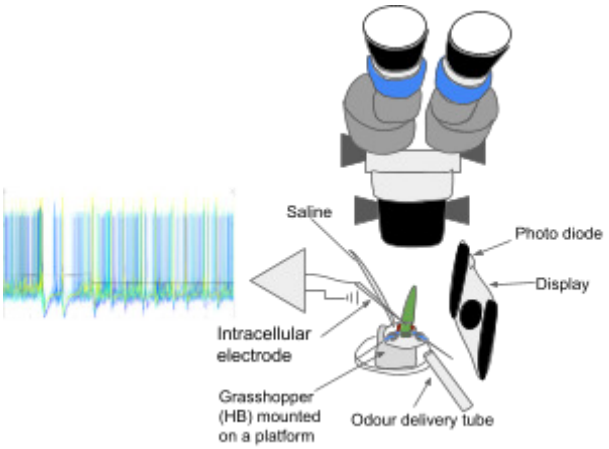

Figure 2.4: Schematic of the intracellular recording setup.

2.5 Extracellular field potential recording

Also called blunt electrode recordings. Custom made borosilicate glass electrodes were pulled using an electrode puller (P-97,Sutter Instrument Co., Novato, CA, USA). Electrodes having 1-10MΩ were used in extracellular recordings, electrodes were filled with ringer's saline instead of KCl which is used in intracellular recordings. Extracellular signals were amplified by a factor of 100X-1000X times based on the signal strength. Then the signal was Bandpass filtered between 0.1-80 Hz and digitised by a digitizer (Digidata 1440A) with a sampling frequency of 10000 Hz.

2.5.1 Electroretinogram (ERG)

ERG is an extracellular technique, where a ground electrode is placed either in saline or in the body of the animal and the reference electrode is placed over the eye. ERG recorded while presenting red,blue, green, white, less bright white and least bright white colours on a mobile screen.

2..5.2 Local field potentials (LFP)

LFP is another extracellular technique where we place a reference electrode at an interested region of the brain and measure the potential difference with respect to the ground electrode, which is similar to the ERG.

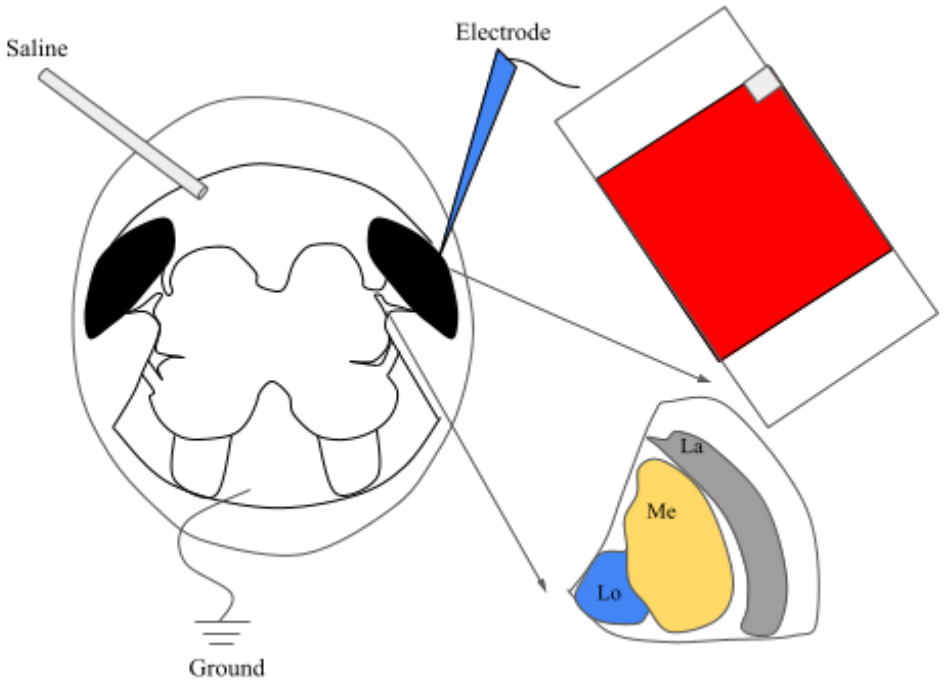

Figure 2.5: Schematic of the *Hieroglyphus banian* ERG recording procedure.

2.6 Neuronal tract tracing through bulk filling

To find out the major connectome of the brain dyes like dextran biotin (DB;D7135, Invitrogen), dextran tetramethylrhodamine (DTMR;D3308,Invitrogen), dextran 488(), dextran texas red () were used. Either of the dye is placed at a particular region of the brain using sharp electrodes/ toothpicks/ forceps. After placing the dye, the brain is washed with saline to avoid dye distribution all over the brain externally. After placing the dye, the animal is perfused with saline for 12-14 hours, then the brain is dissected out and fixed in 4% PFA.

2.7 Immunohistochemistry

For fixation brains were put in 4% PFA for 4-6 hours. Then washed in 1X PBS thrice for 20 minutes each. The brains which wer e injected with dextran biotin, neurobiotin, which require conjugated fluorescent molecules were kept in 0.5 ml 1XPBST for one hour for permeabilization. Then avidin 488/633 were added in the ratio of 1:1000 and incubated for 4-5days with intermittent mixing. After that, brains were washed in 1XPBST for thrice , 20 minutes each wash. Then washed in 1X PBS for thrice, 20 minutes each. For brains which are injected with dextran 488,TMR,Texas red and hydrazide dyes which do not require any fluorescent conjugate were washed with 1X PBS. Then all the tissues (brains which require fluorescent conjugate and brains which do not require fluorescent conjugate) were dehydrated in ascending alcohol series (30%, 50%, 70%, 80%, 90% and 100%). Then brains are cleared in methyl salicylate and mounted on a cavity slides.

2.8 Anti-GABA and nc82 staining

To find out the major neuropils and GABA positive cells, PBS washed and PBST permeabilized brains were incubated with presynaptic marker nc82 (monoclonal antibody against bruchpilot which is an active zone (AZ) protein homologous to human active zone protein ELKS/CAST) raised in mice and anti-GABA raised in rabbit, respectively in 1:1000 proportion for five days with intermittent mixing.After five days incubated brains were washed with PBST and PBS thrice in each solution for 20. Then again permeabilized with) 0.5ml PBST for an hour and incubated with either of the (633/488) anti-mouse for nc82 and (633/488) anti-rabbit secondary antibody for anti-GABA for 5 more days with intermittent mixing. After the incubation washing,clearing and mounting is performed same as described in above procedure.

2.9 Confocal microscopy

Both intracellularly filled brains and bulk tracing brains were scanned using confocal laser scanning microscopy (Leica TCS SP8 STED) with an objective of 10X, with a resolution of 1024 X 1024 pixels, speed 400Hz and the line average of 4 was used with step size of 1.14. Bidirectional scanning was used for faster scanning.Excitation wavelengths of the lasers used were 633or 561 or 488. Gain and intensity were changed manually based on the requirement. After the scanning images were analysed using Fiji ImageJ 1.47v (National institute of health, Bethesada,MD) (Scheindelin et al. 2012). All the images were presented as it is, combining a few optical sections along the z-axis, modified only for brightness and intensity changes.

2.10 Stimulus presentation

The synthetic stimuli, loom in, loom out , gratings and white noise for the video were created in matlab. The natural stimuli recorded using a video camera and images were also read in matlab and a single video file was created and used. The video was
Written at 60fps.

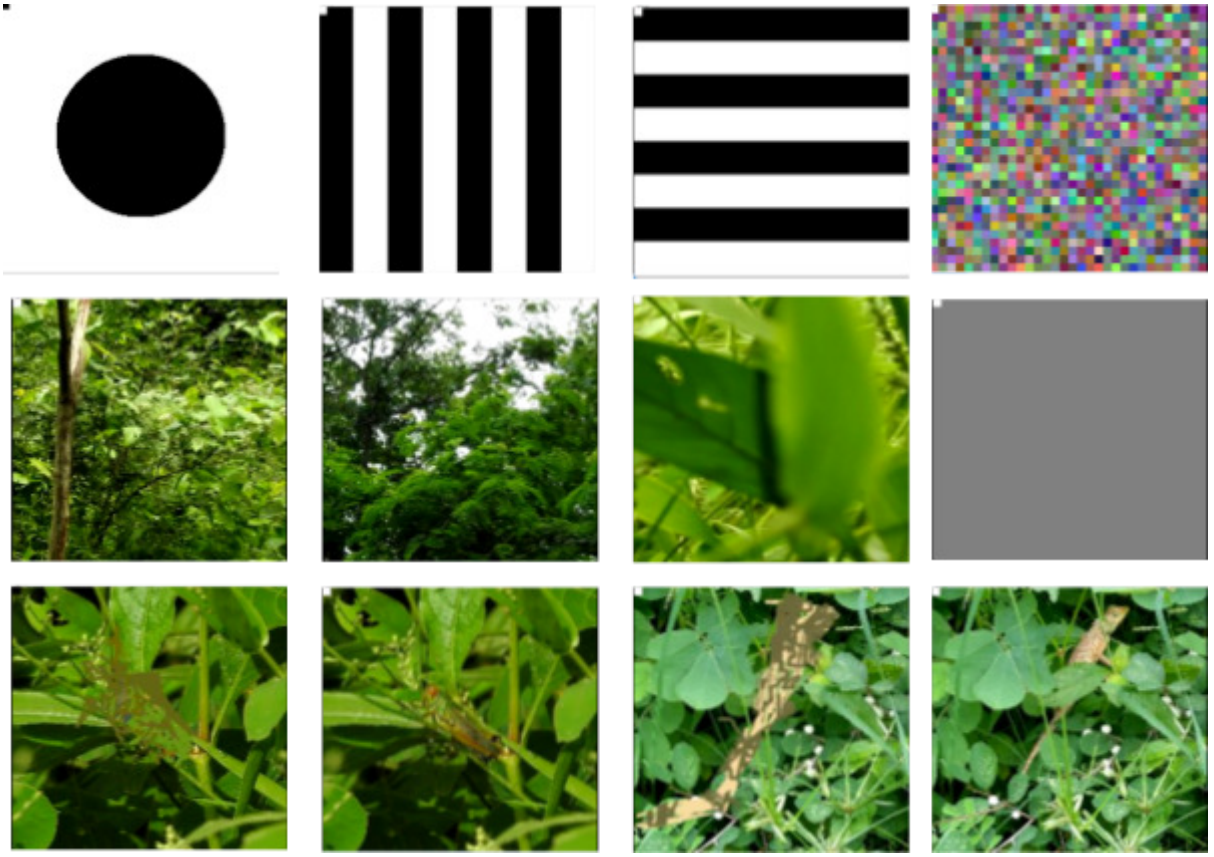

Figure 2.6: Few frames of visual stimulus video presented through mobile screen (white or black square appearing on top left corner of the frame is where the photodiode is placed).

All the synthetic stimuli used 8 bit representation. The grating stimuli have average pixel brightness of 127.5 and they were preceded by uniform grey background of 127.5. All the grating stimuli had an initial stationary phase and then a moving phase. The white noise was 32x32 square matrix with each element having R, G and B values chosen as random numbers ranging from 0 to 255. The white noise changed every other frame making it have a presentation rate of 30fps (Fig 2.6). The white noise stimuli lasted for 39 sec (1170 distinct frames) of which 90% is used to construct STA and 10% for testing how good the prediction by STA. The white noise duration was less than ideal, restricted by the duration for which we could record intracellularly and fill dyes.

2.11 Data analysis

Data is analysed using a custom made programme written in Matlab. The coding sequence in the video at the photodiode location was resampled in time to match the sampling rate of the recorded signals (10kHz). The correlation between the photodiode signal and the coding sequence was calculated to find the shift at which the recorded signals, intracellular signal and photodiode signal, can align in time with the video. This is done for every trial and intracellular data is aligned accordingly.

2.11.1 Peri stimulus time histogram (PSTH)

Spikes were detected in the intracellular traces by thresholding the waveform that was bandpass filtered between 100 and 1000 Hz. Detection was verified for each trial visually and by checking the ISI histogram. The spikes from all the trials were collected and PSTH was computed with a bin size of 1/60 seconds.

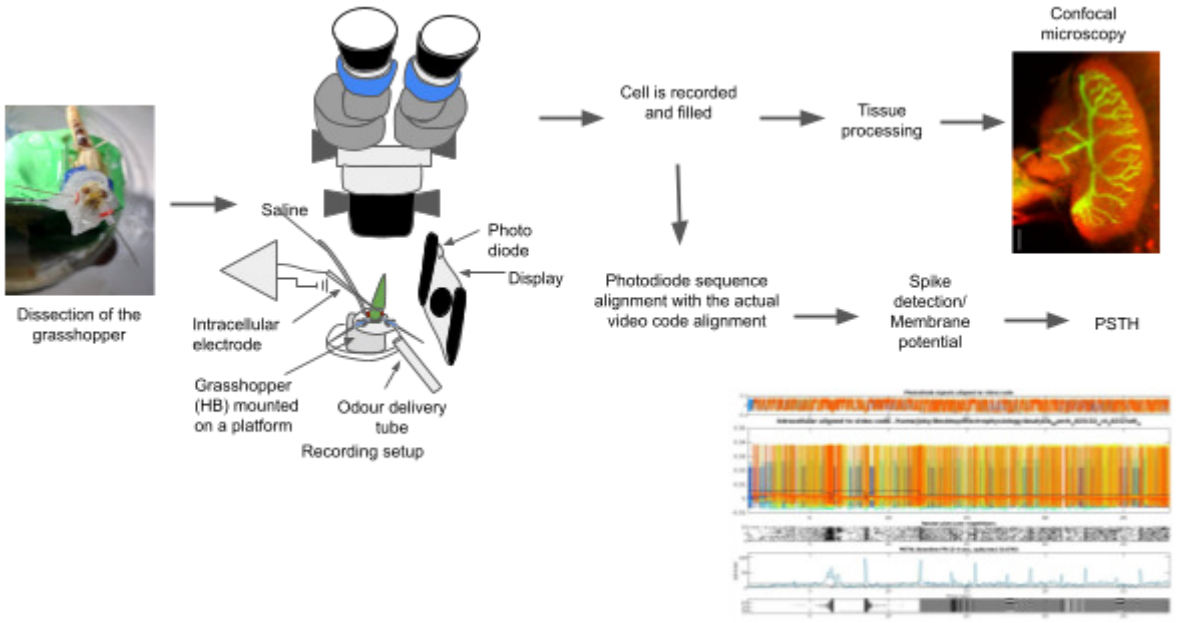

Figure 2.7: Schematic of the whole experimental procedure of intracellular recording, filling the recorded cell, imaging under confocal microscope and analysing the intracellular data to find out the PSTH.

2.11.2 Hierarchical classification tree

Hierarchical clustering was carried out using linkage function in matlab with euclidean metric.

2.11.3 Comparing euclidean distance matrices

Euclidean distance matrices were created by taking pairwise distances between the response of each of the cells. The two matrices were created for the synthetic and natural stimuli. The correlation coefficient between the upper triangle elements of the two matrices was calculated as the true value. The upper triangle of these matrices were compared by shuffling one of the matrices and finding the probability of getting the correlation coefficient to be the true value or greater by chance.

2.11.4 K-means clustering based classification

The vectors of PSTH for the stimuli for each of the stimulus set were stacked together to form a matrix. Svd was computed and based on the knee in the scree plot three components were used to reduce the dimension of the data. K-means clustering was performed on this and visualised as a 3D scatter plot to see the neighbourhood relationships of the cell specific responses.

Chapter 3

Gross anatomy and physiology of the visual processing centres of *Hieroglyphus banian*

"When brains of different species share common arrangements of centres, this indicates their phyletic relatedness whereas differences of brain organisation reveal divergence"

- Nils Holmgren and Bertil Hanstrom

3.1 Introduction

Visual systems across different organisms exhibit similarity in structure and function either by convergent evolution or conservation of traits. Visual sensory system first appeared in marine arthropods (Trilobites) around 541 mya during the early Cambrian era (Martinsson, 1975; Clarkson et al., 2006;Honkanen et al., 2019). Although as we go higher in the taxonomy category, complexity of the brain and the complexity of the visual processing increases, visual systems of insects have been used to understand the principles of visual information processing. Various theories of components of visual processing have been tested on insect systems (Haag et al., 2017; Honkanen et al., 2019; Turner-Evans et al., 2020; Dombrovski et al., 2023).

Most organisms, ranging from insects to higher vertebrates like birds and mammals, have to process visual information and often store it to sustain their life. These visual information include shape and form, colour, motion, depth and polarisation often involving delineable pathways and processing centres. To understand how insects process visual information, first we should understand what are the major neuropiles and the connectivity between them (Sanes and Zipursky, 2010; Joly et al., 2016). Many insects in the order Diptera, Orthoptera, Lepidoptera and Hymenoptera have been well studied to understand their vision (Bausenwein et al., 1992; Fischbach and Dittrich, 1989; Homberg et al., 2003; Heinze and Reppert, 2012; Habenstein et al., 2020).

Insects have compound eyes and compound eyes of all the arthropods have the following functional components, a lens and a crystalline cone that collects and focuses light onto the ciliated parts of the retinula cells. Based on optical properties of the eye, at least seven types of compound eyes have been described. A number of retinula cells forms a circular arrangement with the ciliated structures in the centre into a light guide structure called rhabdome. The light coming from the crystalline cone is guided over the celia by the rhabdomere. Each of the lenses looks at a distinct cone of space and light transduced by a rhabdomere is determined by which all crystalline cones focus the light on to that rhabdome. One such processing element centred around a rhabdome is called an ommatidia and each ommatidia is optically isolated from the others around it by pigmented cells (Nilsson, 1989).

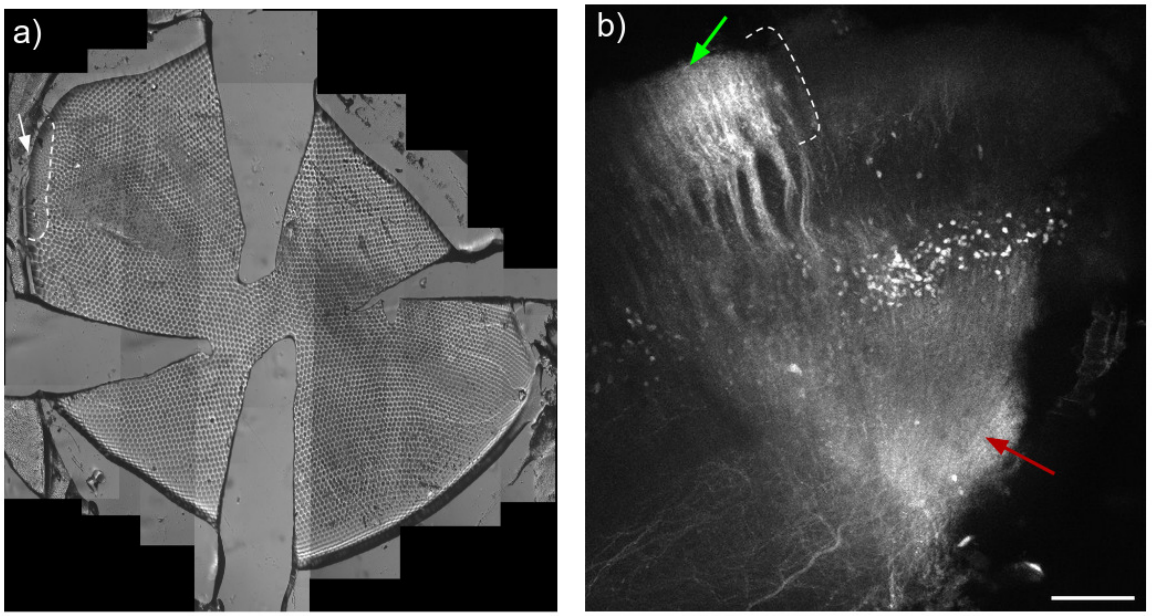

Figure 3.1: a) Replica of an eye casted using nailpolish. White arrow indicates the dorsal rim area (DRA) of the eye. White dashed lines denote the demarcation of the DRA from the rest of the ommatidia. b) Dextran conjugated dye injection in medulla (red arrow) filled lamina neurons (green arrow) and the dashed bracket indicates the layer forming the lamina. Scale: 100µm.

Lamina and medulla are distinct neuropils having layered structure, conserved across different insects. Lamina receives input from the receptor neurons in the retina, and medulla receives input from both retina and lamina. The number of layers of lamina and medulla differ across species evidenced by staining for different markers (Gokan and Meyer-Rochow, 1990; Heinze and Reppert, 2012; Rosner et al., 2017). There is a chiasma that crosses over, between lamina and medulla (Fischbach and Dittrich,

1989; Rosner et al., 2017). Lobula complex is the proximal most structure in the optic lobe. In Diptera and other orders there is a chiasma between the medulla and some of the lobula neuropils (Fischbach and Dittrich, 1989; Rosner et al., 2017).

The structure of lobula complex differs vastly from species to species, in the number of neuropils and their arrangement. Lobula is made up of a single neuropil in bees (Gowda and Gronenberg, 2019) and ants (Habenstein et al., 2020), two neuropils lobula and lobula plate in flies (Fischbach and Dittrich, 1989), butterflies (Heinze and Reppert, 2012) and in dung beetles (Gokan and Meyer-Rochow, 1990). Lobula complex in the locust (Ito et al., 2014), mantis and cockroach (Rosner et al., 2017) have multiple neuropils. The identifiable neuropils are outer lobula, inner lobula and multiple sub-neuropils, anterior lobula and dorsal lobula. Tracts from the optic lobe terminate in various centres in the protocerebrum, namely the optic tubercles and accessory lobe of the central complex that are by and large conserved in the insects (Homberg et al., 2003; Mota et al., 2011).

In this work, we characterise the visual system of *Hieroglyphus banian* (a grasshopper endemic to south Asia) in terms of the major neuropiles and the connections between them. We identify all the major reported neuropils of the optic lobe, anterior optic tubercle (AOTu), posterior optic tubercle (POTu) and lateral accessory lobe (LAL) by tract tracing and immunohistochemistry and thus show that these are similar to locust species (Table 3.1). We identify two new centres receiving inputs from the optic lobe.

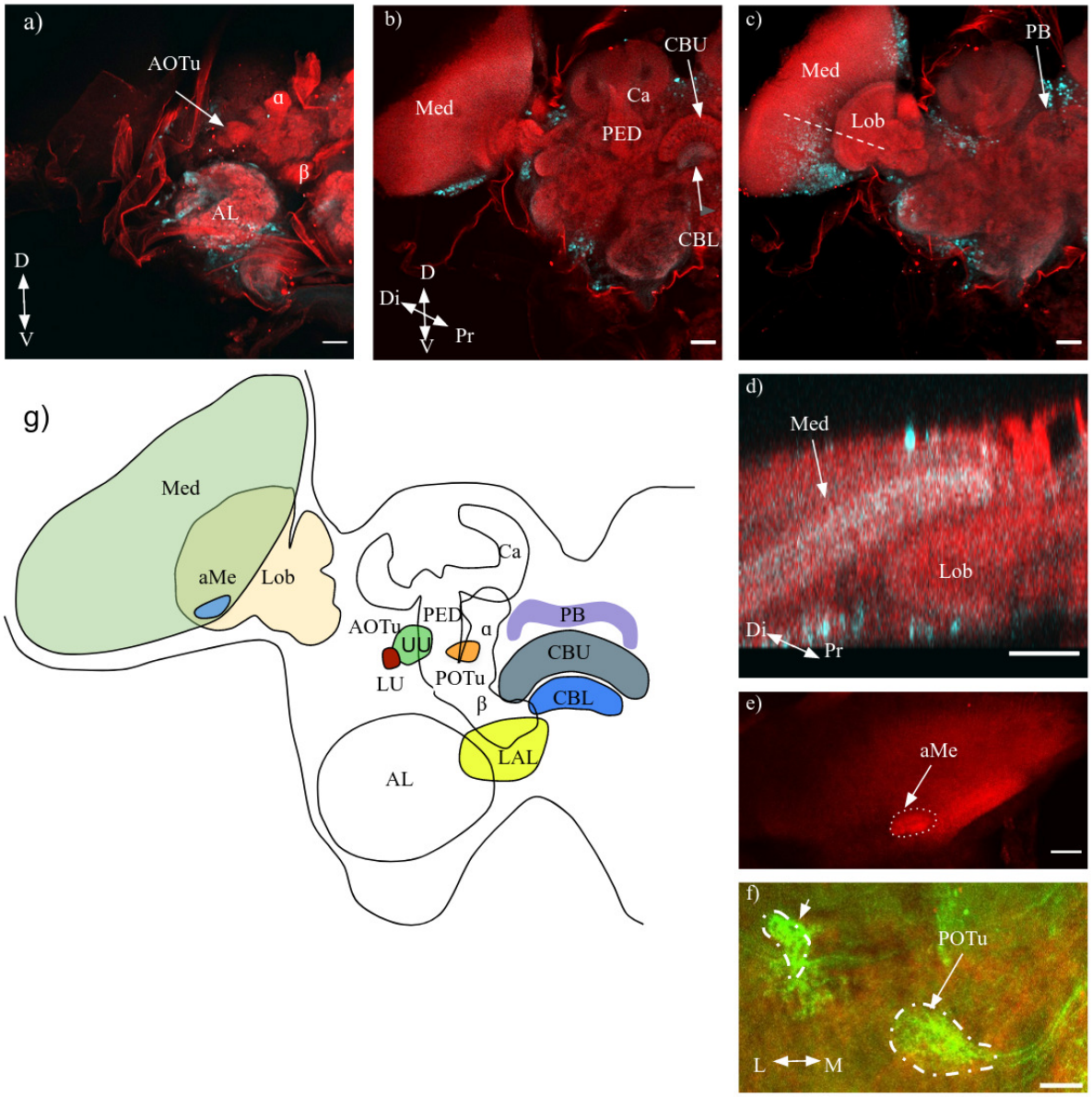

Figure 3.2: Schematic of the *Hieroglyphus banian* brain based on nc82 (red), anti-GABA (cyan) immunohistochemistry and tract tracing (green). a) Section depicting AOTu upper (AOTu-UU) and lower units (AOTu-LU) relative to alpha and beta lobes of mushroom bodies and antennal lobe (AL). b) Section depicting Calyx (Ca), peduncle (PED) of the mushroom body, upper (CBU) and lower (CBL) divisions of the central body and medulla (Med) of the optic lobe. c) Section depicting Medulla (Med) and Lobula (Lob) of the optic lobe and protocerebral bridge (PB) of the central complex. d) Cross section through the plane represented by a dashed line in (c) showing medulla (Med) and lobula (Lob) of the optic lobe. e) nc82 stained section of another animal showing accessory medulla (aMe). f) Stack showing POTu and a novel structure (arrow head) (nc82-red; Dextran-green) filled by dextran tracing from aMe from a different animal. g) Schematic of the *Hieroglyphus banian* brain based on nc82 and anti-GABA staining. Scale bars : 100µm (a-d), 50µm (e-f) Di and Pr represent distal and proximal respectively.

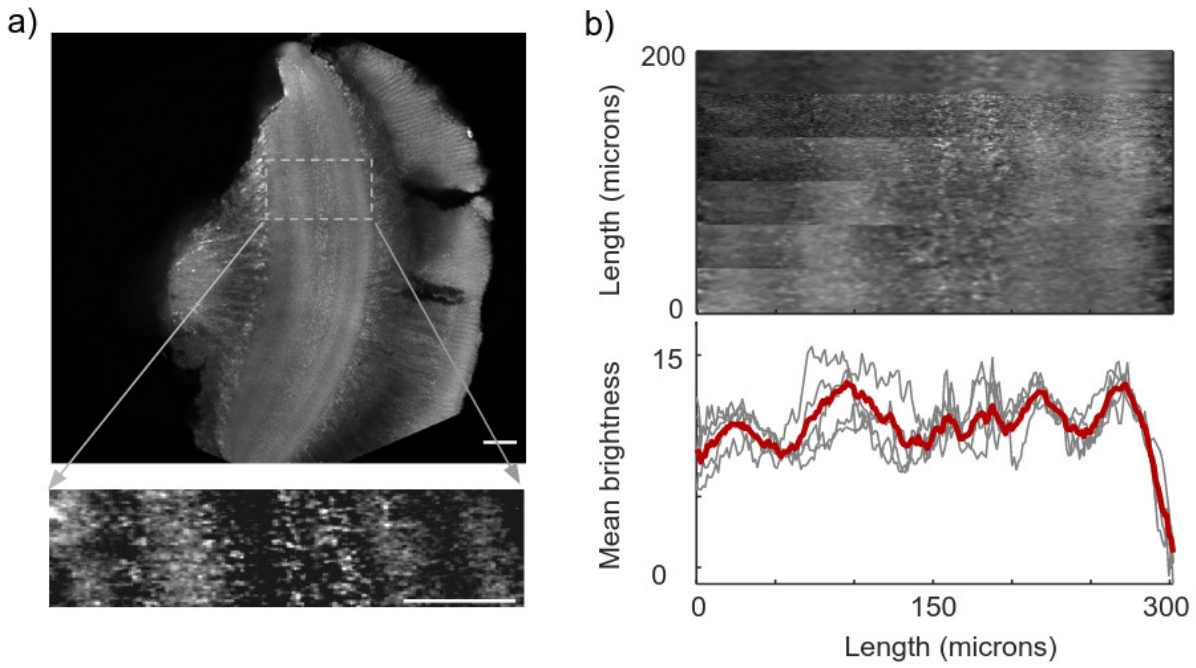

Figure 3.3: Identifying medulla layers based on brightness changes in an autofluorescence image. **a)** Section of a Medulla from autofluorescence image of the optic lobe and a zoomed view of a small section. Scale: 100 µm. **b)** Six ROI's selected from the medulla of figure (a) and scaled them to the same number of pixels horizontally and stacked on top of each other (top). Mean of each ROI was taken along the dorsal to ventral axis for each ROI to obtain the intensities (grey in the upper plot), mean of the six ROIs (red).

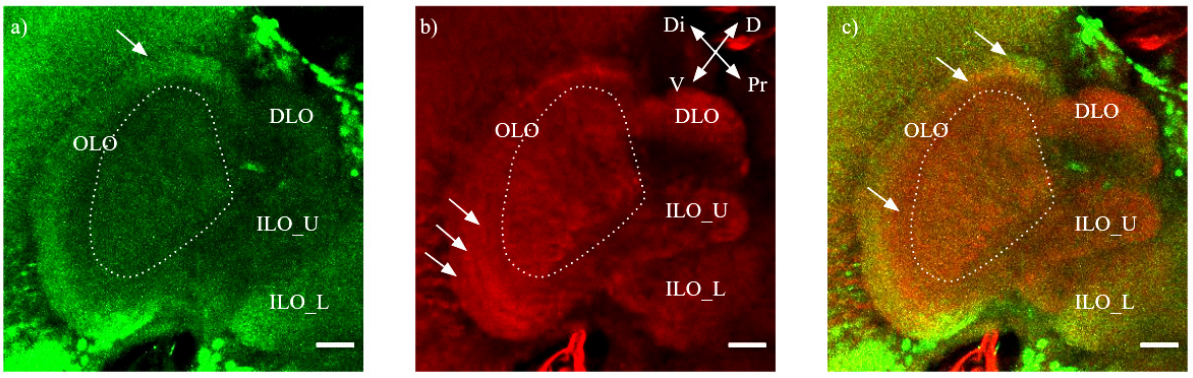

Figure 3.4: Lobula complex of the *H. banian* Optic lobe **a)** Anti-GABA staining of the lobula complex of the *H. banian* optic lobe. **b)** nc82 staining of the lobula complex of the *H. banian* optic lobe. **c)** Merged image of anti-GABA and nc82 staining of the lobula complex of the *H. banian* optic lobe. Scale : 50µm (a-c)

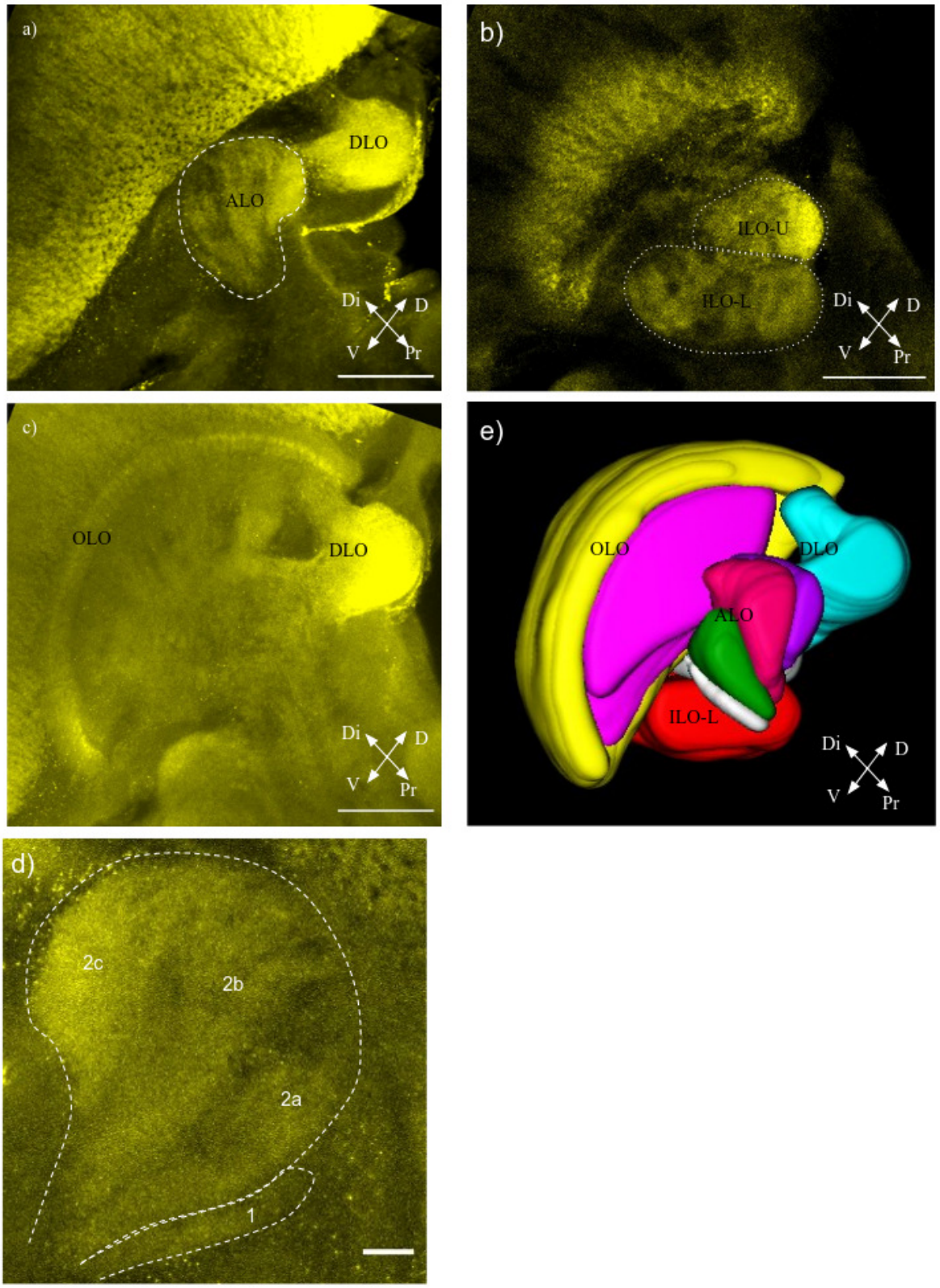

Figure 3.5: Reconstruction of lobula complex based on nc82 immuno-histochemistry. **a)** Section showing dorsal (DLO), anterior (ALO) parts of the lobula complex. **b)** Section showing upper and lower units of the inner lobula (ILO). **c)** Section showing dorsal(DLO) and outer (OLO) lobula. **d)** Section showing sub-compartments of the anterior lobula. **e)** Reconstruction of the lobula complex drawn based on nc82 staining. Scale bars : 100µm (a-c), 20µm (d).

3.2 Results

3.2.1 Number of Ommatidia

Image of the whole cast of the eye (Fig 3.1) was used to count the number of the ommatidia using a multi point tool in ImageJ. We have counted a total of 8 animals (4 Males + 4 Females). In females, ommatidia number varied from 5679 to 8277 including the ommatidia in dorsal rim area (DRA) which had approximately 210 of them. In males, the ommatidia number varied from 5248 to 6880 including the 177 ommatidia in the dorsal rim area. In both males and females, the size of the ommatidia in the dorsal rim area is much smaller than the ommatidia in the other part of the eye. It was not the case that the larger animals necessarily had more number of ommatidia because in our set, larger animals (Male: 5248; Females: 5679 ommatidia) had less number of ommatidia than smaller animals (Male: 6560; Female: 7054 ommatidia).

3.2.2 Major neuropiles visualised by immunostaining with nc82 and anti-GABA antibodies

Immunohistochemistry with nc82 (against bruchpilot) revealed major neuropiles of the brain and the partitions in the visual pathway. nc82 positive Presynaptic marker could distinguish synaptic densities associated with optic lobes, lateral horn, mushroom bodies, central complex, lateral accessory lobes, anterior optic tubercles, posterior optic tubercles and antennal lobes. Immunohistochemistry with anti-GABA revealed inhibitory neuron cell clusters and regions of dense arborizations. Stronger GABA positivity in some of the subcompartments visualised via nc82 pointed to synaptic regions with strong GABAergic interactions. The differential density of staining was used to visualise compartments of optic lobe, lamina, medulla and lobula complex. Lobula complex could be further compartmentalised into outer lobula (OLO), inner lobula (ILO), anterior lobula (ALO) and dorsal lobula (DLO). OLO has four layers, 1st layer of the OLO is highly GABA positive and 2nd layer has almost no GABA staining. Third and 4th layers are GABA positive. Fourth layer is a triangular structure (maximal extension of 250µm) where LGMD branch B is innervated (Fig 3.8b). All the four

layers of outer lobula are clearly visible in nc82 staining (Fig 3.4). Anterior lobula (ALO), upper and lower units of the inner lobula (ILO) and dorsal lobula (DLO) are GABA positive. A central complex consisting of the protocerebral bridge (PB), central body upper (CBU) and lower (CBL) are visible in the nc82 immunoreactivity. CBL is more reactive to anti-GABA than PB and CBU. Anterior optic tubercle contains upper (AOTu-UU) and lower units (AOTu-LU). Upper unit is further divided into the outer (AOTu-UU-OL) and inner lobe (AOTu-UU-IL), both are highly reactive for nc82 (Fig 3.2a).

3.2.3 Optic lobe of the *H. banian*

H. banian optic lobe is further compartmentalised into lamina, medulla and lobula from distal to proximal end.

Lamina: Lamina is a single layered structure, containing multiple columnar structures called cartridges (Fig 3.1b).

Medulla: Autofluorescence image of the optic lobe scanned using laser 488 (Fig 3.3a) is used to calculate the number of layers in medulla based on pixel intensity of the scanned image. Six ROIs from the medulla were chosen at different locations along the dorso-ventral axis (proximal end left and distal right in each ROI) that is approximately 300u wide and 45 pixels vertically. They were all scaled to the same number of pixels along the lateromedial axis. Then they are stacked along the dorsoventral axis as shown in (Fig 3.3b top). Mean of each ROI, shown in red (Fig 3.3b bottom), was taken along the dorsal-ventral axis for each ROI to obtain the intensities shown in grey. Both the crest and through of the mean plot are considered as the presence of a layer to calculate the number of layers of medulla to reveal 11 layers .

Accessory medulla is clearly visible as an anterior structure at the proximal medulla, visible in the nc82 staining (Fig 3.2e) and in the tract tracing from medulla as well (Fig 3.5f).

3.2.4 Lobula complex

Based on the nc82 and anti-GABA staining (Fig 3.4), lobula is compartmentalised into outer lobula (OLO) (Fig 3.4 and Fig 3.5c), inner lobula (ILO) (Fig 3.5b), anterior lobula (ALO) (Fig 3.5d) and dorsal lobula (DLO) (Fig 3.5a,c and Fig 3.4). Outer lobula has four layers (Fig 3.4). The 1st layer of the OLO is highly GABA positive, similar to that of the 1st layer OLO of *Schistocerca gregaria* and the 2nd layer of the OLO is highly nc82 positive. The arborisation pattern of individual neurons also supports this anatomical and functional segmentation of the lobla complex. Here, we present two neurons arborising in distinct regions of the lobula to show segmentation of the lobula complex in grasshoppers (Fig 3.8). In Fig 3.8a-c, showing LGMD type 1 branches A, B and C innervation into the 2nd layer of OLO, 4th layer of OLO and DLO respectively. Fig 3.8d, shows another neuron (putatively LGMD type 2) with innervation into the 2nd layer of OLO.

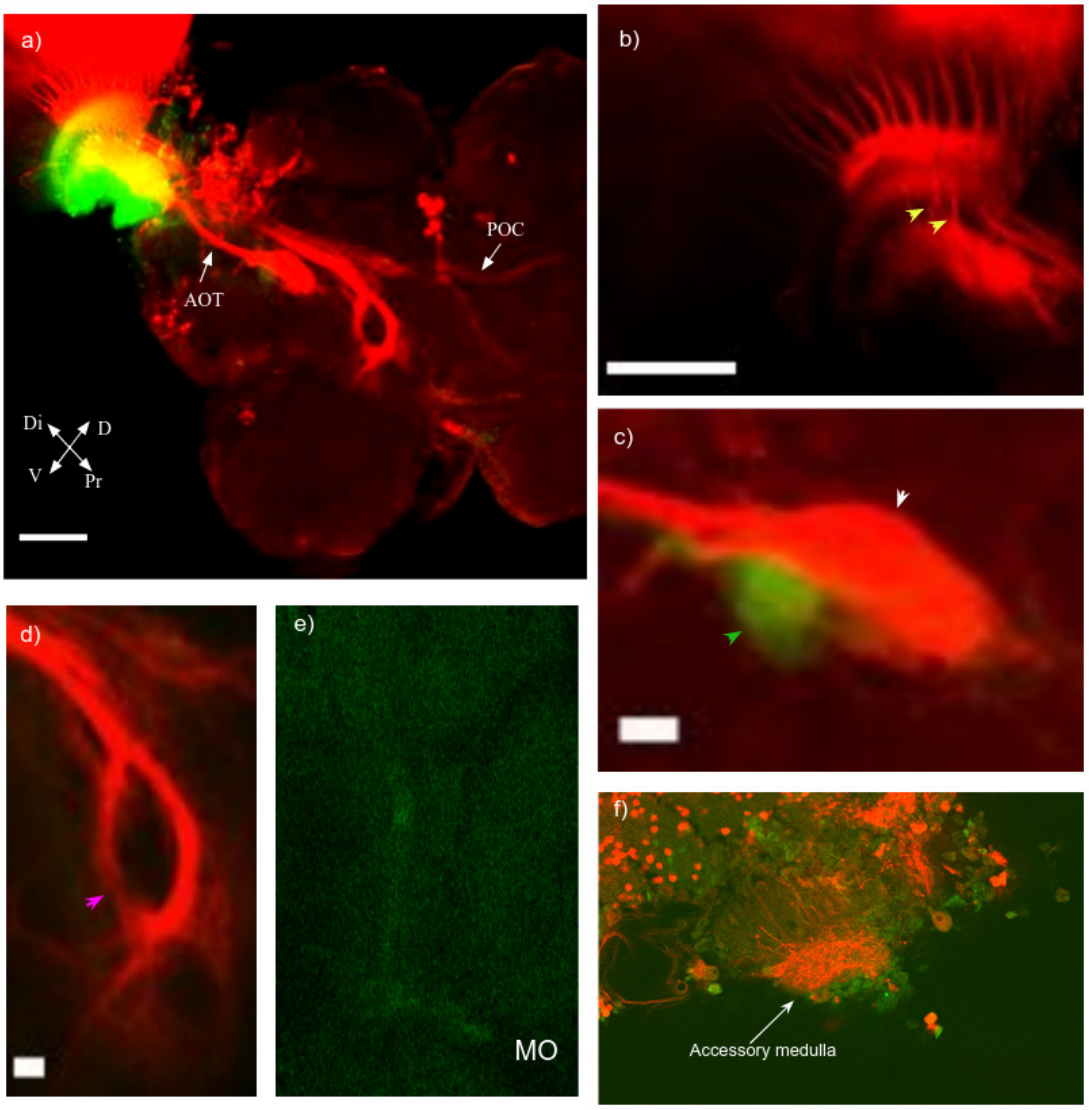

Figure 3.6: Dextran conjugated Texas red injection at anterior-dorsal medulla and Dextran 488 injection in anterior-ventral lobula revealed optic lobe connections with the rest of the brain. **a)** Tracts connecting the optic lobe with the other parts of the brain. White arrows indicate anterior optic tubercle (AOT) and posterior optic commissures (POC). **b)** Transmedulla neurons crossing the OLO (yellow arrowheads) and arborising onto the ALO2. **c)** Trans medulla neurons have filled ALO2 and then transported via the tract and filled anterior optic tubercle upper unit (AOTu-UU) (white arrowhead) and fibres from ALO1 filled anterior optic tubercle lower unit (AOTu-LU) (green arrowhead) through the anterior optic tract. **d**) Transmedulla neurons have also filled two novel oval structures (pink arrowhead) on the ipsilateral side protocerebrum, located posterior most region. **e)** Tubercle accessory lobe neuron terminals innervating median olive (MO) of lateral accessory lobe (LAL). **f)** Trans medullary neurons terminals filling accessory medulla (aMe). Scale bars: (a-b) 50µm (c-d) 10µm.

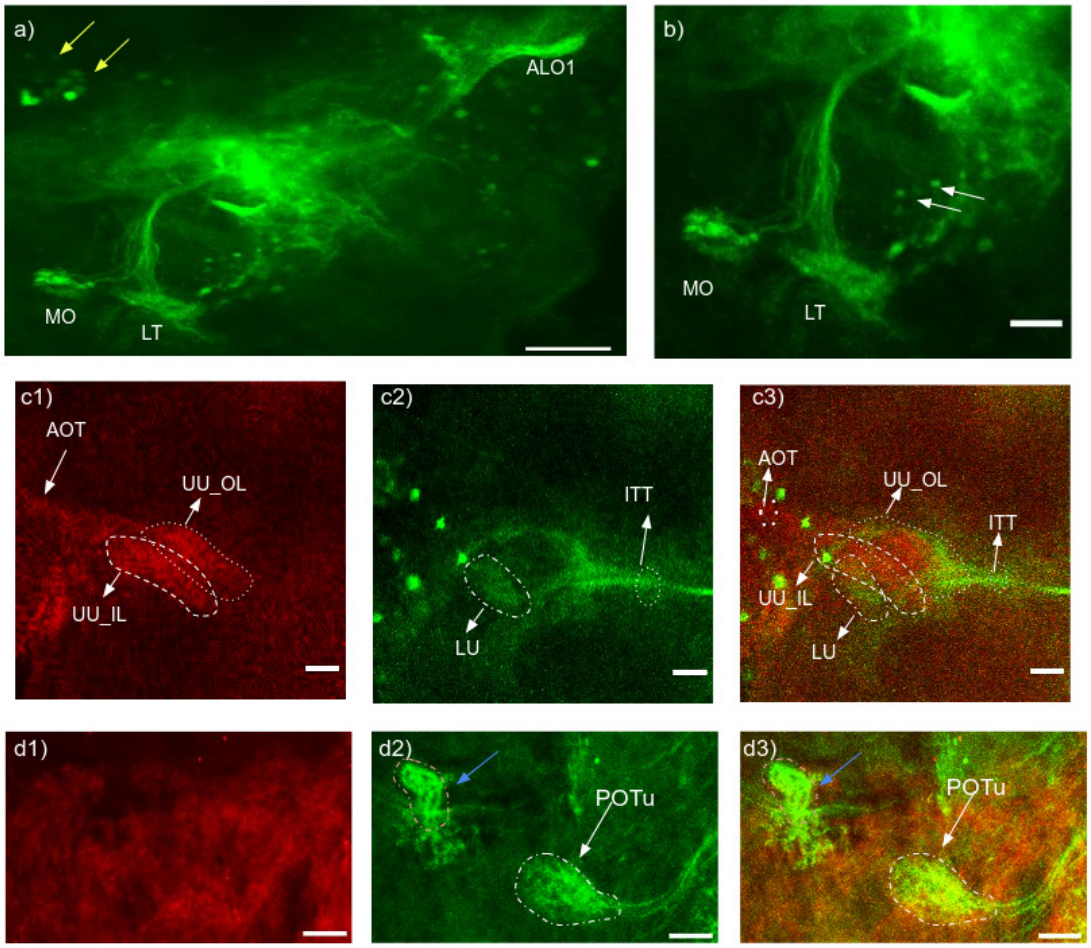

Figure 3.7: Innervations of the Anterior optic tubercle (AOTu) and posterior optic tubercle (POTu) **a)** Dextran injections in AOTu filled ALO1, MO and LT of LAL. Yellow arrows indicate the cell bodies filled through the tubercle protocerebral tract. **b)** MO, LT and the putative cell bodies (white arrows) of tubercle lateral accessory lobe neurons are visible in the enlarged image. **c)** Dextran injections in medulla filled AOTu_UU_OL and AOTu_UU_IL of the ipsilateral side and dextran injections from contralateral AOTu in the same preparation filled ipsilateral AOTu. **d)** Dextran injections in the accessory medulla filled the ipsilateral POTu (white dashed line) and also filled a novel structure (blue arrow). Scale bar : (a) 100µm (b-d) 50µm

3.2.5 Major tracts

Targeted injection of dextran conjugated dye at several subcompartments of the neuropils, identifiable by landmarks revealed major tracts connecting the optic lobe to the other regions in the visual pathway.

3.2.5.1 Optic lobe and anterior optic tubercle

AOTu (Fig 3.6c and 3.7c) is one of the major neuropil located in the medial protocerebrum anteriorly, latero-ventral to the alpha lobe tip visible in the nc82 staining (Fig 3.2a). AOTu is divided into upper (AOTu-UU) and lower units (AOTu-LU) (Fig A1). AOTu-UU is further divided into outer (AOTu-UU-OL) and inner lobes (AOTu-UU-IL) (Fig 3.7c). AOTu is a small structure (maximal extension of 200μm). AOTu can be seen connected to the rest of the brain through four major connectives as visualised by dextran based tract tracing. 1) To the optic lobe through anterior optic tract (AOT) (Fig 3.6a and 3.7c). 2) Inter-tubercule tract (ITT) connects it to the contralateral AOTu (Fig 3.7c). 3) Tubercle protocerebral tract connects it to the superior protocerebrum (Fig 3.7a). 4) Tubercle accessory lobe tract connects it to the lateral accessory lobe (Fig 3.7b). Anterior optic connective connecting AOTu and optic lobe has three major bundles of fibres. Dextran injections at anterior-dorsal medulla revealed that the trans-medullary neurons having cell bodies distal to the medulla entered the medulla and has side branches in the serpentine layer (7th layer). These tracts then cross the medulla and enter the OLO followed by the stratum 2 of the anterior lobula (ALO2). Cells from the same region of the medulla also densely innervated the accessory medulla (Fig 3.6f). The AOT continues beyond ALO2 and innervates both the outer and inner lobes of the upper unit of the ipsilateral anterior optic tubercle (AOTu-UU) (Fig S1d).

Dextran injection at the contralateral lower unit of the anterior optic tubercle (AOTu-LU) filled stratum 1 of the contralateral anterior lobula (ALO1) through anterior optic connective (Fig 3.7a), and it also filled the ipsilateral AOTu through inter-tubercle tract (Fig 3.7c). This innervation of the

ipsilateral AOTu could be confirmed with the AOTu visualised by dextran injection in the ipsilateral medulla leading to filling of the ipsilateral AOTu (Fig 3.7c).

Dextran injection in the AOTu filled many fibres arborising in lateral triangle (LT) and median olive (MO) in lateral accessory lobe (LAL) through tubercle accessory lobe tract (Fig 3.7a,b). Dextran injection at anterior ventral lobula also filled the median olive (MO) of the LAL (Fig 3.6e) as well as many cell bodies in the superior protocerebrum through tubercle protocerebral tracts (Fig 3.7a). Dorsoventral partitioning of lobula to AOTu connection is observed upon injecting dextran tagged alexaflour 488 in dorsal lobula and texas red in ventral lobula. Ventral lobula is connected to the AOTu-UU & AOTu-LU on contrary to the dorsal lobula, which is connected only to the OL and IL of AOTu-UU (Fig S1).

3.2.5.2 Novel structures in the posterior protocerebrum innervated by fibres from medulla

Very prominent tracts from the anterior-dorsal medulla also innervated two bulb-like novel structures near the ipsilateral side of the central protocerebrum, posterior to the central complex (Fig 3.6d). These fibres travel as a thick bundle and terminate in a distribution shaped around ovals at the very posterior protocerebrum with dense fine branches. There was no structure that was distinguishable in our nc2 or GABA immunohistochemistry demarcating this region.

3.2.5.3 Posterior optic tubercle and a novel innervation

Posterior optic tubercle (POTu) is another major neuropil located posterior to the junction of peduncle, alpha lobe and beta lobe. POTu is a smaller structure (maximal extension of 80µm), which is almost half of the size of AOTu. Dextran injection into accessory medulla (aMe) (Fig 3.6f) filled the POTu (Fig 3.7d) through posterior optic connective. It has also filled a novel structure which is 120µm lateral to the POTu (Fig 3.7d, blue arrow), posterior to the CBU at the protocerebral bridge terminal. Dextran injection at anterior dorsal lobula also filled this novel structure (Fig S1a, blue arrow).

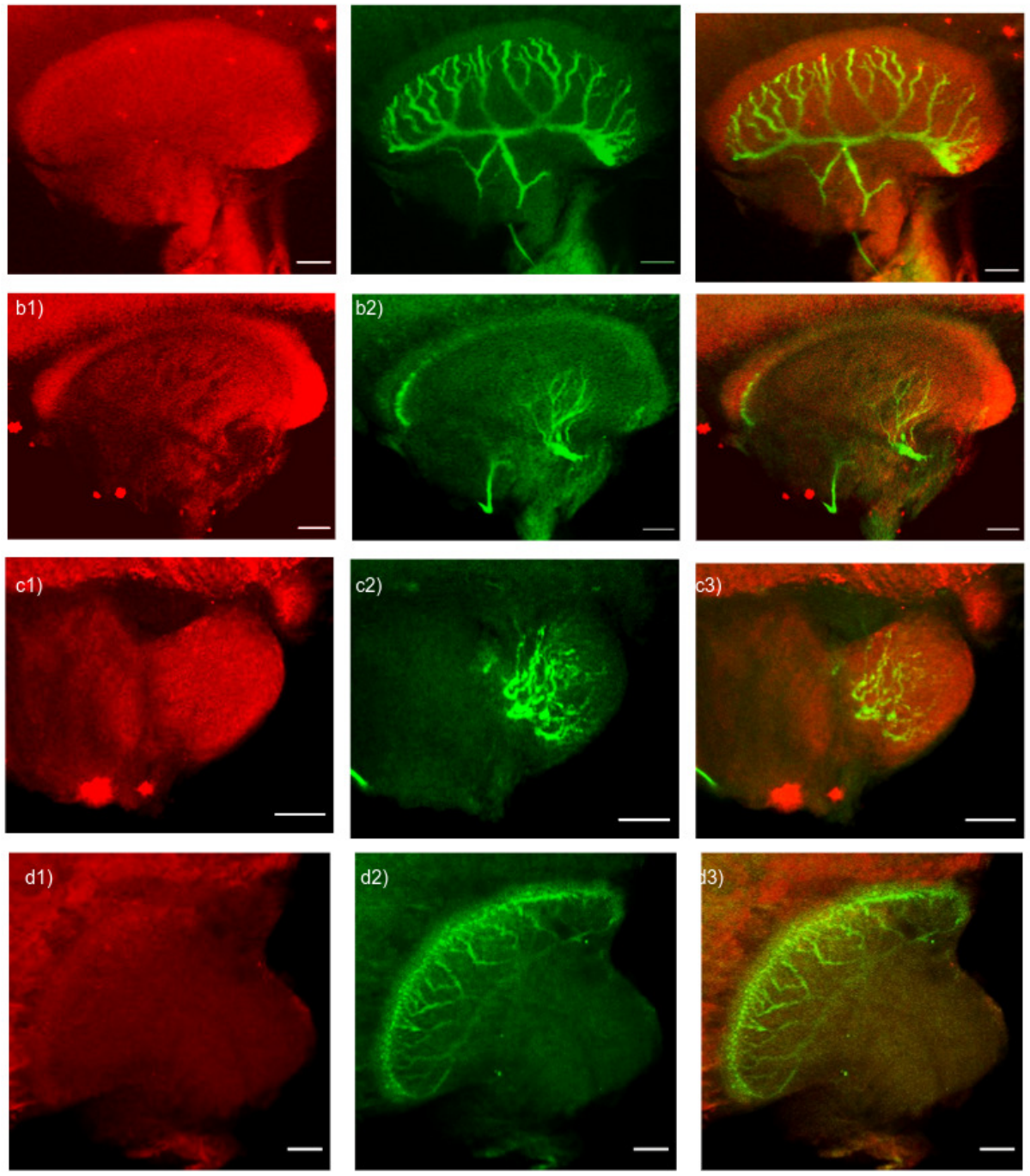

Figure 3.8: Anatomy of lobula neurons to show segmentation of neuropils (Red - nc82, Green - intracellular fills). **a)** LGMD neuron branch A innervation. **b)** LGMD type I neuron branch B innervation. **c)** LGMD neuron branch C innervation. **d)** Another lobula neuron (putatively LGMD type II) innervating the 2nd layer of OLO with fine branches, but having no prominent branches in other parts of the lobula. Scale bar : 50µm (a-d)

3.3 Discussion

It has been shown that the *Hieroglyphus banian* olfactory circuit is conserved through 4th order neurons and analogous to *Schistocerca americana* which have ~57 million years of divergence (Singh and Joseph, 2019). Unlike locust, *H. banian* species is univoltine, is found to inhabit somewhat lush vegetation and rarely seen in open grounds. In this work, we have studied optic lobes and other major visual processing centres of *Hieroglyphus banian*. We counted the number of ommatidia and found them to be similar to that reported in *L. migratoria* (Shaw, 1978). Variation in the number of ommatidia within the species is consistent with the variation observed in the number of ommatidia in a single strain, Canton-S^{BH} strain of Drosophila (Ramaekers et al., 2019). Though most of the structures and the connections were identical to that reported in *S. americana*, we found two novel structures in the central protocerebrum innervated by neuronal innervations from the optic lobe (Fig 3.6d). One of them was filled by dextran injections in the anterior dorsal medulla and anterior dorsal lobula which lies in the very posterior protocerebrum posterior to the LAL. Another novel structure dorsal to the POTu (Fig 3.7d,blue arrow), posterior to the CBU at the protocerebral bridge terminal was filled by dextran injection targeting either in the anterior dorsal lobula or aMe. Innervations of the intracellularly filled visual neurons in the lobula, partitioned consistent with the subcompartments detected from immunohistochemistry. This study thus enabled comparison of major visual processing centres with already well studied locust species Schistocerca gregaria and could identify some novel features about their structure and function.

3.3.1 Comparison of major visual processing centres of *H. banian* and *Schistocerca gregaria*

In visual systems of the locusts, *Schistocerca gregaria* is well studied. Similar to *H. banian*, *S.gregaria* OL has following neuropils lamina, medulla and lobula complex arranged distal to proximal. Anti-GABA staining showed 10 layers in the medulla of *S. gregaria* (Beetz et al., 2015; Rosner et al., 2017). *H. banian* optic lobe scanned under 488 laser, showed layered structure of medulla due to autofluorescence. Upon analysing these images for brightness changes in the medulla

portion of the brain, it also showed 10-11 layered structure. Here, the method used to calculate the number of layers is similar to the method used for calculating medulla and lobula layers based on pixel intensity plots on confocal scans of anti-synapsin and anti-serotonin stained brains of dragonfly (Fabian et al., 2020). For better understanding of the relationship of these layers to function, we need to carry out anti-GABA immunostaining studies on sections of the brain, as these layers were not clear in our whole mount preparations. Lobula complex of *S. gregaria* has OLO, DLO, ALO and ILO similar to *H. banian*. *S. gregaria* OLO showed 4 layered structure for anti-GABA. Distal most layer stained strongly for GABA, second layer is free of GABA and the fourth layer has more densely stained fibres than the third layer. In *H. banian*, a similar pattern of GABA staining is observed in OLO. In *H. banian*, nc82 staining showed all the four layers of the OLO and the second layer is the most densely stained among all the four.

In *H. banian*, anti synapsin immunoreactivity is clear in ALO, DLO and ILO, same as in *S. gregeria*. DLO stained brighter than ALO and ILO, whereas ILO also showed substructures such as upper and lower units. In *S. gregaria*, antibodies against Locust Tachykinin II (Lom-TK II) revealed two layers in ALO, (ALO1 & ALO2). ALO2 showed three sub layers (Homberg et al., 2003). Similarly, *H. banian* also has 4 layers, including the 3 sublayers of ALO2 and one layer of the ALO1 (Fig. 4d).

In *S. gregaria*, optic lobes are connected to the rest of the brain especially through two tracts, anterior optic tract (AOT) and posterior optic tract (POT). Through AOT, optic lobes are connected to the anterior optic tubercle (AOTu) and to regions in the rest of the brain. AOTu has upper and lower units. Upper unit is further divided into the outer and inner lobe. AOTu is connected to the contralateral AOTu through inter tubercle tract (ITT) and to LAL through TuLAL tracts. Innervation in the LAL region shows two bulbous structures called median olive (MO) and lateral triangle (LT). AOTu also connects to the superior protocerebrum through tubercle protocerebral tracts (Homberg et al., 2003).

Through POT, optic lobes are connected to the posterior optic tubercle (POTu) (Homberg and Würden, 1997). Both the POTu's are connected through inter tubercle tracts (ITT), POTu is connected to the protocerebral bridge through tangential neurons (el Jundi and Homberg, 2010). Similarly in *H.*

banian, the AOTu is connected to the optic lobe through AOT, LAL through TuLALT, superior protocerebrum through TuPBT and contralateral AOTu through inter tubercle tract. Though POTu is filled through accessory medulla (aMe), we couldn't visualise all the tracts leaving the POTu, as it was difficult to access and target specifically. Thus, we can conclude that the visual system of *Hieroglyphus banian* is anatomically very similar to that of the *Schistocerca gregaria*.

3.3.2 Novel structures

In our tracing of tracts in *H. banian*, two novel tracts could be seen which are not described before in locust visual systems. Dextran injection at the anterior dorsal medulla filled two bulb-like structures in the central protocerebrum, posterior to the central complex. This tract was prominent and consistently filled in our preparations. Dextran injection in the anterior dorsal lobula also filled this structure possibly because the tracts going from medulla to these structures were hit. Why the prominent tract from medulla to the posterior protocerebrum was not visible in *S. gregaria* though it was consistently visible in all our *H. banian* fills is puzzling. Dextran injection at anterior dorsal lobula and aMe filled another novel structure dorsal to the POTu (Fig 3.7d, red arrow), posterior to the CBU at the protocerebral bridge terminal, dextran injection at accessory medulla also filled this structure. It is tempting to call this structure POTu2 because the originally reported close-by structure is called POTu1 and they get filled from similar regions in the optic lobe.

3.3.3 Comparison of optic lobes of *H. banian* and other insects

Drosophila melanogaster is another insect but from the order diptera whose visual system is well studied. The Drosophila medulla is a 10 layered structure, consisting of outer (1-6 layers) and inner medulla (8-10 layers), which are separated by serpentine layer (7th layer) (Fischbach and Dittrich, 1989). Medulla compartmentalization in *H. banian* resemble the other species of insects, varying in number of layers, 6 layers in cockroach (Rosner et al., 2017), 10 layers in Monarch butterfly (Heinze and Reppert, 2012) and Mantis (Rosner et al., 2017). 11 layers observed in dung beetles (Immonen et al., 2017) and 21 layers observed in dragon flies (Fabian et al., 2020). Though there is a similar

arrangement for lamina and medulla in these species they differ distinctly in the arrangement of the lobula complex. In Drosophila (and in other dipterans and butterflies reported so far), the lobula complex is made up of lobula and lobula plate. In this arrangement, lobula plate is involved in directional motion vision and lobula carries out associated computations. In orthoptera systems, a few identified neurons innervating the lobula complex have been shown to be involved in detecting looming stimulus to mediate escape response, a motion related computation but a specialised one. It is not clear why the arrangement of lobula complex is so different between orders of insects, nor is it clear if there are divisions in the orthoptera lobula complex that are equivalent to lobula and lobula plate in other insects. According to Strausfeld, lobula plate receives retinotopic input from medulla and lobula via uncrossed bundle (Lin and Strausfeld, 2013). Lobula plate has 4 layered structure, each layer corresponds to a cardinal direction (Maisak et al., 2013). In *H. banian,* we could not resolve which part can be equivalent to the lobula plate. AOTu, in drosophila, consists of a large spherical medial compartment (AOTUm), and lower unit complex (AOTU_LUC) which has two smaller domains intermediate AOTU [AOTUin] and lateral AOTU [AOTUl]) (Omoto, J. J. et al.,2017). In *H. banian*, the counter parts are upper unit (UU) and lower unit (LU) respectively. Lateral complex of Drosophila consists of gall (GA), bulb (BU, lateral triangle). LAL has a ventral body and crepine (CRE) whereas in locusts, GA is reduced and BU is present in two parts: lateral triangle (LT) and median olive (MO). Upper lateral accessory lobe (ULAL) corresponds to parts of the CRE of Drosophila and the lower lateral accessory lobe is the counterpart of the ventral body in drosophila (Honkanen et al., 2019).

Table 3.1: Comparison of major visual neuropils of *Hieroglyphus banian* and *Schistocerca gregaria*

	Hieroglyphus banian	***Schistocerca gregaria***
Eye	Ommatidia:~8000	Ommatidia:~9400
Lamina	Columnar structure	Columnar structure
Medulla	~10 layered structure (Based on brightness change across the medulla of a autofluorescence	10 layered structure (Anti-GABA staining) (Rosner et al., 2017)
Lobula complex	Four sub-neuropils, OLO,ILO,ALO,DLO	Four sub-neuropils, OLO,ILO,ALO,DLO (Rosner et al., 2017)
AOTu	AOTu consists of upperunit(UU) and lowerunit (LU) UU is further divided into outer lobe (OL) and inner lobe (IL). AOTu is connected to the rest of the brain through 4 distinct fiber tracts., 1. anterior optic tract: connects to theoptic lobe. 2. inter tubercle tract: connects two AOTu's. 3. Tubercle protocerebral tract: with the superior protocerebrum. 4.Tubercle accessory lobe tract: with LAL.	AOTu consists of upperunit(UU) and lowerunit (LU) UU is further divided into outer lobe (OL) and inner lobe (IL). AOTu is connected to the rest of the brain through 4 distinct fiber tracts., 1. anterior optic tract: connects to theoptic lobe. 2. inter tubercle tract: connects two AOTu's. 3. Tubercle protocerebral tract: with the superior protocerebrum. 4.Tubercle accessory lobe tract: with LAL.
POTu	POTu is present as a single neuropil. POTu is filled through aMe through the posterior optic tract.	POTu is present as a single neuropil. POTu is connected to other brain regions through 3 tracts., 1.Posterior optic tract: connects to the optic lobe 2. Inter tubercle tract: connects both POTu's 3. Tangential neurons (TB): connects POTu and protocerebral bridge(PB).

LAL	Ipsilateral LAL shows two bulb-like structures called median olive (MO) and lateral triangle (LT) upon being filled with dextran coupled dye in LU of the AOTu.nc82 staining showed dS,vS,MO and LT .	Ipsilateral LAL shows two bulb-like structures called median olive (MO) / (MBU) and lateral triangle (LT) / (LBU) upon filling with dextran coupled dye in LU of the AOTu. nc82 staining showed dS,vS,MO and LT.Neurons from AOTu-LU and lower division of CB (CBL) synapse at median olive (MO) and lateral triangle (LT) of lateral accessory lobe (LAL).
Novel structures	Two novel structures were observed. 1. Two bulb-like structures are present in the posterior central protocerebrum connected to the optic lobes. 2. Another novel structure is observed posterior to the POTu, connected to the optic lobe through posterior optic tract.	These structures were not reported in *S. gregaria*/ any other locust.

Chapter 4

Nature of the field potentials along the visual pathway and insights into the mechanism of their generation

4.1 Introduction

Field potentials like ERG, LFP and EEG can reflect the population activity of neurons in and around the recording electrode. They are changes in potentials produced at the recording electrodes by transient changes in the charges outside the neurons. These transient changes are caused by membrane currents caused by channel mechanisms involved in sensory transduction, synaptic current generation and spikes. Of these, the fast changes (high frequency components) attenuate rapidly with distance and thus often the ERG and LFP are contributed to by channel mechanisms involved in sensory transduction and synaptic current generation. When large populations of neurons are arranged in parallel and get correlated inputs or, if the network interacts locally and produces correlated activity in the population, the field potentials produced by these can add up and can be picked up on a electrode quite a distance away from the source of the transient excess charge. These field potential responses can be insightful about mean population activity. Their changes under different treatments can infer us about mechanisms involved at the circuit level.

World is full of varied colours, living and nonliving. These variations in spectral properties are mostly produced by the differential reflectivity at different wavelengths, though in some cases the objects may be fluorescent or even generate light. Detecting these differences in spectral properties in space is important for organisms' survival. Organisms may themselves have evolved colour schemes for various purposes given the visual properties of the conspecific or predator. Some use these bright colours as warning signs for their predators, some mimic others colours to escape predators, some to hide from enemies, some to attract mates, and some to fight a rival.

The light sources that the organisms perceive have both spatial and temporal variation of intensities at different wavelengths that constitutes the scene. These have to be detected and processed by the visual systems to enable the capacity for vision.

Transduction of light intensity at various wavelengths is important to the organism which leads to the neural representation of vision.The differential sensitivity to different wavelengths is due to the properties of the opsins that form part of the photo transduction machinery. Different opsins have different wavelengths at which they are maximally activated and they are less activated by wavelengths more distant from this. This transduction is carried out by receptor neurons that usually express a single opsin type. Thus the representation of the arrival of photons of a wavelength at a point is mediated by a combinatorial activity of receptor neurons expressing different opsin types.

Colour vision is well studied in vertebrates and invertebrates. Karl von Frisch first showed that bees (*Apis mellifera*) can identify colours (von Frisch, 1914). As mammals have rods and cones for dim light and bright light vision respectively, in insects we can relate retinula cells R1-R6 as rods which involve in monochromatic vision and R7-R8 as cones which involve in polychromatic vision and respond to a broad spectrum of light. To understand spectral sensitivity and the nature of visual processing at major processing regions, electroretinogram (ERG) and local field potential (LFP) recordings were performed.

4.1.1 Electroretinogram

ERG is the electrical activity recorded using a blunt electrode by placing it over the eye and measuring the potential difference with respect to ground electrodes in the body of the animal. ERG's can be used to access many physiological properties. For example, using ERG's we can identify the spectral sensitivities of the retinula cells (Stark et al., 1976) and also flicker fusion frequencies of an eye (Cosens & Spatz, 1978). In general compound eyes of all the arthropods have following functional components in common, they are cornea, cone, a rhabdom and screening pigment. Compound eyes contain thousands of hexagonal structures called ommatidia/facets, each of the ommatidia have

photoreceptors called retinula cells. Number of ommatidia and retinula cells varies from insect to insect. Microvillar structures of retinula cells give rise to photosensitive structures called rhabdomeres, which collectively form rhabdom. Rhabdoms are also called light guides which help in directing the photon signals further into the eye. Ommatidia & rhabdoms are separated by screening pigment.

Table 4.1: Spectral sensitivities of different insects

Name	**Photoreceptor spectral sensitivity maxima**	**References**
Danaus plexipus	340, 435, 540	(Stalleicken et al., 2006)
Manduca sexta	345,440,520	(Bennett & Brown, 1985)
Bombyx mori	380,520	(Peitsch et al., 1992), (Briscoe & Chittka, 2001)
Periplaneta americana	365,507	(Mote et al., 1970)
Locusta migratoria	**360,430,530**	**(Vishnevskaya et al., 1986)**
Schistocerca gregaria	**339,441,514**	**(Schmeling et al., 2014)**
Gryllus bimaculatus	332,445,515	(Zufall et al., 1989)
Aedes aegypti	345,523	(Stavenga et al., 2017)(Perkins et al., 1992)(Stavenga et al., 2017)
Calliophora erythrocephala	360,490	(Paul et al., 1986), (Hardie, 1986)
Musca domestica	335,355,460,490,530	(Hardie et al., 1979; Stavenga et al., 2017),
Drosophila melanogaster	**345,370,440,480,520**	**(Stavenga et al., 2017); (Salcedo et al., 1999)**

Apis mellifera (male)	346,445,529	(Peitsch et al., 1992), (Briscoe & Chittka, 2001)
Apis mellifera (female)	356,430,540	(Peitsch et al., 1992), (Briscoe & Chittka, 2001)
Cataglyphus bicolor	350,510	(Briscoe & Chittka, 2001)

4.1.1.1 Drosophila compound eye

If we look into the detailed anatomy of the drosophila eye, posterior to the cornea visibly we can see hexagonal structures (Ommatidia/facets).Ommatidia contain eight photosensitive cells (R1-R8 retinula cells) of which R1-R6 retinula cells are arranged in a circle,R7 is present at the centre of the circle and posterior to it R8 is present. R1-R6 express single type of opsin (Zuker et al.,1985; O'Tousa et al., 1985) which conveys achromatic information, and responds to a broad spectrum of wavelengths (Hardie, 1979) whereas R7 express UV sensitive opsins and R8 express blue-green sensitive opsins (Zuker et al.,1987;Montell et al., 1987; Fryxell and Meyerowitz, 1987; Papatsenko et al., 1997; Chou et al., 1996)which conveys chromatic information (Heisenberg and Buchner,1977; Yarnaguchi et al., 2008). With respect to the vertebrate (Zuker et al.,1987;Montell et al., 1987; Fryxell and Meyerowitz, 1987; Papatsenko et al., 1997; Chou et al., 1996) visual system, we can consider R1-R6 as rod equivalents and R7-R8 as cone equivalents. Photo signal from a single source is received by multiple ommatidia in the neighbourhood, which form an inverted image by each ommatidia. Signal from all these ommatidia is 180° twisted and pooled together in the lamina (first neuropil, Fischbah and Hiesinger 2008). There are four neuropils which together make the optic lobe of the Drosophila. They are lamina, medulla, lobula and lobula plate.

The lamina contains lamina monopolar neurons arranged in columns called cartridges.Each cartridge contains five lamina monopolar neurons (L1-L5) (Meinertzhagen and Oneil, 1991; Meinerzhagen and Hanson, 1993; Meinerzhagen and Sorra, 2001), of which L1 and L2 are necessary for motion vision (Riester et al., 2007).

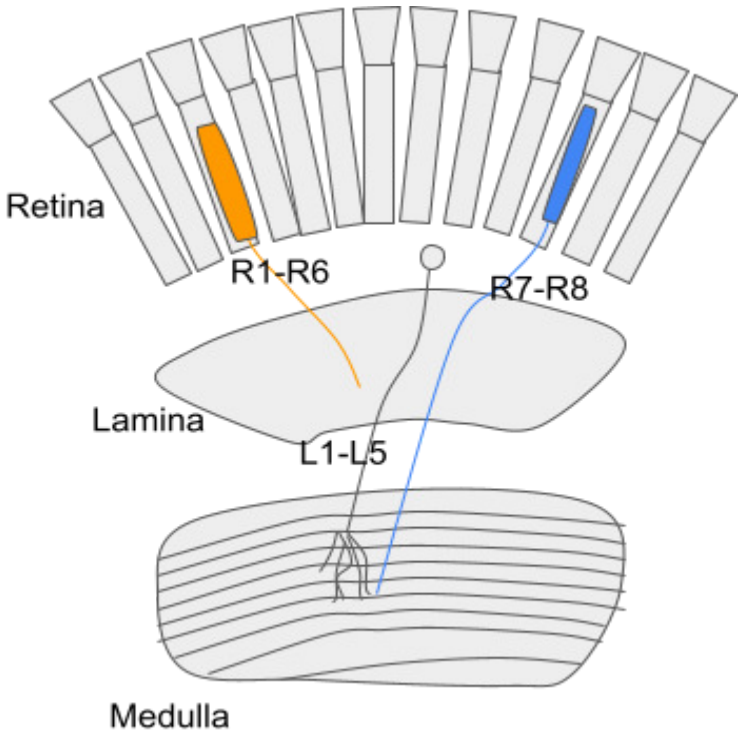

Figure 4.1: Schematic representation of retinula cells and lamina monopolar cells innervation in Drosophila optic lobe.

4.1.1.2 Components of ERG

If we record ERG from drosophila by placing one electrode (+) over the cornea and the second electrode (-) near the basement membrane. This gives the negative sustained monophasic potential for sustained illumination with white light (Fig 4.2a) (Pak et al., 1969). Whereas if we perform the same experiment by moving the electrode (-) further into the thorax region of the drosophila, ERG contains monophasic negative sustained potentials, similar to what Pak et al.1969 have observed, and the positive on and negative off transients (Fig 4.2c) (Heisenberg, 1971; Pak, 1975).

4.1.1.3 Neurons responsible for the shape of ERG

Sustained monophasic potential in ERG is due to the retinula cells (Fig 4.2a) (Heisenberg, 1971) and ON, OFF transients are thought to be due to the lamina monopolar neurons (Fig 4.2b) (Goldsmith & Bernard, 1974; Heisenberg, 1971). In blowfly it has been shown that contrast response curves and intensity response curves of ERG transients and lamina monopolar cells are similar. And low pass

filtering of intracellular recordings from retinula cells and lamina monopolar cells can be used to reconstruct ERG waveform (McCook 1984).

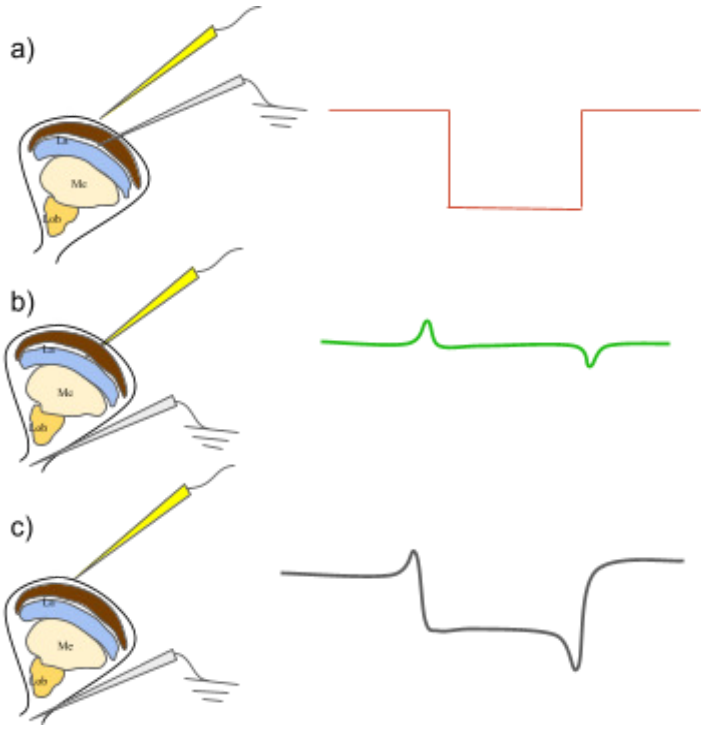

Figure 4.2: Drosophila ERG, recording procedure (left); shape of the potential (right). a) Receptor potential, monophasic response. b) Lamina currents recording, ON and OFF transients. c) ERG recording, which is the sum of receptor potential (monophasic response) and lamina currents (ON & OFF transients).

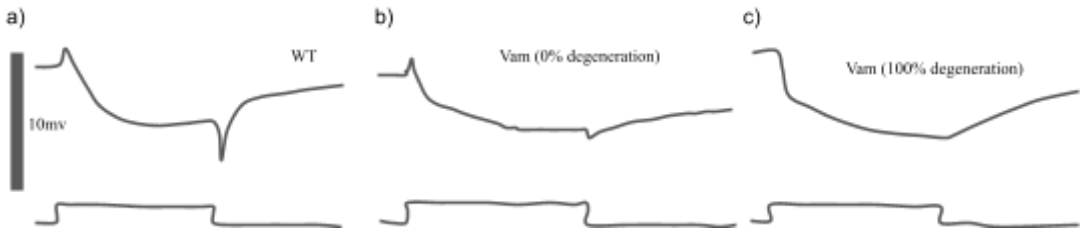

Figure 4.3: L1 and L2 are responsible for transients and the transients are absent when L1 and L2 are degenerated. a) Drosophila WT ERG response. b) ERG response of the Vam (which causes degeneration of lamina monopolar neurons L1 and L2) with 0% degeneration. c) Case of Vam with 100% degeneration. ERG response. (adapted from (Coombe, 1986))

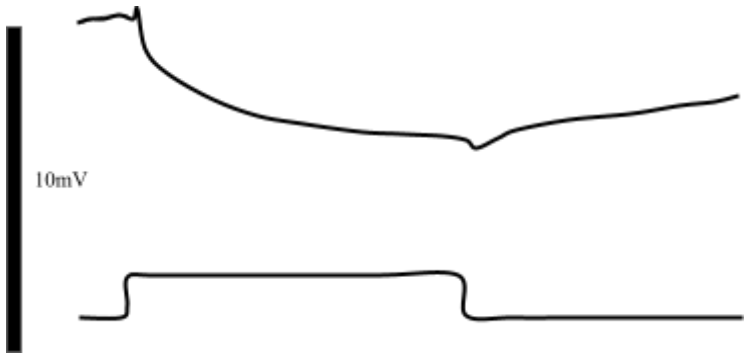

Figure 4.4: ERG response from the Drosophila triple mutant (rol mnb sol) that has reduced number of facets, reduced number of lamina monopolar cells per column showing reduced receptor potential, reduced ON and Off transients (adapted from (Coombe, 1986)).

Coombe, 1986 showed that lamina monopolar neurons L1 and L2 are responsible for the ERG transients using Vam (Fig 4.3) and triple mutant rol mnb sol (reduced optic lobes, minibrain and small optic lobes) (Fig 4.4) of Drosophila. Vam stands for vacuolar medulla, it is a semi dominant mutation. It causes the age dependent degeneration of the lamina monopolar neurons L1 and L2. Triple mutant rol mnb sol has disorganised lamina with most of the cartridges having no lamina monopolar neurons and few of the cartridges have one LMC axon. In the triple mutant, number of ommatidia reduced to 500 compared to 700-800 in WT and lamina size is reduced.

ERG recordings from dark adapted Vam drosophila mutant with 0% degeneration for yellow-green light diffused light stimuli for 1 second showed normal ERG with reduced transients (Fig 4.3b) whereas 100% degenerated mutant showed no transients (Fig 4.3c). Same experiment repeated with triple mutant rol mnb sol showed reduced transients in the ERG (Fig 4.4) (Coombe, 1986). While recording ERG in Drosophila by placing probing electrodes just above the lamina and ground electrode in thorax resulted in just on & off transients without any receptor potential for white light stimuli from quartz-iodine light bulb for a duration of 0.65 seconds (Fig 4.2b). Whereas recording ERG by placing a probing electrode over the cornea and the ground electrode just above the basement membrane gave rise to negative monophasic potential (Fig 4.2a).

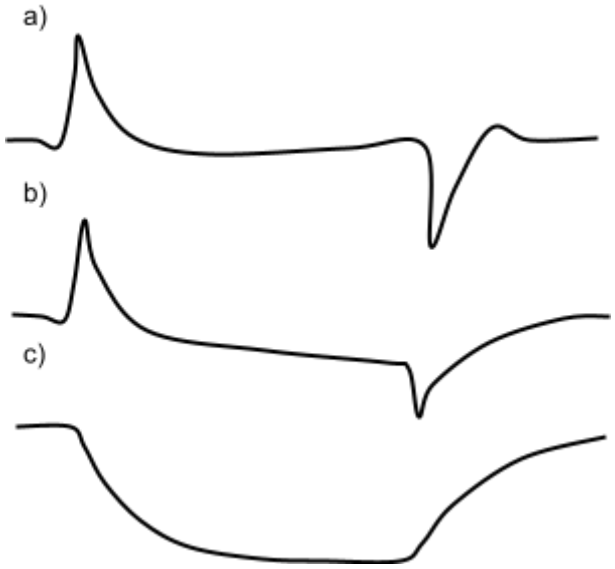

Figure 4.5: Lamina is responsible for transients in calliphora ERG. a) ERG response of calliphora intact eye. b) ERG response of medulla ablated calliphora eye. c) ERG response of lamina and medulla ablated calliphora eye (adapted from Autrum, 1952).

Combining ON, OFF transients and negative monophasic potential resulted in the construction of normal ERG (Fig 4.2c) (Heisenberg, 1971). Autrum performed ERG experiments on calliphora by removing different parts of the optic lobe microsurgically. ERG of normal calliphora contains both positive on transient and negative off transient and negative sustained potential. When medulla is removed and performed the experiment.There is no much change in the ERG shape (Fig 4.5b). When both medulla and lamina are removed and performed the experiment, transients disappear whereas only negative sustained potential is obtained (Fig 4.5c) (Autrum 1952). With the above observations it is clear that lamina monopolar neurons are responsible for transients in ERG.This confirms the Autrum hypothesis that "transients of the flies ERG are due to the lamina neurons and retina response alone which is monophasic and negative.

Local field potentials (LFP) are similar to ERG, where a blunt electrode is placed in the region of interest in the brain instead of the eye.

4.1.1.4 Oscillations

Oscillations are periodic variations that swing around the central value in the time domain. Oscillations in the range of 100Hz-200Hz were observed while recording from the optic lobe of the blow fly by illuminating one of the eyes. Amplitude of the oscillations increased upon increasing the illumination area and/or intensity of the light (Kirschfeld, 1992). Gamma oscillations were observed in the visual cortex of the cat, which are one-third of the oscillations frequency observed in the blowfly optic lobe (Kirschfeld, 1992). In the mammalian olfactory system, 40–100 Hz oscillations were observed in the olfactory bulb and piriform cortex during an inspiration (Adrian, 1950; Freeman, 1978). Stopfer et.al 1997 showed that in *Apis mellifera*, 30Hz oscillations were observed upon presenting odour stimuli for 1sec to the antenna while recording LFP from the calyx of the mushroom body .

Laurent showed that in Schistocerca americana ~ 20Hz oscillations were observed while recording local field potentials from the mushroom body. Oscillations were maintained throughout the stimulus duration (10ms) and disappeared at the end of the stimulus. Autocorrelation of the LFP oscillations for different odours revealed that oscillation frequency was independent of the odour. Simultaneous LFP recordings from ipsilateral mushroom body regions separated by 300µm showed almost exact LFPs without any phaselag, indicating the entire population of kenyon cells synchronisation (Laurent & Naraghi, 1994) .

Stopfer (1999) showed that in Locust (*Schistocerca americana*), LFP oscillatory power around ~20Hz increased maximally from trial 1 to trial 8 while recording from mushroom body, which was unaffected upon further odour stimulation. The coherence of firing patterns between LN membrane potential and LFP waveform and between PN spikes and LFP waveform has increased 4-5 times over the trials. And PN spikes became more precise over the trials as the odour became familiar (Stopfer & Laurent, 1999). Singh and Joseph 2019 has recorded LFP from *Hieroglyphus banian* mushroom body calyx.They have observed ~25Hz oscillations, and the power of the high frequency components(15-40Hz) has increased over the trails where as the power of the low frequency components (1-5Hz)

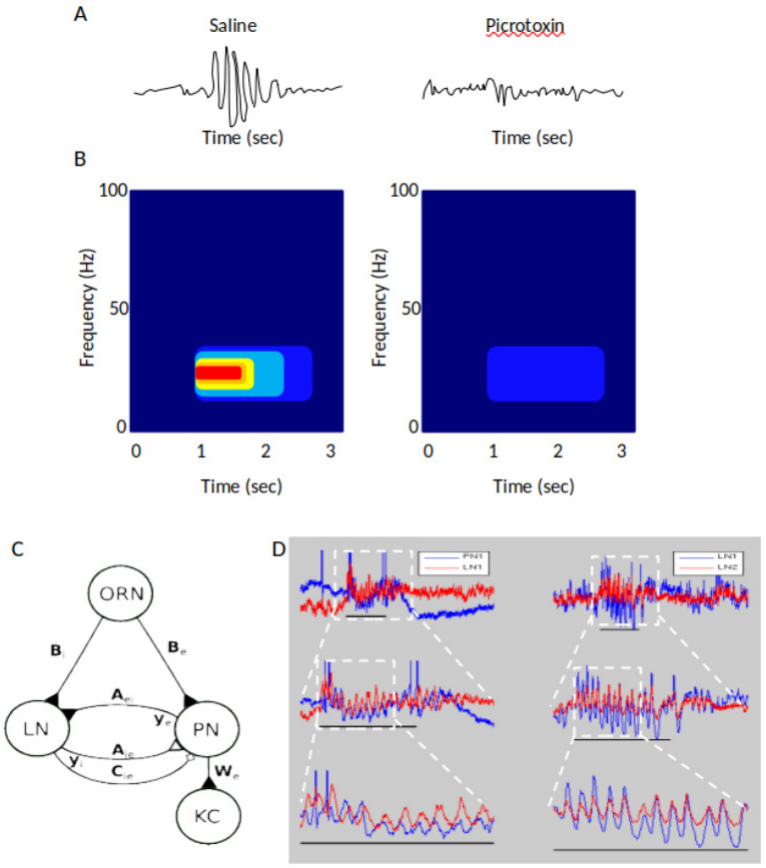

Figure 4.6 : 20-30 Hz oscillations recorded from mushroom body calyx while presenting the odour are abolished by picrotoxin. A). During an olfactory experiment, 20-30 Hz oscillations were recorded from the calyx of the mushroom body (left); whereas these oscillations were abolished by injecting Picrotoxin (PTX) (right). B). Spectrogram showing the power of frequencies present while recording LFP's from the calyx of the mushroom body by presenting an odour in saline (left); Spectrogram showing the power of frequencies after the injection of PTX (right). C). ORN-LN-PN connections, ORNs are connected to LNs and PNs. LNs are connected to PNs with inhibitory synapses. LN to LN and PN to KC are connected with excitatory synapses (Bhavana Penmetcha and Joby Joseph, unpublished). D). Phase relationship of LN and PN in HB in response to an odour. PN depolarization happens before LN depolarization, and LN depolarisation happens before PN hyperpolarisation (Singh & Joseph, 2019; Stopfer & Laurent, 1999).

decreased over the trials. In *Apis dorsata* ~25Hz oscillations were observed while recording LFP from the mushroom body. Oscillations were also observed in the intracellular membrane potentials of the antennal lobe interneurons for odour stimuli. LFP oscillations recorded from the mushroom body showed a phase lag compared to the intracellular membrane oscillations recorded from the antennal lobe (Stopfer et al., 1997).

From the above discussion it is clear that Oscillations are present in different sensory systems (Delaney et al., 1994; Gelperin & Tank, 1990) and they arise in response to stimulus presentation. But the function of those oscillations is still not clear.

In locusts, it has been shown that PN's are inhibited by LN's (Fig 4.6C) by the action of GABA which acts over $GABA_A$ receptors and opens the GABA gated chloride channels (MacLeod & Laurent, 1996). Waldrop et.al. 1987 showed that in *Manduca sexta*, GABA mediated inhibitory interactions in the antennal lobe are abolished by GABA antagonist picrotoxin (PTX) (Fig 4.6A) (Waldrop et al., 1987). In *Apis mellifera*, 30Hz oscillations which were observed while recording LFP from the mushroom body for odour stimuli, were abolished 8 minutes after the application of picrotoxin. PTX application has also affected the discrimination ability of similar odours of the honey bee in PER conditioning experiments (Classical conditioning/ Pavalovian conditioning is a learning and memory assay in which animal associates conditioned stimulus (CS) with unconditioned stimulus (US). In PER conditioning, honey bees associate sugar reward (US) with unfamiliar odour (CS), once they associate the odour with the sugar reward, they extend the proboscis for just odour presentation in further trials) whereas the discrimination ability of dissimilar odours is unaffected. From the GABA antagonist (studies it is clear that oscillations help in fine odour discrimination in Apis mellifera (Stopfer et al., 1997). Stopfer et al., 2003 studied concentration encoding in the locust olfactory system. While recording LFP from the mushroom body, 20-30 Hz oscillations were observed. Oscillation frequency did not change with changing the odour concentration, whereas the power of the LFP has increased with increasing the odour concentration. Increased LFP power is attributed to the increased PNs firing synchronisation and the increased LNs modulation efficacy. There is no change in PNs spikes mean phase during odour response with increasing odour concentration.

With the increased odour concentration, afferent inputs to the antennal lobe (AL) in insects or olfactory bulb (OB) in mammals increases (Cinelli et al., 1995; Friedrich & Korsching, 1997; Joerges et al., 1997; Meister & Bonhoeffer, 2001; Ng et al., 2002; Rubin & Katz, 1999; Stewart et al., 1979; Wang et al., 2003). Despite the concentration increase, overall output from the antennal lobe

integrated in the PNs does not change significantly. This indicates the existence of adaptive gain control mechanisms within the AL, which is consistent with the increased modulatory effect of LNs with increasing odour concentrations. This also indicates that the apparent involvement of LNs in monitoring the PNs output is consistent with PNs synchronisation over the increased odour concentrations. From this it is clear that local circuits in the AL modulate the mean output by compressing the input levels (Wachowiak et al., 2002).

Sandhya and Joby modelled AL to capture the oscillations and LFP responses. From the model it is observed that oscillations have increased from the first to second trial. And upon lowpass filtering the raw LFP trace at 5Hz to compare the oscillations with the change in deflection, deflections have decreased with the increasing oscillations from trial 1 to trial 2. The decrease in deflection component over the repeated trials while recording LFP is attributed to the increased $GABA_A$ synaptic strength which further increases the strength of the oscillations. Based on this observation, change in deflection is used as a proxy to identify the oscillation buildup. With this knowledge, they have performed PER conditioning experiments in one set of bees with 1%, 10% and 100% odour concentrations at 2min and 10min inter trial intervals (ITI) and LFP recordings from the mushroom body in another set of bees. Better similar odour discrimination occurred at 10% odour concentration with 2min ITI whereas the maximum mean change in deflection (which is an indication for oscillation buildup) occurred at 100% odour concentration with 2min ITI. This is a counter-intuitive with the Stopfer 1997, that had shown that oscillations help in fine odour discrimination. Thus we see that local field potentials can be indicative of the ongoing process and manipulations that modify them can give insight into the mechanisms operating in the brain region. It also gives insight into the processing and function.

4.2 Results

4.2.1 ERG of Drosophila

In the literature all the ERG experiments on Drosophila are carried out by presenting stimulus through LED light. Whereas we are using mobile display to present the stimulus (spectrum of visual

stimulus presented through mobile screen Fig 4.7). This was done because the same display will be used to present our white noise stimuli and other stimulus set while recording from cells. We see that by and large each of the colours red, green and blue had a band centred around the corresponding wavelength. However the red and green had some small peak overlapping close to the boundary of green. White of different intensities we sum of the red, green and blue.

To find out whether the display makes any difference, we recorded Drosophila Canton-S ERG by presenting red, blue, green, white (Fig 4.8b) and different intensities of white light stimulus (Fig 4.8a) through the mobile screen. For all the stimuli, ERG response showed positive ON transient, negative sustained receptor potential and negative OFF transient (Fig 4.8). ERG response amplitude (A) and time constant for steepness (τ) are directly and inversely proportional respectively to the intensity of the stimulus (Fig 4.8a). This shows that it is reasonable to use LED light or a mobile screen to present the stimulus..

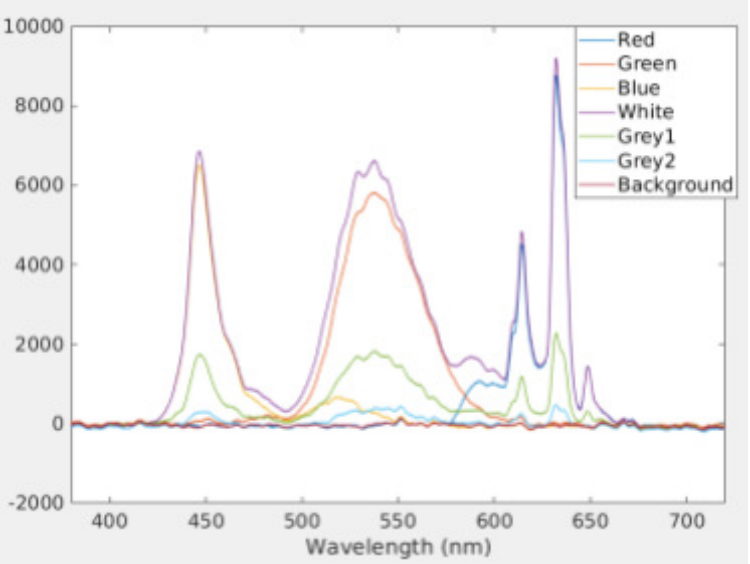

Figure 4.7: Spectrum of the display for different visual stimuli used for ERG. The colours are reasonably separated though there is some amount of leak from blue and red to the green. Whites of different intensities are sums of the red, green and blue with no visible interactions.

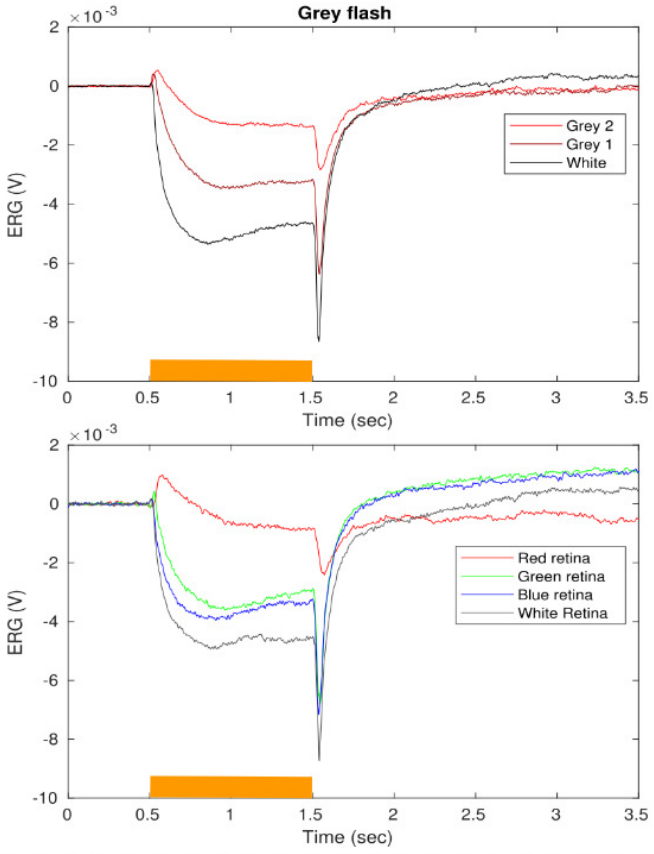

Figure 4.8: Drosophila ERG responses showing all the features seen in previous reports. a) ERG responses for least, less and bright white light stimuli. b) ERG responses for red, blue, green and white light stimuli.

4.2.2 ERG of Hieroglyphus banian

ERG experiments are performed by placing the probe electrode over the eye and ground electrode in the saline (Fig 4.9). Video of red, green, blue and white stimuli was played on the mobile screen sequentially with the same intensity. Each stimulus presented for 1 second and the interval between stimuli was 7 sec

ERG response for red showed negative sustained receptor potential with positive on and negative off transients respectively. Similar to what we have observed in Drosophila ERG(Heisenberg, 1971; Pak et al., 1969). Whereas for green, blue and white stimulus we can see negative sustained receptor potential and negative off transient but not the positive on transient. Receptor potential is maximum for white light followed by green, blue and red (4mv, 3.8mv, 2.3mv and 0.2mv) respectively. ERG

response amplitude (A) and time constant for steepness (τ) are directly and inversely proportional respectively to the intensity of the stimulus, similar to what we have observed for Drosophila ERG.

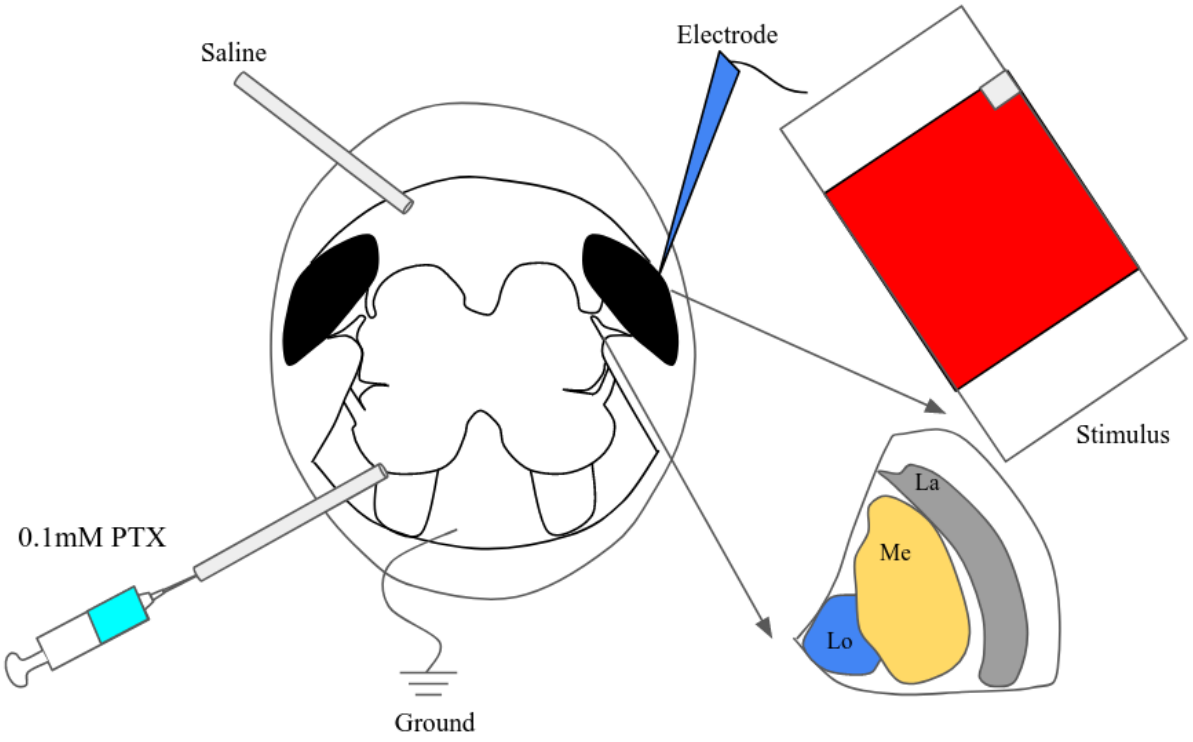

Figure 4.9: Schematic of ERG recording and drug perfusion in *Hieroglyphus banian.*

Positive ON transients observed in response to red stimuli (Fig 4.10a) but not for other stimuli. As red sensitivity is less in grasshoppers, drive from the retina to the lamina for the red stimulus would be less. We tested if positive going ON transient above the baseline in ERG could be revealed if we decrease the retinal drive by presenting lower intensities of white light. There we saw progressive reduction in red receptor potential with decreasing white light intensity (Fig 4.10b,c). At a very less bright white (2-3 Lux) stimulus, the positive ON transient above the baseline became visible (Fig 4.10c). This ON response was similar to what we have observed for red light stimulus including the time of on transient appearance (Fig 4.10c). This supports the hypothesis that the reduced input to the eye, reduces the drive results in reduced receptor potential and we can see the positive on transients.

However if the drive from the retina is the reason that the transient becomes visible of invisible it would imply that the processing in the lamina is similar for different power and spectral properties and

possibly the ON transient is hidden in the fast downward on transient phase of the receptor potentials at higher retinal drive. This turned out to be true and the ON transient riding on the receptor potential was visible as change in slope in the onset transient for higher light intensities of green, blue and white light stimulus (Fig 4.10d).

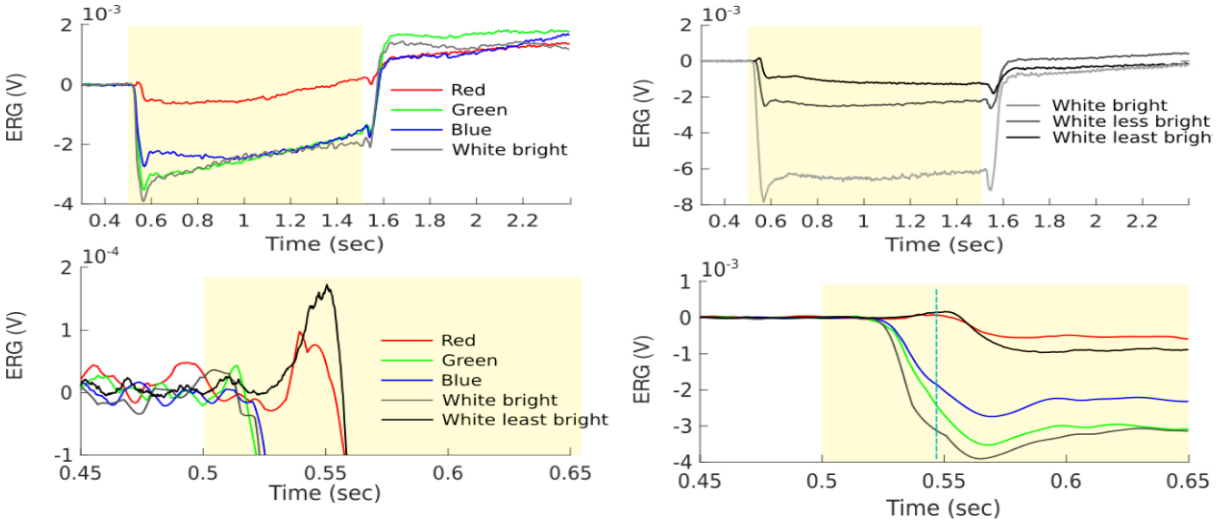

Figure 4.10: ERG responses of HB. a) ERG responses for red, blue, green and white light. b) ERG responses for different intensities of white light. c) Zoomed in version of ERG to show the On transients due to red and least bright white light stimulus. d) Zoomed in version of ERG to show the hidden On transients (kink at blue dotted line) for blue, green and white light stimuli.

4.2.3 Modelling of ERG

From the literature, the neural circuit responsible for ERG is reasonably well understood (Fig 4.11b). And from above experiments it is seen that the ERG response amplitude (A) and time constant for steepness (τ) are directly and inversely proportional respectively to the intensity of the stimulus. Stimulus evokes excitatory response in the retinula cells. Retinula cells further excite the lamina monopolar neurons. The linear computing part of the lamina processing involves differentiation of the input signal and saturate which gives ON and OFF transients. We propose a saturating nonlinearity at the lamina processing level. In the model, these constitute the proposed circuit level model of the retina and lamina.

As we are measuring the potentials from the surface of the eye, the electric field contributed by retina and lamina are inversely proportional to the distance from where we are measuring the ERG (Fig

4.11a). From Drosophila ERG experiments (Heisenberg, 1971a) it is known that ERG is the sum of receptor potentials and effect of lamina currents (Fig 4.2c). Thus the ERG was modelled by summing these from the circuit level model.

We simulated similar observations in the model for bright light and low light flash. The receptors components and the lamina components have the nature we attempted to model (Fig 4.11c). In line with the observations in the experiments, for bright stimulus, the ON transients are hidden in the fast negative receptor potentials, whereas for low intensity light stimulus, the ON transients going above the baseline become visible(Fig 4.11c).

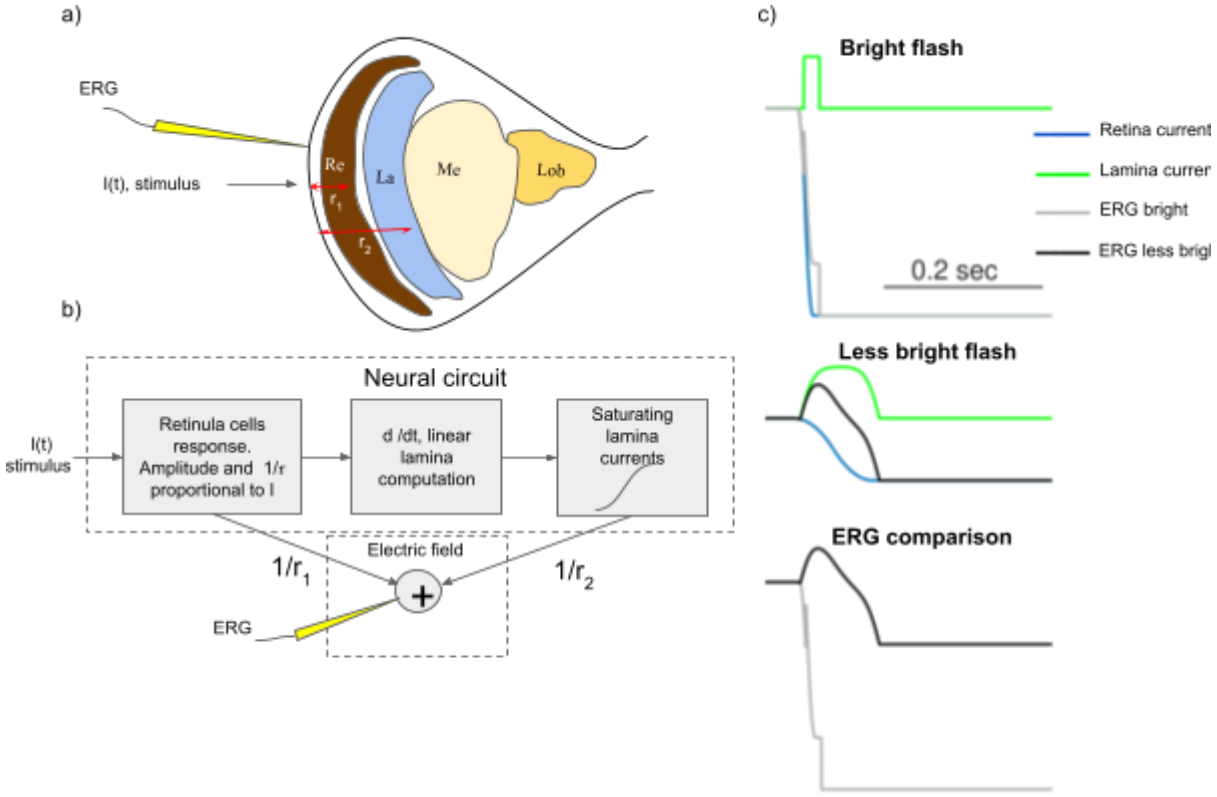

Figure 4.11: Modelling of ERG. a) Schematic of eye and the layers spatial relationship affecting ERG. b) Neuronal circuit responsible for ERG and electric field recorded from them. c) ERG responses for bright stimulus and less bright stimulus showing the appearance of ON response above baseline at low intensities.

4.2.4 Local field potentials at different regions of the HB brain

Local field potentials (LFPs) have been recorded from different regions of the brain while presenting the red,green,blue and white light stimulus. All the LFP recordings from medulla, lobula, AOTu, mushroom body (Fig 4.12b-e) (Calyx) looked like an inverted form of ERG, except that upward deflection is observed for both onset and offset of the stimulus whereas in ERG upward deflection is observed for onset of the stimulus and downward stimulus for offset of the stimulus. LFP recordings showed propagation delay from medulla to lobula to AOTu to mushroom body. Sustained potentials in LFP recordings from medulla and lobula showed maximum response for white light, followed by green, blue and least for red which is the same as in ERG response. Whereas sustained potentials in LFP recordings from AOTu (Fig 4.12d) and mushroom body (Fig 4.12e) showed maximum response for white light followed by blue, green and least for red. LFP recordings from mushroom body calyx and from the somatic layer of the mushroom body showed positive correlation. LFP recordings from contralateral central brain and from contralateral calyx also showed responses similar to LFP recordings from ipsilateral central brain and calyx. Contralateral eyes are closed with acrylic paint and LFP recorded from contralateral calyx showed reduced response compared to the LFP response recorded from contralateral calyx without covering the eyes with acrylic paint. Covering both the eyes with acrylic paint and recording LFP from contralateral calyx showed further reduced response compared to the LFP response recorded from contralateral calyx by closing the contralateral eye.

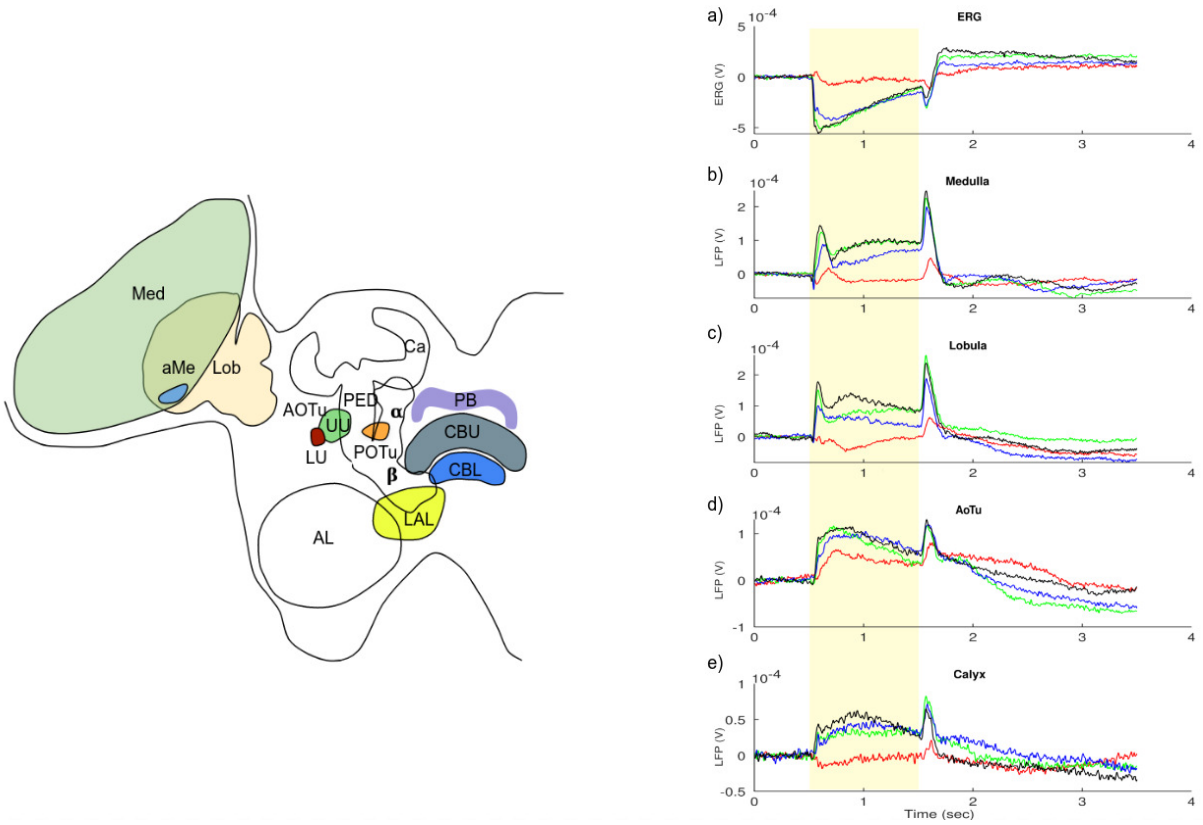

Figure 4.12: Local field potentials at different locations of the brain and GABA A mediated oscillations in the proximal optic lobe. Time of light stimulus indicated in pale yellow. **a)** ERG responses for red, green, blue and white stimuli. **b-e)**. LFP recordings from medulla, lobula, AOTu and calyx of the mushroom body.

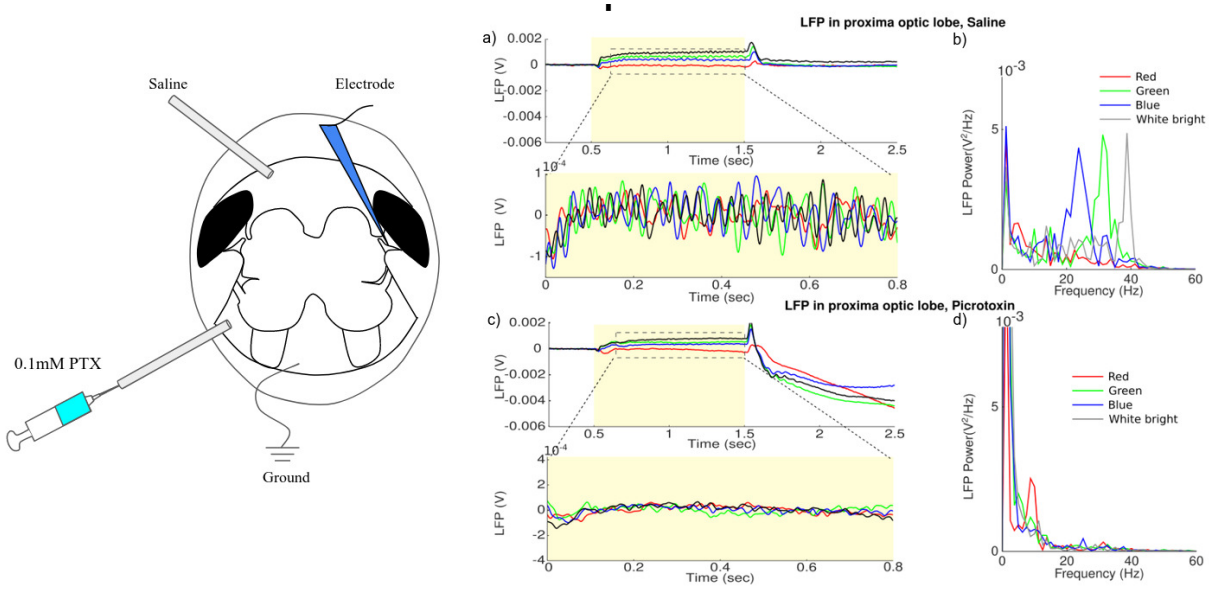

Figure 4.13: a) LFP recording from proximal optic lobe (top) and oscillations present in local field potentials (bottom). b) Power spectrum showing the strength of the oscillations in the proximal optic lobe. c) LFP recording from proximal optic lobe (top) and absence of oscillations in the presence of

picrotoxin (bottom). d) Power spectrum showing the oscillation strength in the proximal optic lobe in the presence of picrotoxin. All traces are average of 5 trials

4.2.5 Oscillations in the proximal optic lobe LFP

While performing LFP recordings from proximal optic lobe (medulla and lobula) (Fig 4.13), 20-40Hz oscillations (Fig 4.12f) were observed for the stimulus red, green, blue and white light. Of which white light LFP responses showed 40Hz osciallations, green light showed 30Hz and for blue light , a range of 20-25Hz were observed. And for red light, hardly we see any oscillations. To check what neurotransmitter is mediating these oscillations, suspecting GABA as the one from previous studies (Stopfer et al., 1997) . To check this, we have used 0.1mM picrotoxin in ringer's saline and mixed fastgreen as a colouring agent to identify whether picrotoxin is injected or not. In our experiments we have used bath application of picrotoxin (Fig 4.13). We have checked the effect of Fast Green mixed saline on oscillations and found out that fast green does not affect the oscillations. Then we injected picrotoxin and fastgreen mixed saline, this abolished the oscillations (Fig 4.12 h-i). This confirms that oscillations are mediated by $GABA_A$ receptors and GABA as the neurotransmitter. After abolition of the oscillations, we immediately replaced the picrotoxin and fastgreen mixed saline with normal saline. As seen in the olfactory pathway the effect of PTX was not reversible (in 8 more hours).

4.3 Discussion

4.3.1 ERG

Electroretinogram of *Hieroglyphus banian* for green, blue and white light stimulus is shown to consist of onset downward deflection, negative sustained potential and offset downward deflection. Whereas for the red light stimulus, ERG response of HB is having positive ON transient, negative sustained receptor potential and negative OFF transient which are same as Drosophila Canton-S ERG for the stimulus presented through mobile screen (Fig 4.8) and Drosophila ERG response for LED stimulus (Heisenberg, 1971; Pak et al.1969).

P.E. Coombe and O. Schmachtenberg reported that 'locusts ERG has negative monophasic response without the transients' (Coombe, 1986; Schmachtenberg & Bicker, 1999). We could reveal ON and OFF transients along with negative monophasic receptor potential in HB ERG response by presenting

red flash stimuli (Fig 4.10a). As there are no reports about red sensitive retinula cells in grasshoppers (see table1), this would be a weak drive caused by the broad spectrum of the red stimuli seen in the screen measurements. Consistent with this on presenting very low white stimulus we saw reduced receptor potential and ON transient above the baseline (Fig 4.10b). In our experiments we could not see the on transients for other coloured stimuli because of the higher intensity of the stimulus as it is hidden in the onset downward transient. Due to higher intensity, input drive has increased to the retinula cells which resulted in higher receptor potential and fast dornward transient which dominated the lamina currents. That is why the positive ON transient is visible as change in slope in the downward onset transient (Fig 4.10d). We could see the similar results in our modelling also (Fig 4.11). This was unlike P.E. Coombe's report, and would imply conserved lamina processing in the orthoptera.

We observed that the amplitude of the transients in HB are much smaller than the transients amplitude in Drosophila. This might be due to the differences in the sizes of retina and lamina. To check this we measured the distance from the surface of the eye to the centre of the lamina (½ (lamina)+retina), Drosophila showed ~82.5µm whereas HB showed ~340µm. That is, HB's distance from the surface of the eye to the centre of the lamina is 4 times the Drosophila distance.

4.3.2 Oscillations

We have shown that oscillations observed in proximal optic lobe are mediated by $GABA_A$ receptor which is similar to what Stopfer et al., 1997 have been observed by perfusing the whole brain with picrotoxin solution while recording LFP from the calyx of the mushroom body of the Apis mellifera. Bicuculline could not abolish the oscillations though it is a $GABA_A$ inhibitor as reported in *Manduca sexta,* as it is ineffective on most of the inhibitory synapses in many insects (Waldrop et al., 1987).

Oscillations have been observed in many sensory systems. Scientists have come up with different explanations for its functional role in the network. Stopfer et al showed that abolishing osillations by PCT compromised similar odour discrimination from which they inferred that oscillations may be

important for this function (Stopfer et al., 1997). Konig et al showed that oscillations are important for synchronising neural responses over large distances (König et al., 1995).

Mogily and Joseph showed that similar odour discrimination best occurred in lower odour concentrations whereas in higher odour concentrations similar odour discrimination did not take place successfully but higher oscillation buildup took place (Mogily PhD thesis). With this they conclude that better discrimination is possible when less $GABA_A$ synaptic strength is required for lower odour concentration compared to higher $GABA_A$ synaptic strength for higher odour concentrations. Their results were consistent with a theory that oscillations can happen when system is carrying out gain control and better similar odour discrimination occurs when there is no requirement of adaptive gain control mechanism. This is not consistent with the theory of oscillations helping fine discrimination (Stopfer et al., 1997).

Chapter 5

Identifying novel neuron types in the proximal optic lobe using intracellular fills and response to a set of diverse stimuli

5.1 Introduction

Visual system, independent of the organism, has to compute and represent elementary features of the visual world including contrast, motion, depth, distance and polarisation. These features then may be used to compute and represent more complex features. Often there is a progression towards computing and representation of more complex features as one moves away from the periphery.

The most elementary feature, a photon of certain wavelength arriving from a particular point in the visual field is registered in the retinula cells in the ommatidia pointed in that direction. Cells in the lamina and medulla that receive input from the retinula cells have been shown to respond to contrast and luminance changes and UV and green colour changes in the stimuli (Currier et al., 2023). Lamina neurons innervate within the lamina or medulla. Medullary neurons have many classes. Some of them innervate within the optic lobe while others send axons to the protocerebral regions or to the contralateral optic lobe.

5.1.1 Neurons of the proximal optic lobe

In the proximal optic lobe neurons have been described that innervate medulla, medulla and compartments of lobula as well as those that innervate one or more compartments of lobula alone. Broadly speaking the neurons innervating lobula and connected to the protocerebral centers respond to large field motion including looming stimuli (Mauss et al., 2014; Mauss et al., 2015; (Paulk et al., 2009); O'Shea & Williams, 1974; (Currier et al., 2023)). Neurons innervating medulla and lobula are involved in computing motion (Borst et al., 2020). Neurons innervating medulla and connecting to

protocerebral centers or to the contralateral optic lobe have been shown to be involved in circadian function. These are results mostly from drosophila, honeybee, dragonflies and locust. In praying mantis, some neurons innervating the lobula and medulla, have been shown to be involved in binocular vision (Rosner et al., 2020). A set of neurons with innervations in medulla express molecules associated with circadian rhythm and have responses that depend on the time of the day (Rojas et al., 2019). A subset of neurons innervating the medulla are polarization sensitive and send their output to anterior tubercles (Jundi et al., 2011). A count of neuron types reported from the proximal optic lobe and their innervation schemes are collated in table 5.1.

Table 5.1: Count of the morphologically identified neuron types reported in the optic lobe of insects with responses to at least one visual stimuli.

S.no	**Species**	**Lobula neurons**	**Medulla neurons**	**Neurons innervating in both lobula and medulla**	**Total**	**Number of papers pooled from.**
1.	Locust	14	9	5	28	7
2.	Cricket	1			1	1
3	Mantis	29	1	2	32	2
4.	Cockroach	1	10	6	17	2
5.	Bees	10	8	2	20	1
6.	Silk moth	3			3	1
7.	Dragonfly	4			4	2
1.	*Hieroglyphus banian* from my recording	5	2	4	11	From our recordings

In orthoptera that includes grasshoppers and crickets, 29 cell types have been reported in the optic lobe including their responses to some subset of stimuli or state. There are some studies that show morphology of the neurons without their response properties.

Previously in our lab we had recorded from the olfactory pathway in *Hieroglyphus banian* (Singh & Joseph 2019) In those recordings they could record from all the cell types that has been reported previously in the olfactory pathway of *S. americana* and no new neuron types. Thus it was concluded that the olfactory circuit in HB to be conserved at this resolution upto fourth order neurons both morphologically and physiologically compared to locust .

On surveying the literature on the optic lobe of insects and pooling together all the known neuron types which have been recorded from and filled, we found a total of 94 cell types to have been reported. Given that the technology involved is fairly old either this is mostly the only cell types present or the sampling of cell types is insufficient in the visual pathway. Given this background we attempt to characterise the cell types in the visual pathway from the proximal optic lobe in *Hieroglyphus banian*.

We have seen in chapter 3 that gross anatomy of the visual pathway of Hieroglyphus banian is similar to that reported in the other orthoptera with notable exception of two novel tracts and their corresponding innervation areas. We also saw in chapter 4 that the ERG, though previously reported to be different in orthoptera compared to other insects in the nature of ON transients, is likely not as much a difference in visual processing as the geometry. We could reveal the presence of ON transients by manipulating the signal strength and spectrum thus demonstrating conserved nature of lamina processing with drosophila. To investigate the nature and distribution of cell types in the visual pathway, we recorded intracellularly from a large number of cells to investigate the response properties to a set of stimuli. We were limited in our stimulus set spectrally to human visible range (Fig 4.7) thus excluding UV stimuli that locust can see. We also did not test for polarisation sensitivity or differential response to binocular stimuli.

For the stimuli we chose one set that spans the class of transitions often tested to investigate early visual processing, namely looming and gratings, fixed and moving. Another set was composed of natural scenes recorded from their habitat (Fig 2.6 showing stimulus in the methods section). We also recorded from these cells while presenting white noise stimuli to test if the response properties can be

explained by constructing linear nonlinear models from white noise analysis (chapter 6) We attempted to fill dye in each of the recorded cells after completion of the recording if the cell was still holding.

We are able to present the morphology and responses to 15 intracellularly filled cell types. We see that only a small subset of them (2 out of 15 cell types) are similar to the types that have been previously reported, indicating that existing sampling of cell types in orthoptera (and also likely in other insects) is likely highly insufficient. We test if the responses to the set of stimuli of all the cells we recorded from are distributed in euclidean space in a similar way for both the classes of stimuli. Using hierarchical clustering we see if cells get clustered in a similar manner for both the stimulus classes. We see that among the filled cells those which cluster together based on response type can be morphologically very different indicating that we need a broader class of stimuli to have critical stimuli in them even when the morphology is very different.

5.2 Results

5.2.1 Classification based on the morphology of neurons

Based on anti-GABA and nc82 staining of the HB brain, the optic lobe has lamina, medulla and lobula complex. Lobula has 4 sub neuropils, outer lobula (OLO), inner lobula (ILO), anterior lobula (ALO) and dorsal lobula (DLO) (Explained in detail in Chapter 3) Here 15 visual neurons are classified into 5 classes based on their innervation pattern. Neurons which are innervating in lobula exclusively, neurons which are innervating in medulla exclusively, neurons which are innervating in both lobula and medulla, neurons which are recorded from the optic lobe but innervation in optic lobe could not be found due to loss of optic lobe during tissue processing and visual neurons in central protocerebrum having arborisations in tritocerebrum. There are 5 lobula neurons (Fig 5.1-5.5), 2 medulla neurons (Fig 5.6-5.7), 4 neurons which are innervating in both medulla and lobula (Fig 5.8-5.11)and 2 neurons recorded from the optic lobe but could not identify the innervations due to the loss of optic lobe while processing (Fig 5.12-5.13) and 2 neurons in central protocerebrum having arborisations in tritocerebrum (Fig 5.14-5.15). There is 1 more lobula neuron (Fig A2) 2 medulla neurons (Fig A3-A4) and 1 lobula-medulla neuron (Fig A5) filled while presenting stimulus through

LED setup (Table A1). Neurons have been named based on the following rules. First letter of the name is either T or C based on their Tangential innervation or columnar innervation. A neuron is defined as tangential neuron if its innervation is parallel to the layers of the neuropil and as columnar if the neuron innervation is restricted only to some part of the neuropil. If the neuron's innervation is neither tangential nor columnar, then the first letter of the neuron is omitted. Second letter of the neuron represents the innervation pattern in the optic lobe. Me is for medulla, Lo for lobula, I for ILO, O for OLO, D for DLO, A for ALO. If the neuron innervation in the optic lobe is in more than one region, then the next letters in the neuron's name represent the neuropil in which the neuron is innervating. Letters pro and tri represent the neuron innervation in protocerebrum and tritocerebrum respectively. Letter com represents the commissural neuron, which connects two neuropils on the both sides of the brain. And for neurons which are recorded from optic lobes but optic lobes lost during tissue processing, such neurons are named as OL for the optic lobe along with the region in which they are innervating.

5.2.1.1 Lobula neurons

1) TOpro/ LGMD1

In HB, LGMD cell body is situated antero-ventrally in the optic stalk. It arborizes in lobula with three subfields and a thicker axon arborises in the superior protocerebrum. In lobula, LGMD subfiled A has thicker and smoother arborizations in the outer lobula (OLO) excluding the first or distal layer of the OLO. Subfield A has curved fan shape appearance restricted upto the second layer of the OLO posteriorly, which is devoid of GABA, which is an indication of receiving excitatory inputs from preceding neuropils (Fig 5.1a). Subfield B has finer and smoother arborisations in the fourth or proximal layer of the OLO, which is prominently GABA positive and Subfield C has smoother arborizations in dorsal lobula finer than subfield B (Fig 5.1b). DLO is also prominently GABA positive. Inferring that both subfield B and C receive inhibitory inputs from preceding neuropils. LGMD has mean spiking activity of 7.0 spikes/sec, responding to loom in and to transition from white to grey, grey to drift, drift to grey, white noise to natural stimuli and for transitions between the natural stimuli with high firing rate (Fig 5.1c and d).

2) TOpro1: Commissural neuron

This neuron cell body is located next to the posterior lateral protocerebrum. This neuron is recorded from the contralateral proximal optic lobe. Main branch of the axon crossing the midline of the brain through the great commissure (GC) and having punctate structured arborizations throughout the contralateral posterior lateral protocerebrum (PLP) (Fig 5.2a), further the main branch has smoother arborizations in the proximal layer of the contralateral outer lobula (4th layer of OLO) (Fig 5.2b). This neuron baseline firing rate is 8 spikes/sec. This neuron is excited only for a few frames of white noise but not for other synthetic stimuli. However this neuron strongly responds when the scene changes to green colour possibly indicating innate relevance.

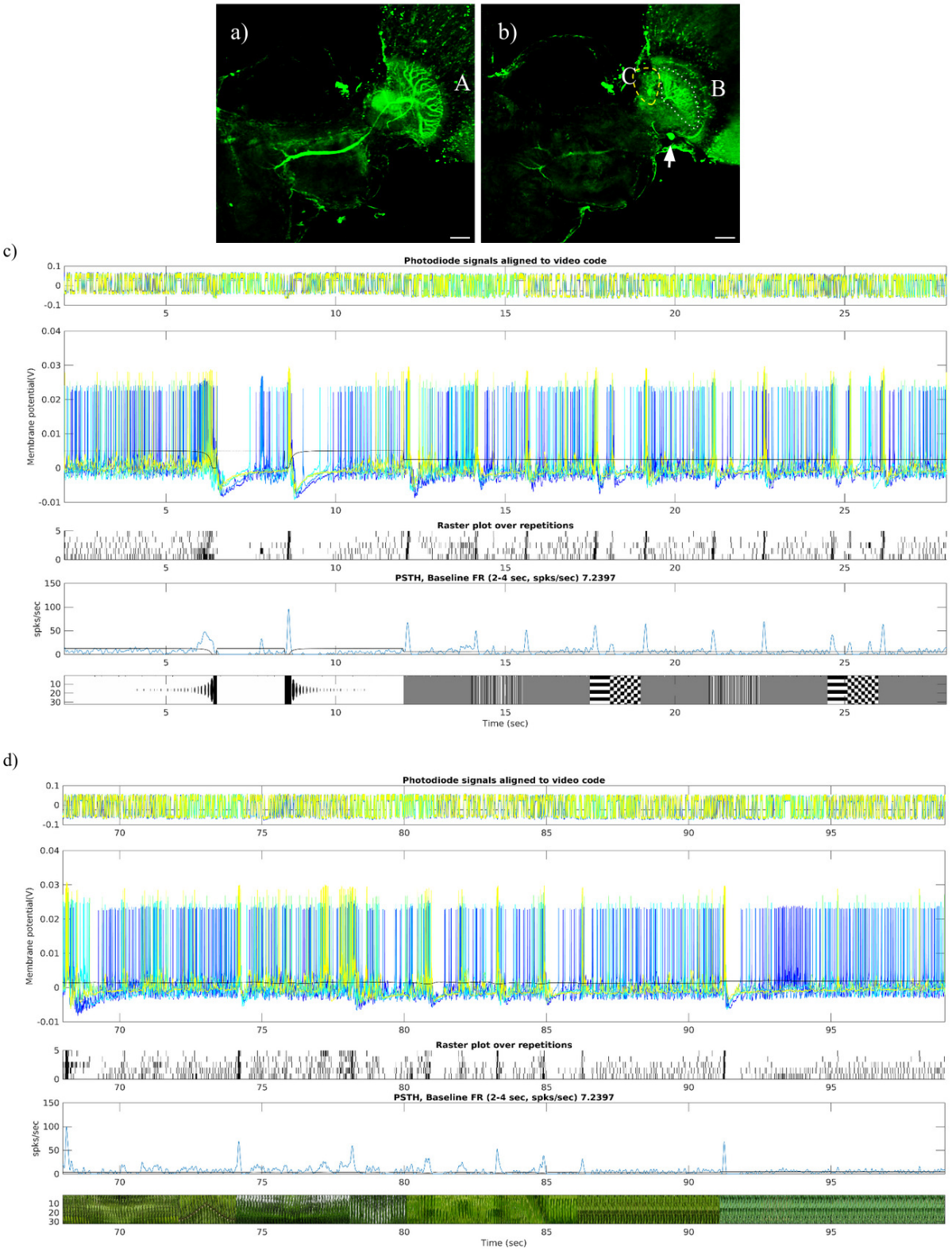

Figure 5.1: LGMD1/TOpro neuron morphology and responses to a set of the stimulus. a) Neuron branch A innervating into the 2nd and 3rd layers of OLO. b) Branch B and C innervating into the 4th layer of OLO (GABA rich region) and DLO respectively. c) Responses for stimulus set A d) Responses for stimulus set B. Scale bars: 100µm.

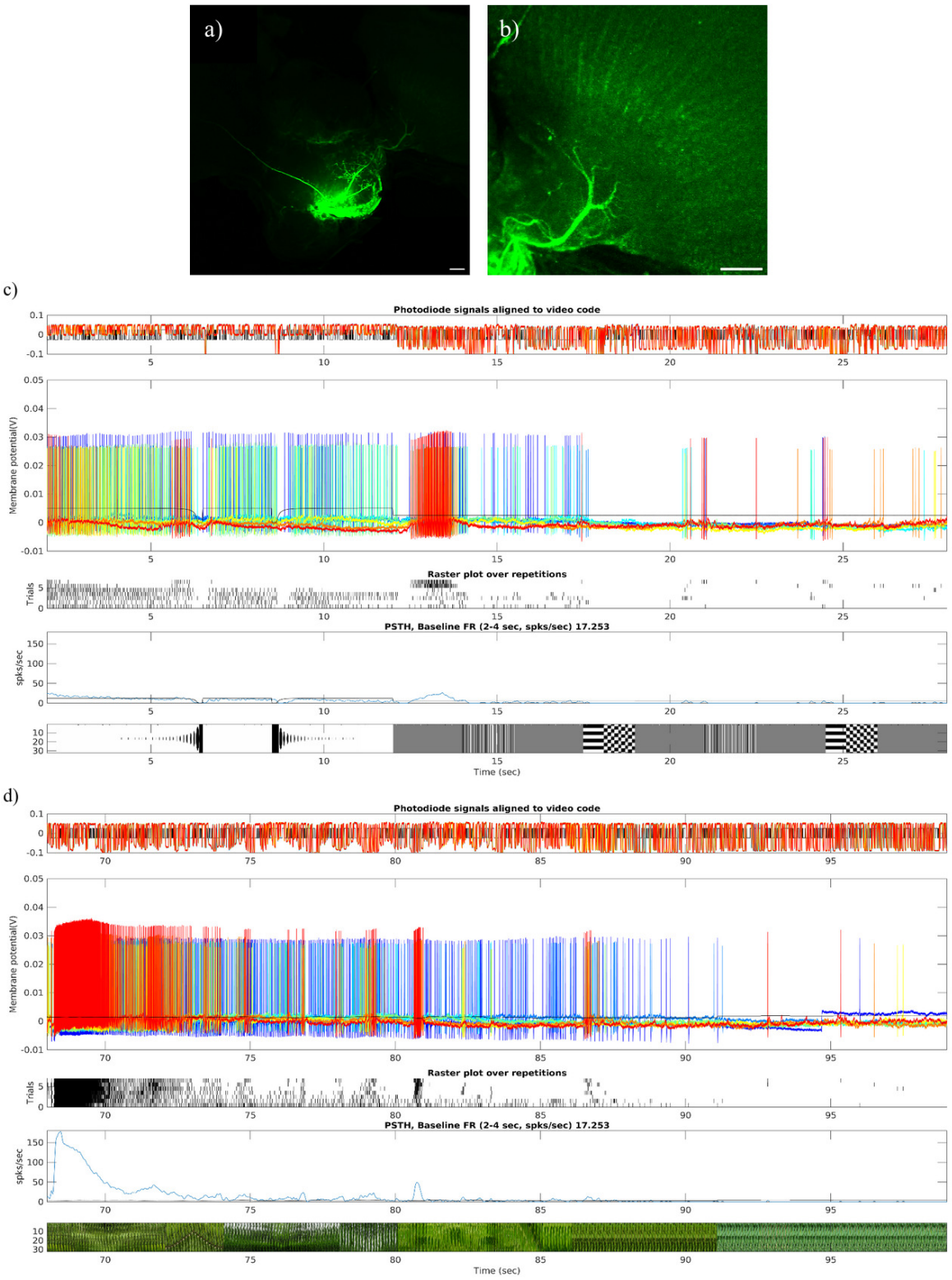

Figure 5.2: TOpro1: Commissural neuron neuron morphology and responses to a set of the stimulus. a) Neuron innervations in the PLP with punctate structures. b) Smooth arborisation of the neuron in the 4th layer of OLO. c) Responses for stimulus set A d) Responses for stimulus set B. This neuron strongly responds when the scene changes to green colour. Scale bars: 100µm.

3) TO neuron:

This neuron is recorded from Lobula. Could not identify its cell body. In one of the nc82 stained brains, there is an unknown structure anterior to the outer lobula, extended from dorsal to ventral. This particular neuron is localised in that region (Fig 5.3 a&b). This neuron is inhibited for loom in off dark and transitioning from grey to drift. Excited to loom out of dark and transitioning from white to grey, drift to grey and white noise to natural stimuli (Fig 5.3 c&d).

4) TLoprocom

This neuron cell body is located at the junction between the optic lobe and central brain anteriorly. This is an interlobular neuron, connecting lobula's in both the optic lobes. This neuron is innervating throughout the proximal outer lobula and inner lobula with smooth arborizations in the ipsilateral optic lobe (Fig 5.4b). Main branch of the neuron which is innervating in the ipsilateral optic lobe, is also innervating in the contralateral optic lobe by crossing the midline of the brain (Fig 5.4a). In the contralateral optic lobe, this neuron has punctate arborisations in DLO,3rd and 4th (proximal) layers of OLO and majorly in the upper unit of ILO, very few arborizations in the lower unit of the ILO (Fig 5.4c-e). In contralateral protocerebrum it has two sub branches (Fig 5.4a). This neuron basal response is 8.0 spikes/sec. It responded to the loom in stimulus, transition from white to initial loom out, transition from white to grey,grey to drifting and back to grey background. And for transitioning from white noise stimuli to natural stimuli (Fig 5.4f-g).

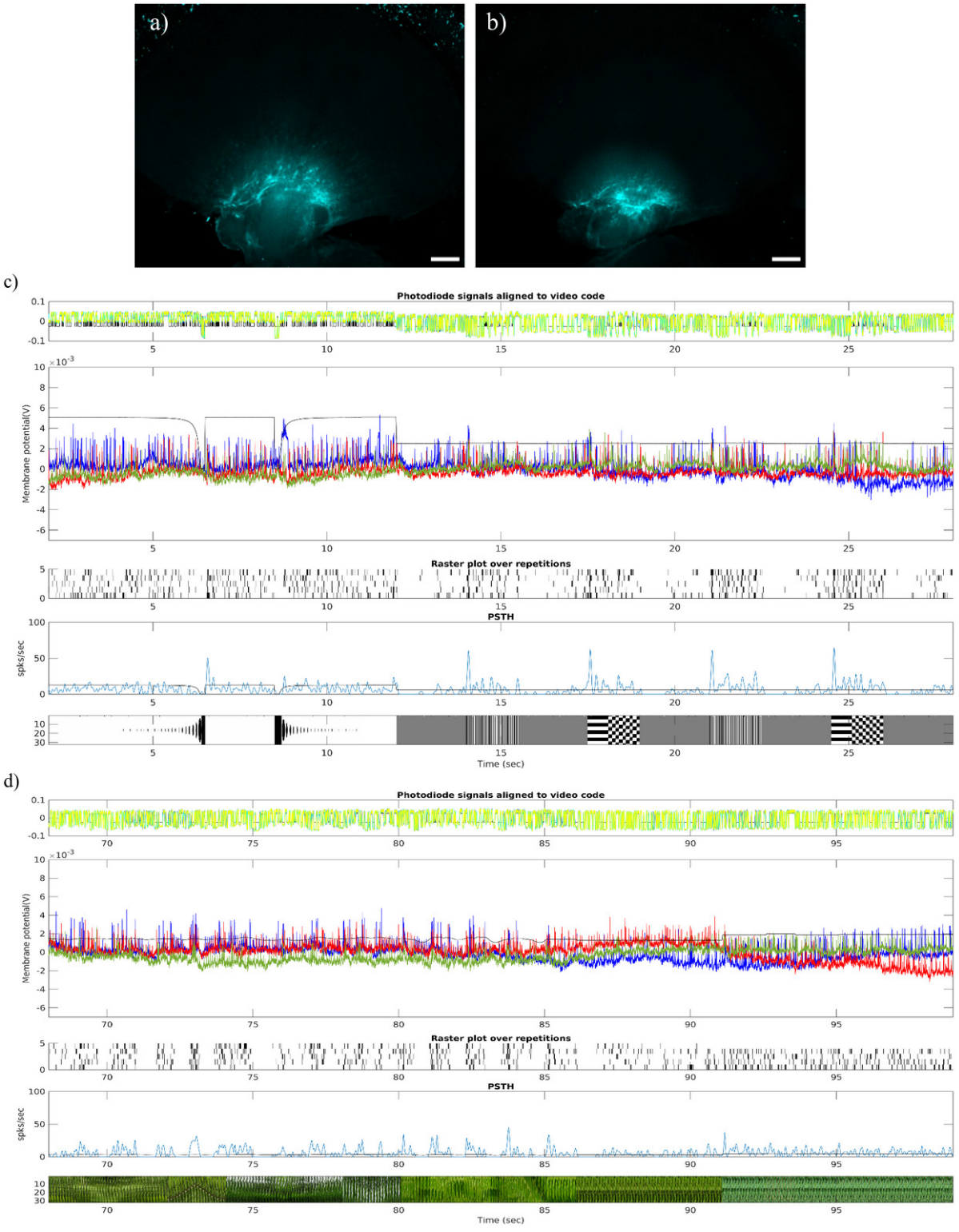

Figure 5.3: TO neuron morphology and responses to a set of the stimulus. a&b) TO neuron innervation in an undefined region in the optic lobe anterior to the OLO. c) Neuron response to stimulus set A. d) Neuron response to stimulus set B. Scale bars: 100µm.

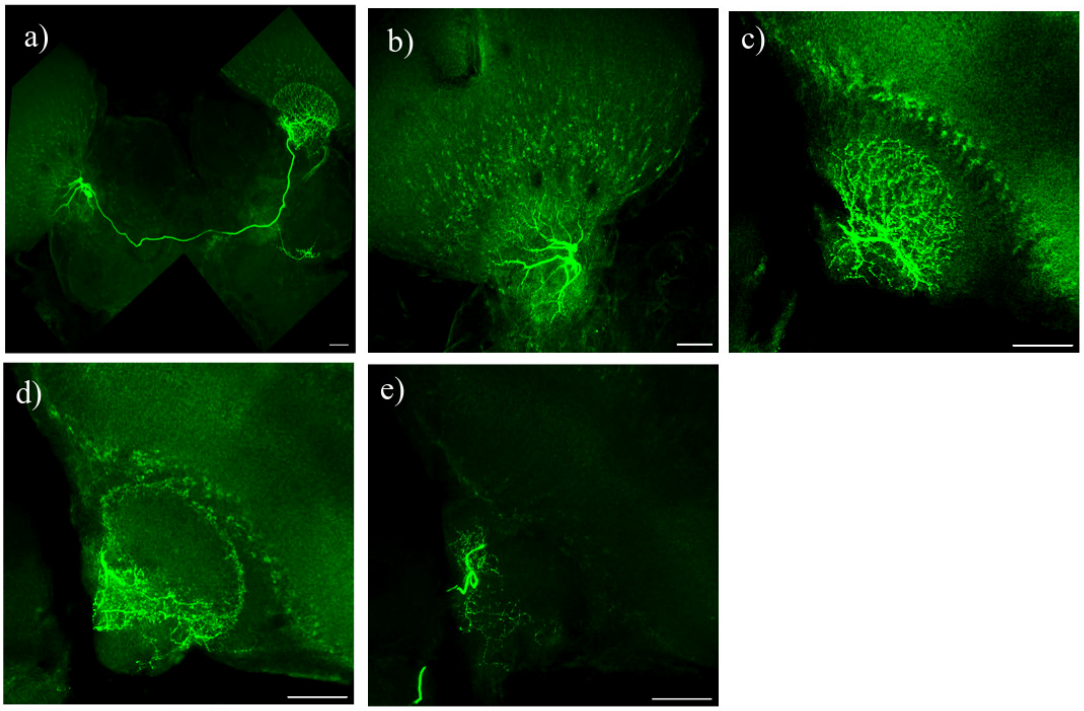
a)
b)
c)
d)
e)

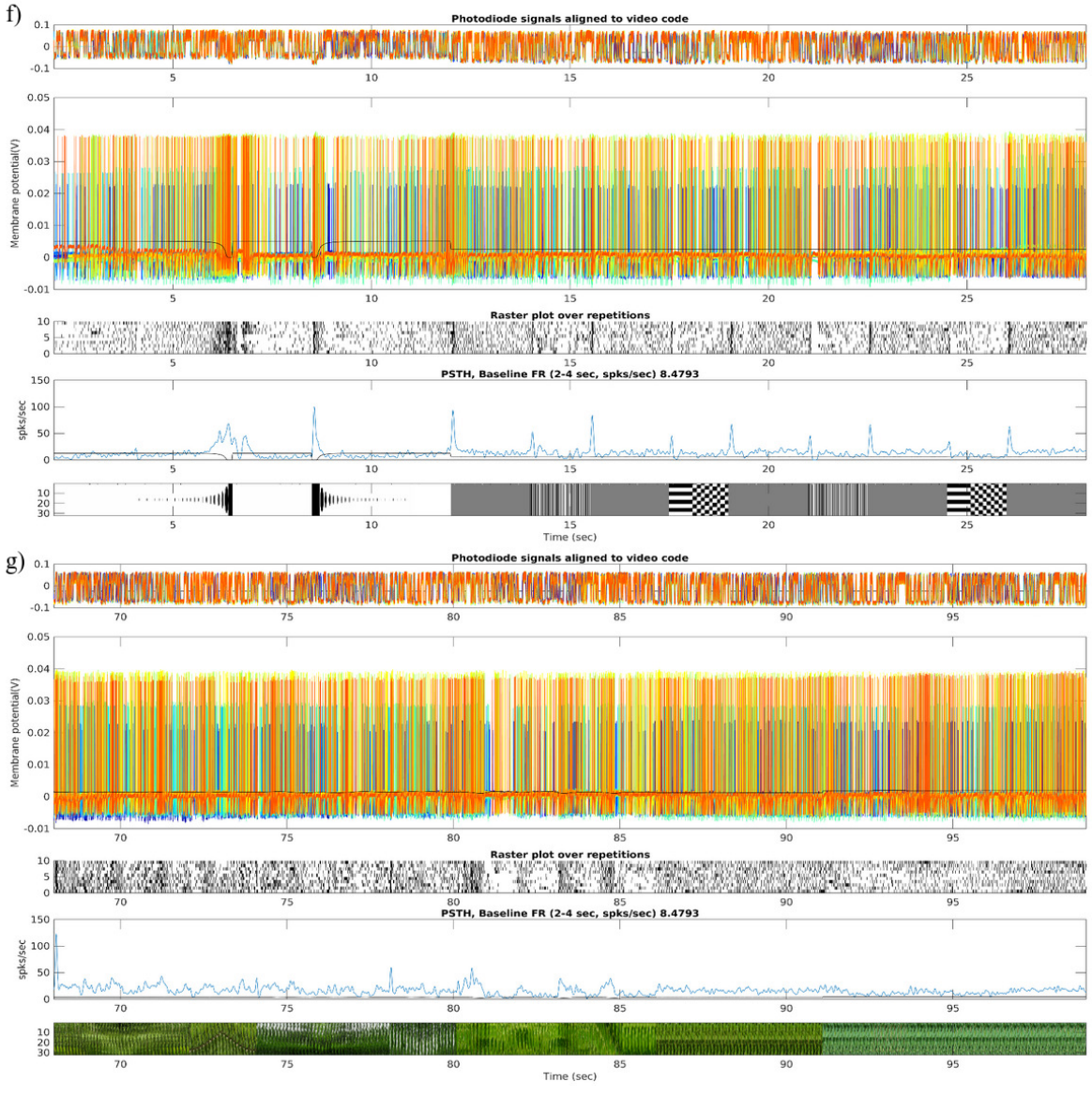
f)
Photodiode signals aligned to video code
Membrane potential(V)
Raster plot over repetitions
PSTH, Baseline FR (2-4 sec, spks/sec) 8.4793
spks/sec
Time (sec)
g)
Photodiode signals aligned to video code
Membrane potential(V)
Raster plot over repetitions
PSTH, Baseline FR (2-4 sec, spks/sec) 8.4793
spks/sec
Time (sec)

Figure 5.4: TLoprocom neuron morphology and responses to a set of the stimulus. a) TLoprocom neuron innervating in lobula's of both the optic lobes and two branches having punctate arborisations in contralateral protocerebrum. b) Zoomed in picture to show the smooth arborisation in the ipsilateral lobula. c-e) Zoomed in picture to show the punctate arborisation in the contralateral lobula. f) Neuron responses to the stimulus set A g) Neuron responses to the stimulus set B. Scale bars: 100µm.

5) TLotri:

This neuron is recorded from the proximal lobula region. Its cell body is located anteriorly just above the antennal lobe. It has two major regions of arborisation. One in optic lobe other in tritocerebral region of the brain (Fig 5.5a). In optic lobe, in posterior lobula this neuron is innervating with five major branches and with many sub-branches having button-like structures, indicating output regions of the neuron. Whereas in tritocerebrum, having three major branches one of them going towards midline of the brain in tritocerebral region. Other two branches having sub branches innervating in tritocerebral region towards the VNC (Fig 5.5a). This neuron has 29 spikes/sec as basal response for white and grey background whereas transitioning from white to grey has a response of 35 spikes/sec. This neuron responded to loom in,transitions between drifting, just above the basal response for loom out and for transitioning natural stimuli (Fig 5.5c-d). This neuron responded to a clap sound also.

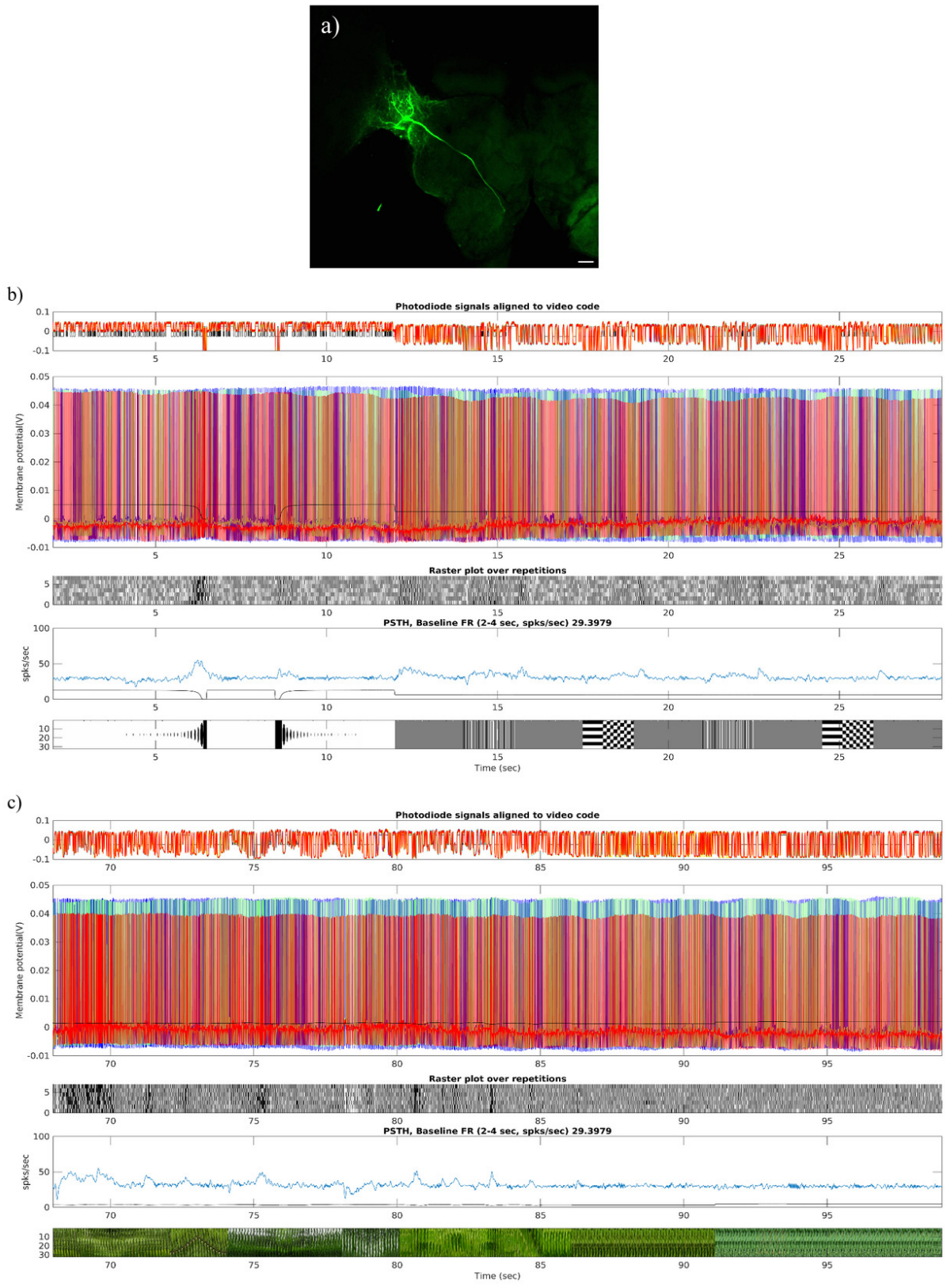

Figure 5.5: TLotri neuron morphology and responses to a set of the stimulus. a) TLotri neuron ipsilateral innervation in posterior lobula and in the tritocerebrum. b) Neuron responses to the stimulus set A. c) Neuron responses to stimulus set B. Scale bars: 100µm.

5.2.1.2 Medulla neurons

1) CMe:

Cell body could not be found. Smoother arborizations throughout the dorsal and ventral portion of the medulla (Fig 5.6a-b). This neuron baseline rate is 6 spikes/sec. This neuron is responding to an increase in brightness (Fig 5.6c-d).

2) TMepro:

Could not identify the cell body of this neuron. In the optic lobe this neuron is arborising in the proximal medulla with punctate structures (Fig 5.7 a-d). Major branch of the neuron also innervating in the posterior lateral protocerebrum (PLP) of the brain ipsilaterally with smooth arborisations. This neuron baseline rate is 9 spikes/sec. This neuron is responding for loom in of dark, loom out of dark and for transitions (white to grey, drift to grey and transitions between the natural stimuli) (Fig 5.7e-f).

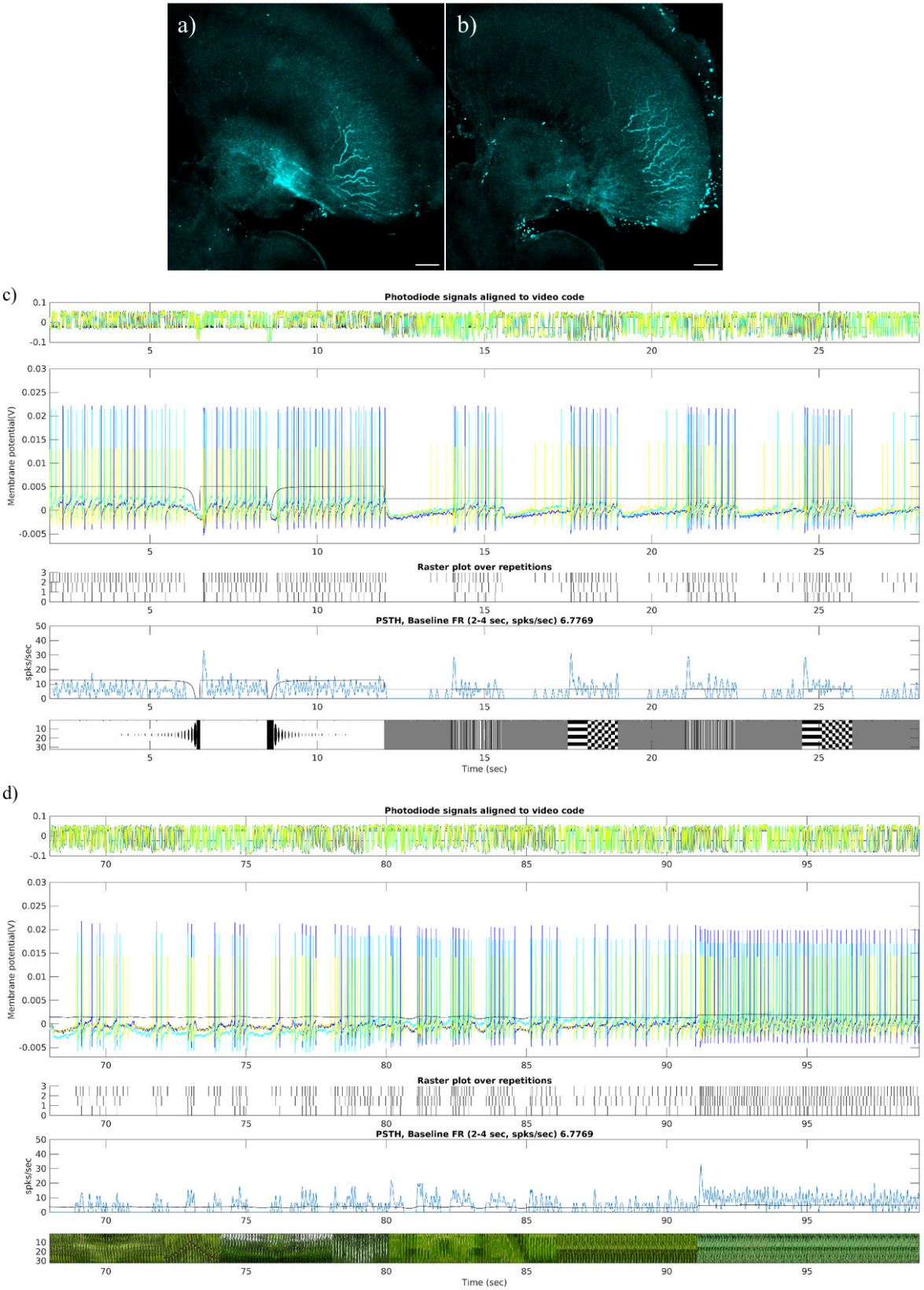

Figure 5.6: CMe neuron morphology and responses to a set of the stimulus. a) CMe neuron is arborised throughout the medulla. c) Neuron responses to stimulus set A. d) Neuron responses to stimulus set B. Scale bars: 100µm.

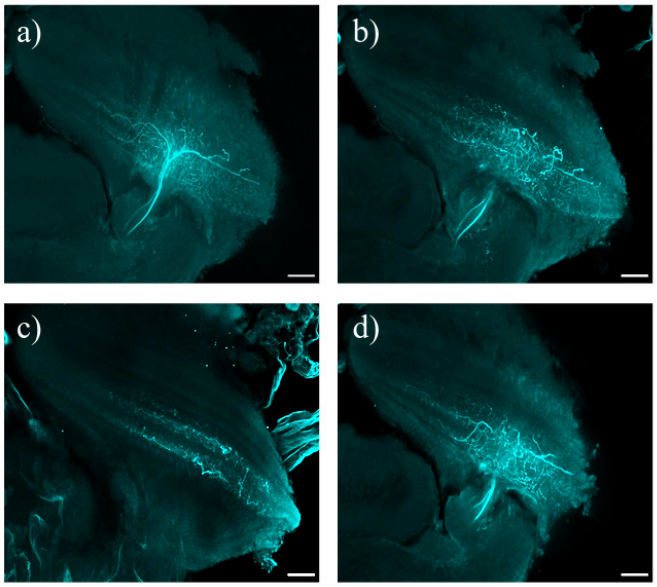
a)
b)
c)
d)

f)

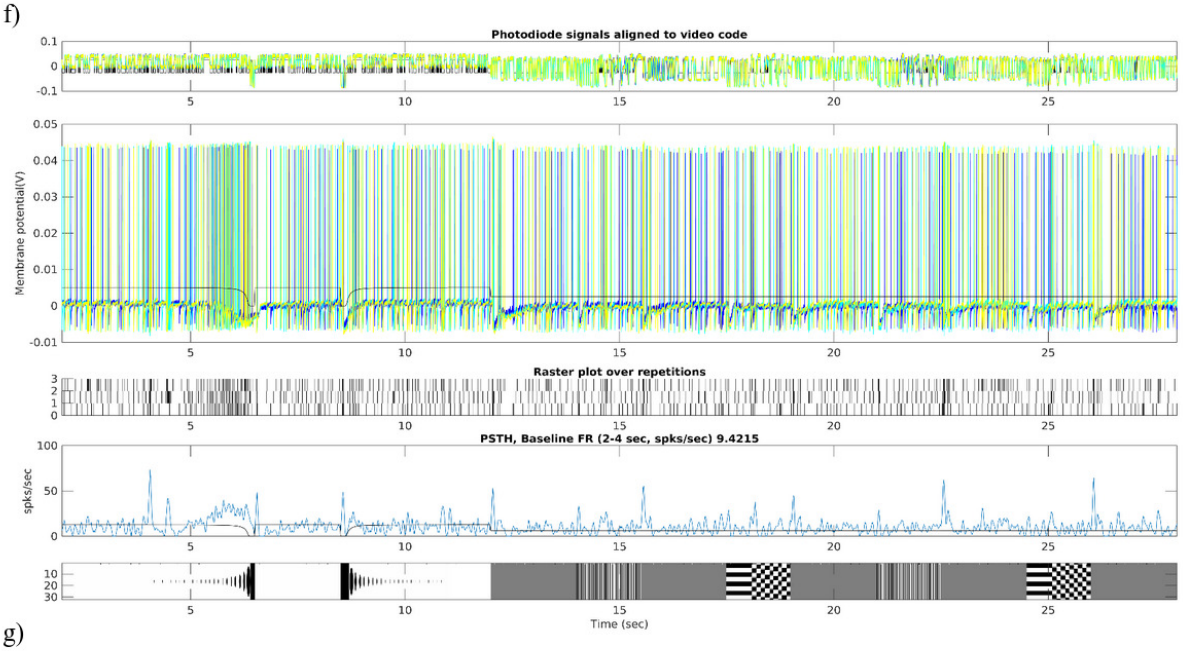
Photodiode signals aligned to video code
Membrane potential(V)
Raster plot over repetitions
PSTH, Baseline FR (2-4 sec, spks/sec) 9.4215
spks/sec
Time (sec)

g)

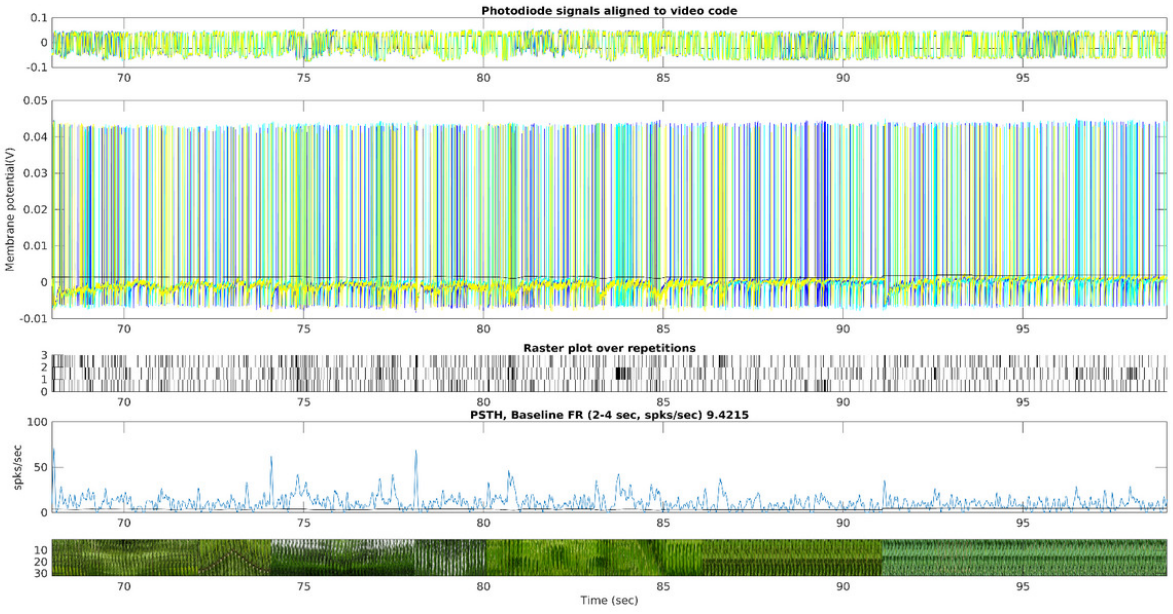
Photodiode signals aligned to video code
Membrane potential(V)
Raster plot over repetitions
PSTH, Baseline FR (2-4 sec, spks/sec) 9.4215
spks/sec
Time (sec)

Figure 5.7: TMepro neuron morphology and responses to a set of the stimulus. a-d) TMepro neuron arborisation in two layers of proximal medulla. e) Neurons responses to the stimulus set A. f) Neurons responses to the stimulus set B. Scale bars: 100μm.

5.2.1.3 Lobula-Medulla neurons

1) CMeOI:

This neuron is recorded from the proximal optic lobe. Its cell body is located anteriorly in between the space of DLO and ILO (Fig 5.8a, white arrow). This neuron arborisation is restricted to the ipsilateral optic lobe. It has one major branch and one sub-branch. Major branch having smooth arborization entering into the medulla anteriorly and innervating throughout the medulla in single layered manner (Fig 5.8a). Main branch is bifurcated at the junction of medulla and lobula. From there the bifurcated sub branch descended into the inner lobula anteriorly. This sub branch bifurcated again posterior to the cell body and this bifurcated branch demarcated the boundary between ILO and OLO. This bifurcated sub-branch has smoother innervations throughout the proximal layer of the OLO (Fig 5.8b-c). Innervations into the medulla and OLO are smooth and innervations into the ILO are punctate. Inferring the input signals are collected from medulla and OLO and give output into the ILO.

This neuron's baseline firing rate is 9.0 spikes/sec. This neuron responded to transition from white background to black loom out, white background to grey transition, and to natural stimuli moving from left to right. However it did not respond to the drifting grating moving left to right (Fig 5.8d-e).

2) *DMe:*

This neuron is recorded from the proximal lobula. In this preparation we could not identify the cell body nor its complete innervation. We could see punctate innervation in DLO and four fibres from DLO entering into the medulla (Fig 5.9b-c).

This neuron basal response rate is 13 spikes/sec. This neuron is getting inhibited for final loom in of dark and initial loom out of dark stimuli, getting inhibited for transitions (white to grey, grey to drift and drift to grey, white noise to natural stimuli and transitions between natural stimuli) Inhibition is greater for grey to drift transition compared to drift to grey transition.And no inhibition for transition from grey to white noise (Fig 5.9d-e).

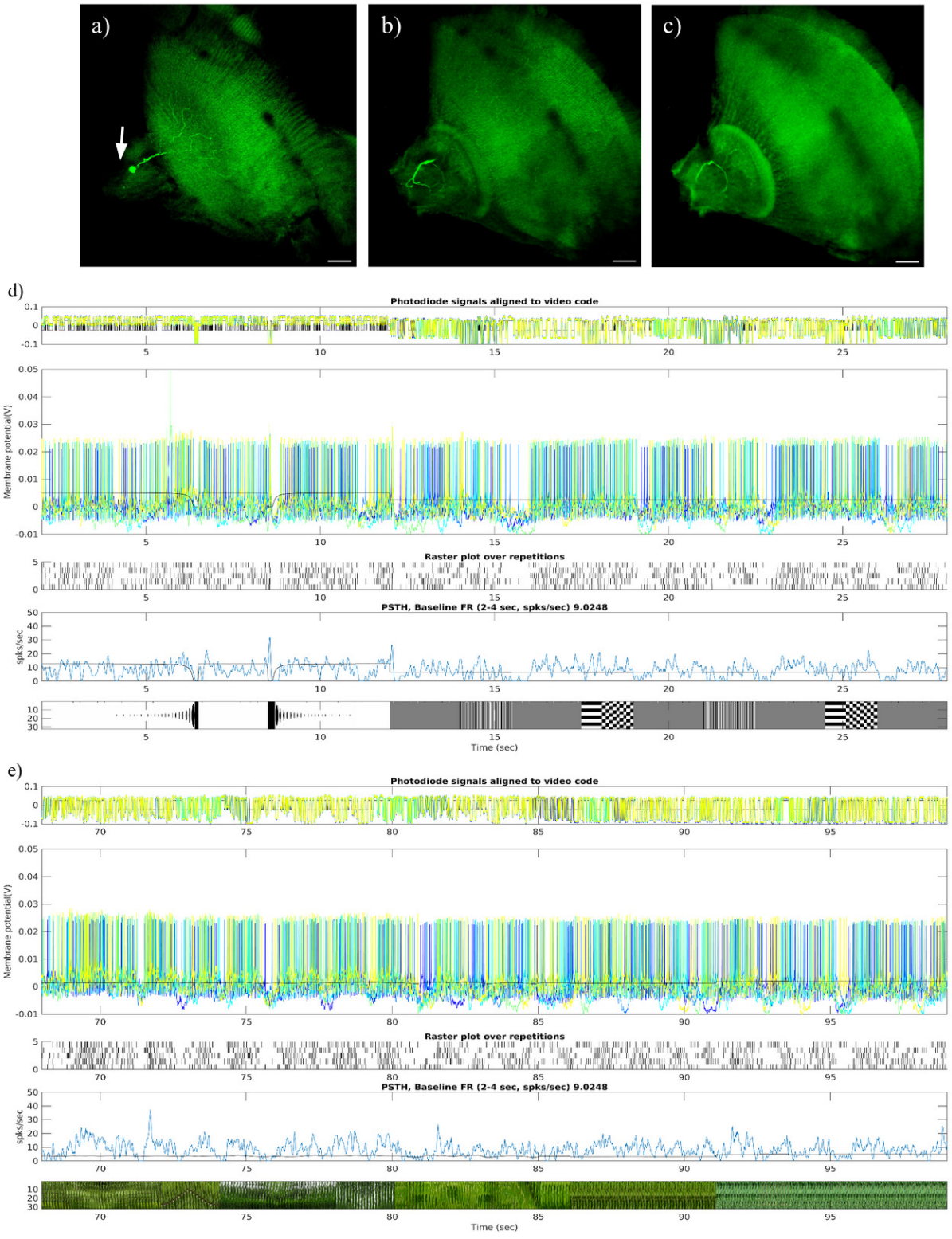

Figure 5.8: CMeOI neuron morphology and responses to a set of the stimulus. a) CMeOI neuron innervation in medulla (cell body is indicated by white arrow). b-c) Neuron innervation in lobula. d) Neuron responses to stimulus set A. e) Neuron responses to stimulus set B. Scale bars: 100µm.

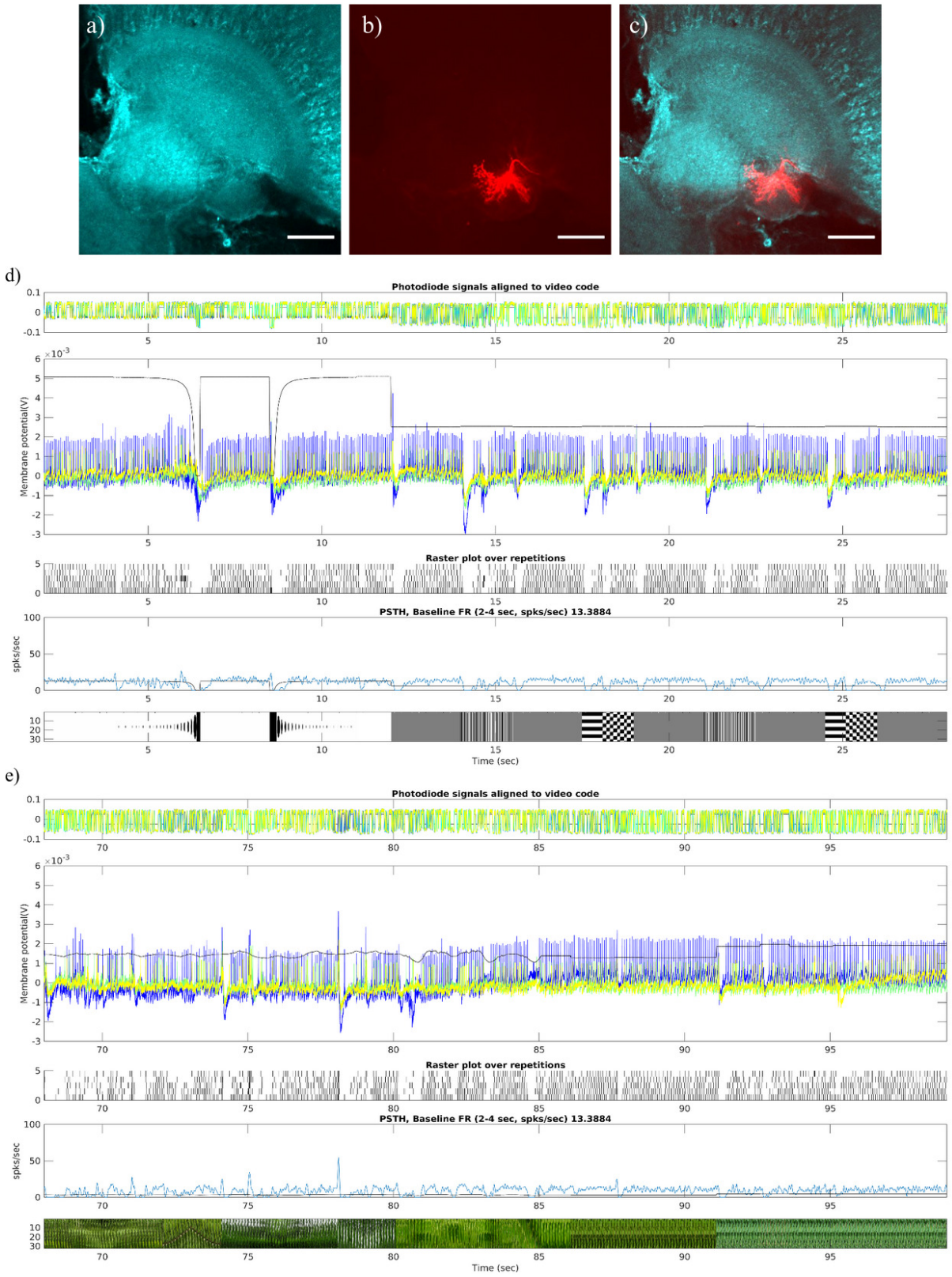

Figure 5.9: DMe neuron morphology and responses to a set of the stimulus. a) Autofluorescence image of the lobula. b) DMe neuron innervation in DLO. c) Merged picture of both a & b. d) Neuron responses to stimulus set A. e) Neuron responses to stimulus set B. Scale bars: 100µm.

3) TMeIpro

This neuron is recorded from the proximal optic lobe. Its cell body is located right to the midline of the brain, anteriorly between the antennal lobes. It has two major regions of arborizations. One in the optic lobe. In the optic lobe one branch arborises throughout the upper unit of the inner lobula (ILO-U) with punctate structures (5.10a), indicating the output regions whereas the other branch enters and has smooth arborizations throughout the medulla forming at least two layers (5.10b). Main branch innervating into the ventro medial neuropils in the protocerebrum has five sub-branches. One of the sub branches has punctate structures arborising throughout the anterior ventro lateral protocerebrum (AVLP) next to the lateral horn. Other branches are innervating AVLP without much arborisation (5.10c). Main branch of the neuron looks like crossing the midline of the brain and entering the tritocerebrum but could not trace further. This neuron has a basal response of 50 spikes/sec. This neuron is responding to all the stimuli except for white noise stimuli. And responding to transitions (Fig 5.10d-e).

4) TMeOpro:

This neuron cell body is located posteriorly left to the midline of the brain, between the antennal lobes (5.11a). This neuron is crossing the midline of the brain and entering the contralateral side of the brain posteriorly, dorsal to the contralateral antennal lobe main branch divided into three branches, both the branches having smooth arborisations in the ventral protocerebrum, among them one branch is innervating posteriorly towards the lower unit of the central complex and other branch is innervating towards antennal lobe posteriorly. Third branch travelling anteriorly and arborising in the anterior lobula (ALO) and dorsal portion of the proximal OLO and then entering the medulla and innervating throughout the medulla (5.11d). All innervations in the optic lobe are having punctate structures (Fig 5.11a-e). Indicating that this neuron is receiving inputs from the contralateral ventral protocerebrum and giving output into the optic lobe. This neuron basal level response is 23.0 spikes/sec. This neuron is responding to loom in of dark, initial loom out of dark and getting inhibited as loom out happens. This neuron is responding for transitions grey to drift and drift to grey and also for transitions between natural stimuli (Fig 5.11f-g).

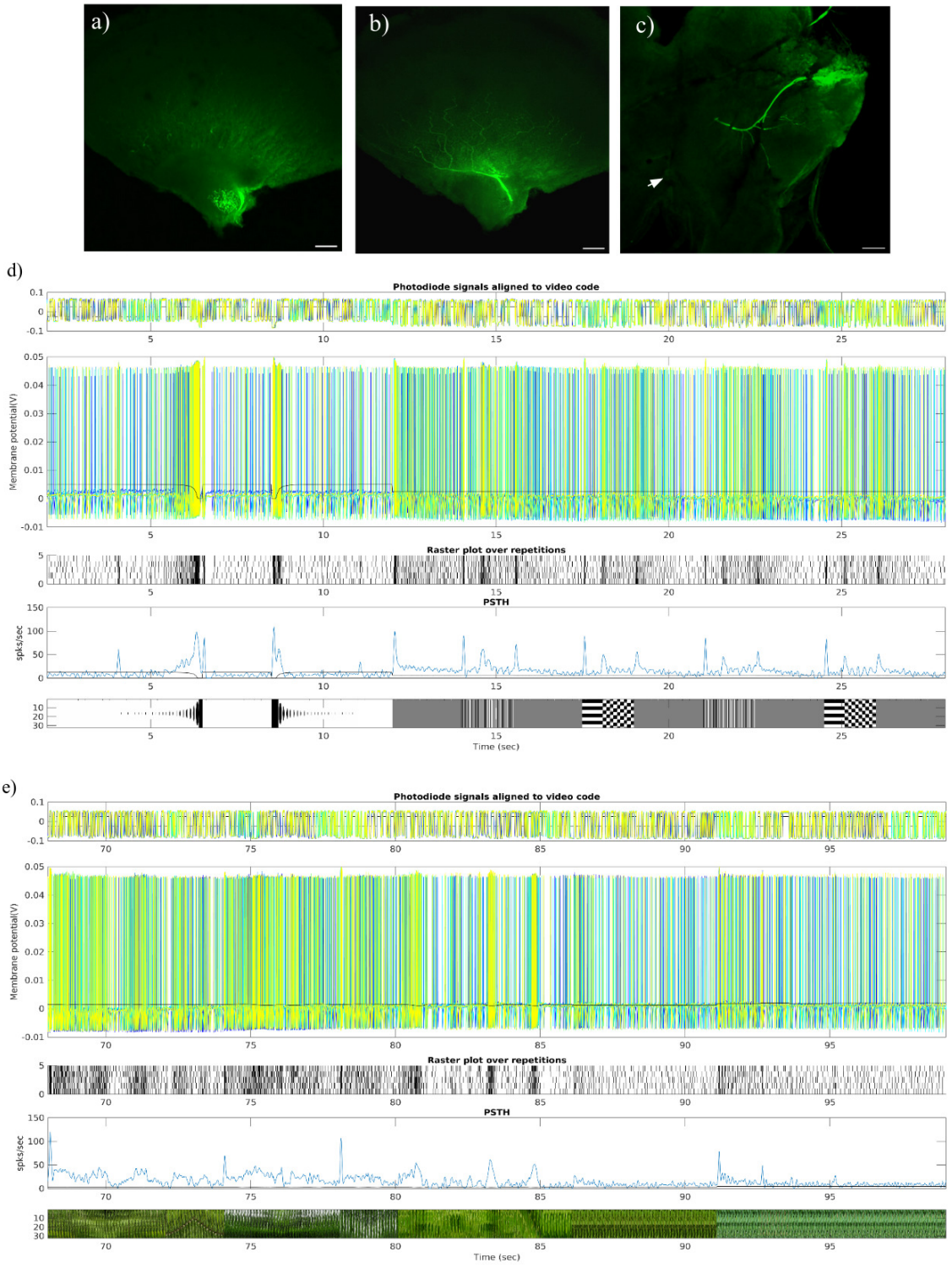

Figure 5.10: TMeIpro neuron morphology and responses to a set of the stimulus. a) TMeIpro neuron innervation in the upper unit of the inner lobula (ILO-U). b) TMeIpro neuron innervation in medulla. c) TMeIpro neuron innervation in anterior ventrolateral protocerebrum (white arrow indicates cell body). d) Neuron responses to the stimulus set A. e) Neuron responses to the stimulus set B. Scale bars: 100µm.

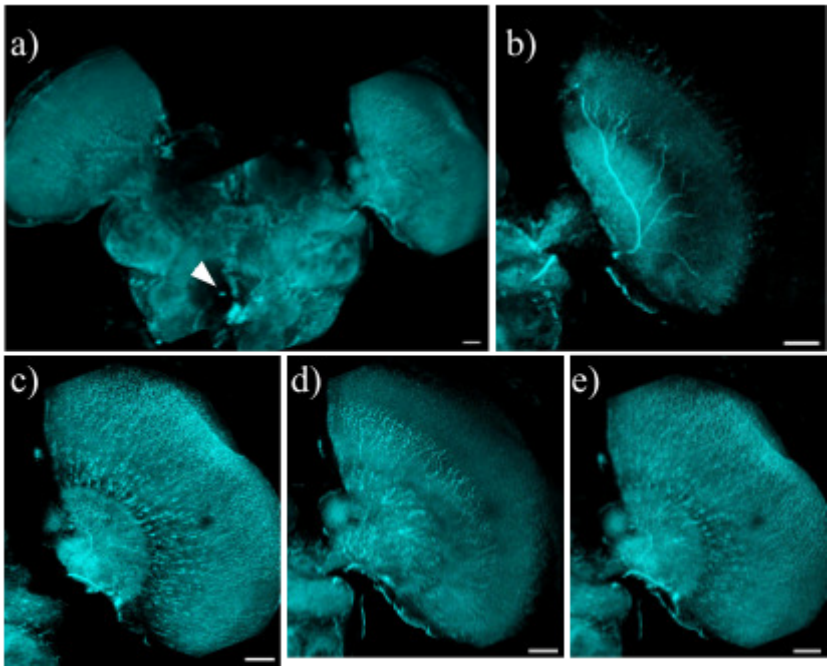
a)
b)
c)
d)
e)

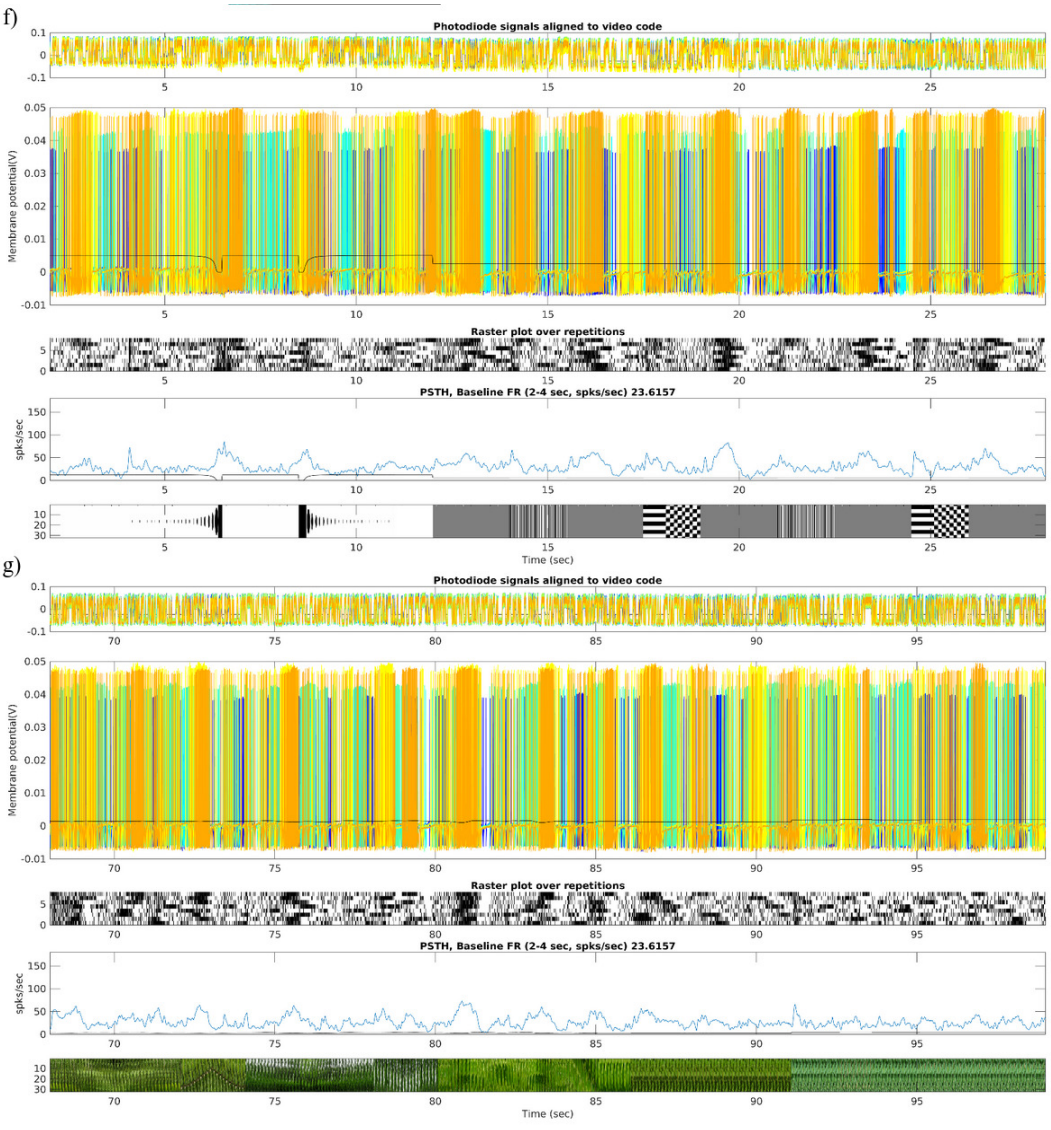
f)
Photodiode signals aligned to video code
Membrane potential(V)
Raster plot over repetitions
PSTH, Baseline FR (2-4 sec, spks/sec) 23.6157
spks/sec
Time (sec)
g)
Photodiode signals aligned to video code
Membrane potential(V)
Raster plot over repetitions
PSTH, Baseline FR (2-4 sec, spks/sec) 23.6157
spks/sec
Time (sec)

Figure 5.11: TMeOpro neuron morphology and responses to a set of the stimulus. a) TMeOpro neuron innervation in contralateral optic lobe (white arrowhead indicates the cell body of the neuron). b-e) TMeOpro neuron zoomed in to show the punctate arborisation into the ALO, OLO and medulla. f) Neuron responses to the stimulus set A. g) Neuron responses to the stimulus set B. Scale bars: 100µm.

5.2.1.4 Neurons recorded from optic lobe but optic lobes are lost during tissue processing

1) *OL+ procom*

This neuron is recorded from the junction between the optic lobe and central brain. Lobula part of the optic lobe is missing and we could not find any innervations in the remaining optic lobe. In the central brain, the neuron is innervating posteriorly in the ventral protocerebrum of the brain on both sides of the midline with punctate structures (Fig 5.12a). Even at the midline of the brain also there are few arborizations with punctate structures. As the neuron is recorded from the optic lobe & central brain junction, and there are no innervations in the left over brain (Lobula is missing) It might be possible that somewhere in lobula this neuron is receiving inputs and giving outputs into the ventral protocerebrum. This neuron baseline firing rate is 2 spikes/sec. This neuron is getting inhibited for all the transitions (dark to white, white to dark,white to grey,grey to drift,drift to grey,white noise to natural stimuli) but not responding for transition from grey to white noise stimuli. This neuron is excited for stationary gratings and stationary natural stimuli but gets inhibited for moving gratings and moving natural stimuli (Fig 5.12b-c).

2) OL+pro :

This neuron is recorded from the proximal optic lobe. This neuron has punctate structure arborisations in the posterior slope of the protocerebrum (Fig 5.13a). This neuron baseline firing rate is 6 spikes/sec.This neuron is getting inhibited for almost all the transitions (Fig 5.13b-c).

3) *pro-tri:*

This neuron cell body is located anteriorly at the knob of the peduncle where alpha lobe and beta lobe structures join, in anterior ventrolateral protocerebrum (AVLP) main branch of the neuron having finer branches is entering into the ipsilateral tritocerebrum (Fig 5.14a). This neuron baseline rate is 5 spikes/sec. This neuron is responding for loom in of dark, loom out of dark and transitions between the stimuli (Fig 5.14b-c).

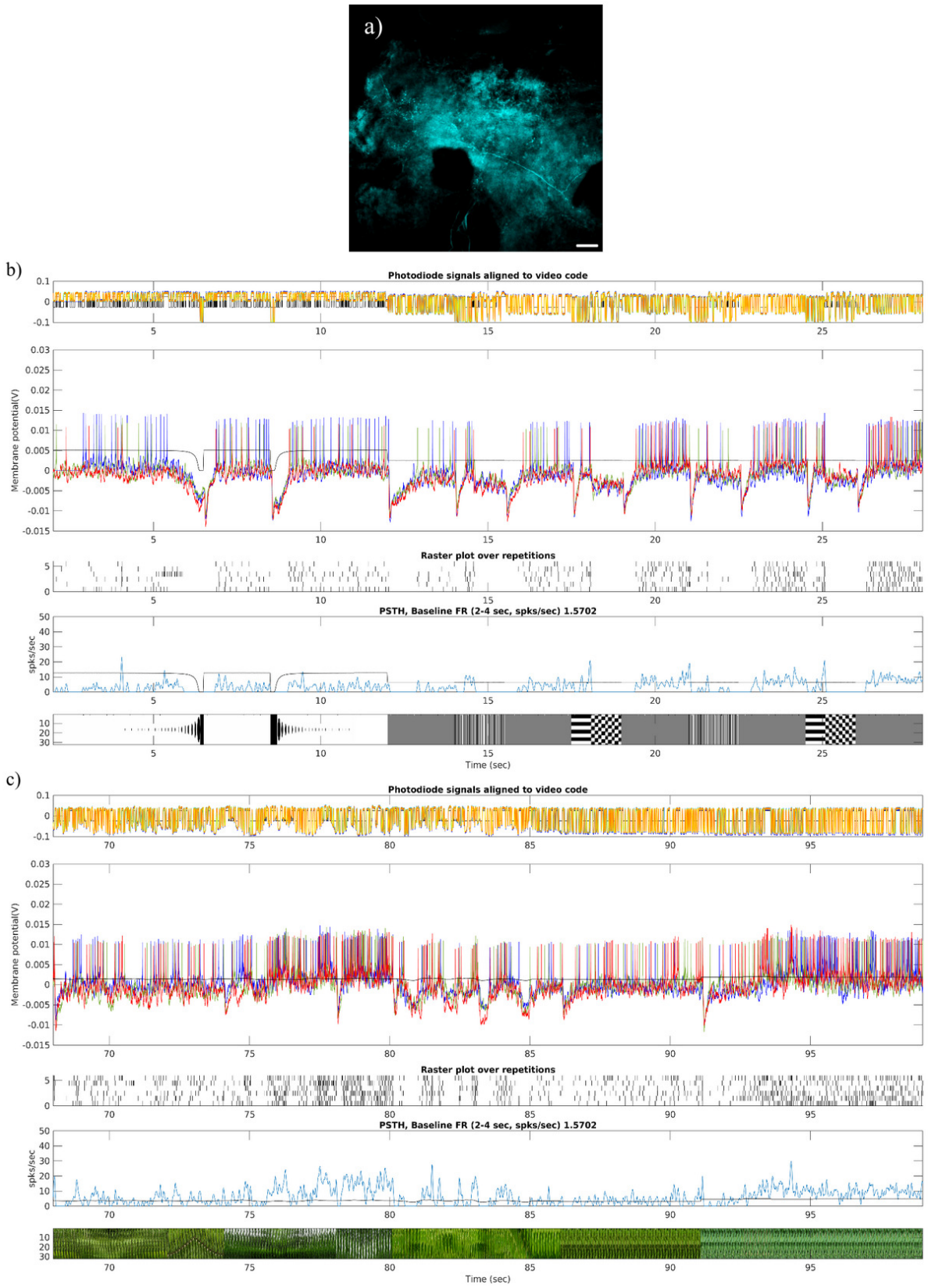

Figure 5.12: OL+procom neuron morphology and responses to set of the stimulus. a) Neuron innervation in the ventral protocerebrum with punctate structures. b) Neuron responses to the stimulus set A. c) Neuron responses to the stimulus set B. Scale bars: 100µm.

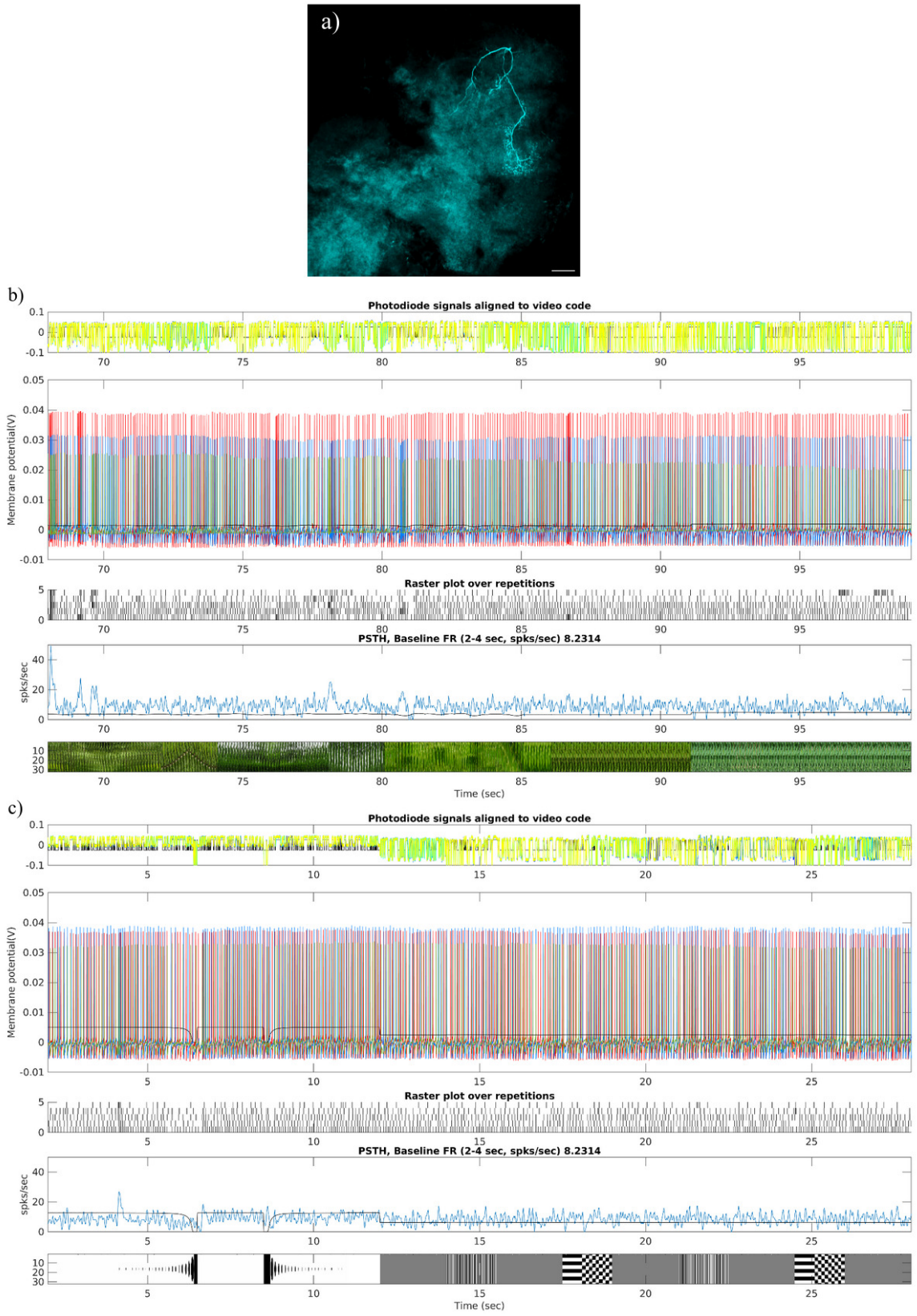

Figure 5.13: OL+pro neuron morphology and responses to a set of the stimulus. a) OL+pro neuron punctate structure arborisations in the posterior slope of protocerebrum. b) Neuron responses to stimulus set A. c) Neuron responses to stimulus set B. Scale bars: 100µm.

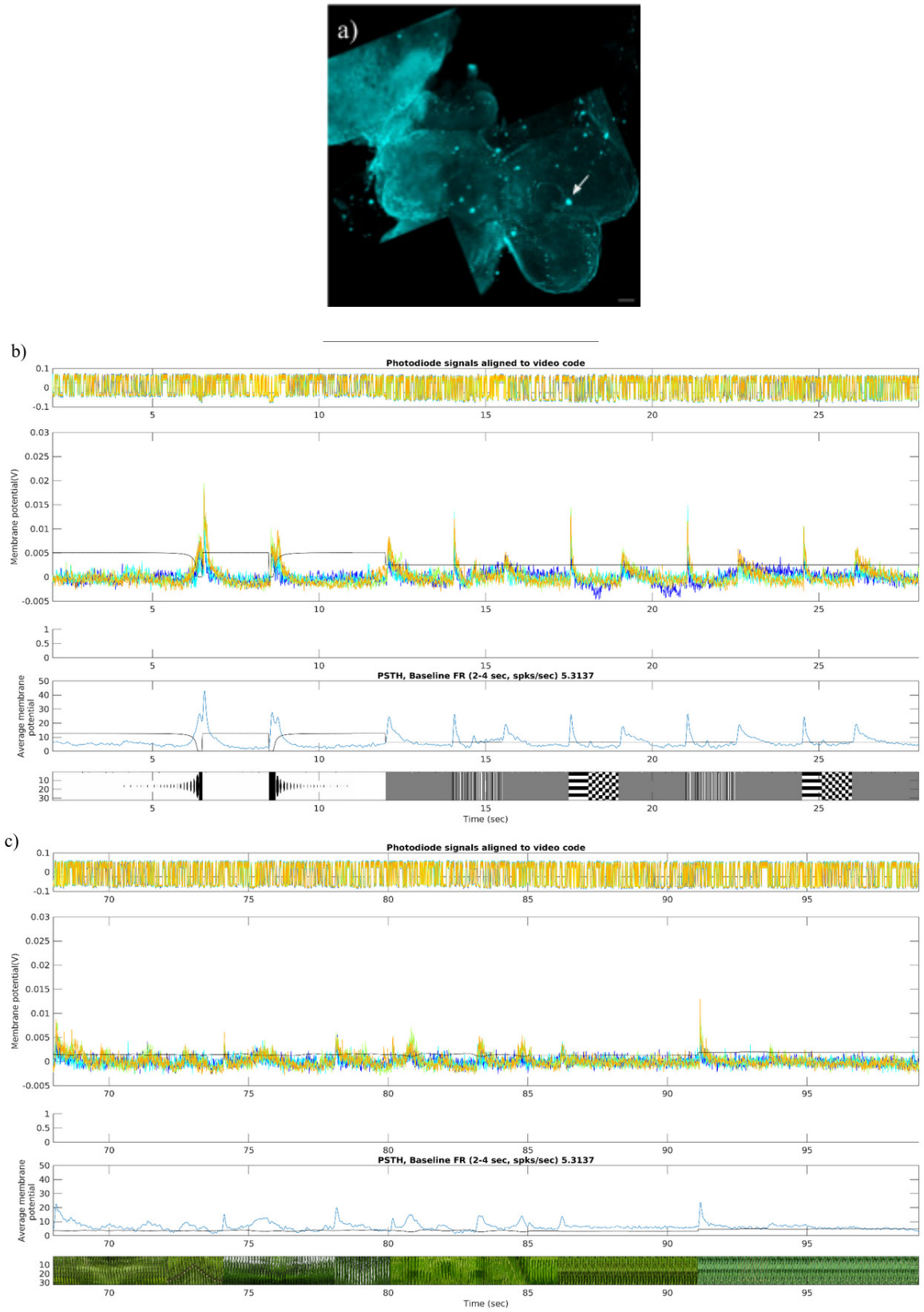

Figure 5.14: pro-tri neuron morphology and responses to a set of the stimulus. a) pro-tri neuron innervation in ventral protocerebrum (white arrow indicates the cell body of the neuron). b) Neuron responses to stimulus set A c) Neuron responses to stimulus set B.

4) pro-tri1:

This neuron is recorded from right to the midline of the brain, ventral to the calyx. Cell body is located in the superior intermediate protocerebrum (SIP) (white arrow in Fig 5.15a). This neuron has many smoother arborisations in the medial protocerebrum, the main branch of the neuron further innervating into the ventral protocerebrum having punctate arborisation structures. And then the neuron is innervating into the tritocerebrum (Fig 5.15a). This neuron baseline firing rate is 7 spikes/sec.This neuron is responding for loom in of dark, loom out of dark and all transitions (white to grey, grey to drift, drift to grey,white noise to natural stimuli and transitions between natural stimuli) This neuron is also excited to the left to right grating movement and for natural stimuli moving left to right (Fig 5.15b-c).

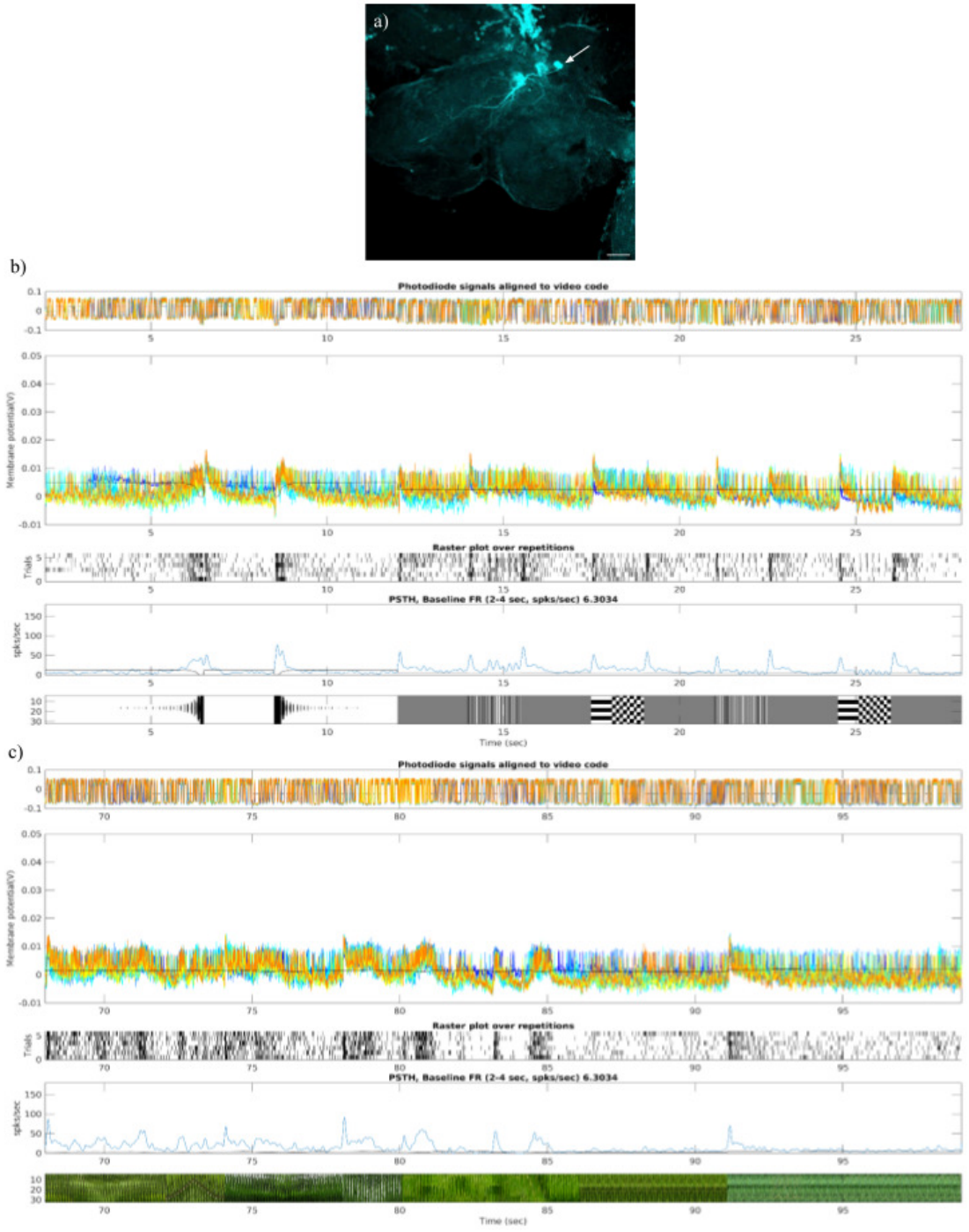

Figure 5.15: pro-tri1 neuron morphology and responses to a set of the stimulus. a) pro-tri1 neuron innervation into the medial protocerebrum (cell body is indicated by white arrow). b) Neuron responses to stimulus set A. c) Neuron responses to stimulus set B. Scale bars: 100µm.

Table 5.2: Neuron's morphology and their responses.

S.No:	Neuron	Cell body	Innervation	Excitatory response to
01	TOpro	Antero-ventrally in optic stalk	In the optic lobe, branch A innervates 2 and 3rd layers of OLO, branch B innervates 4th layer of OLO and branch C innervates in DLO. And in the protocerebrum, thich axon arborises in the superior protocerebrum.	Responding to loom in and to transition from white to grey, grey to drift, drift to grey, white noise to natural stimuli and for transitions between the natural stimuli with high firing rate
02	TOpro1	PLP	Commissural neuron, having smoother arborization in the contralateral OLO and punctate arborization in the contralateral PLP.	Responded to a few frames of WN stimuli, but not for other synthetic stimuli. This neuron strongly responds when the scene changes to green colour.
03	TO	Could not identify	Smoother arborizations in the OLO	Inhibited for loomin of dark, transitioning from grey to drift. Exciting for loom out, transitioning from white to grey,drift to grey and WN to natural stimuli.
04	TLoprocom	Junction of OL and central brain	Interlobular neuron, smoother arborizations in ipsilateral lobula and punctate arborizations in contralateral lobula.	Exciting for the loom-in of dark and for transitions between the stimuli.
05	TLotri	Anteriorly just above the AL	Smoother arborizations in ipsilateral tritocerebrum and punctate structured arborization in posterior lobula.	Exciting for loomin, loom out and transitions between the stimuli. Responding to clap sound..
06	CMe	Could not identify	Smoother arborizations throughout the dorsal and ventral portions of the medulla.	Exciting for increase in brightness
07	TMepro	Could not identify	Punctate structured arborisation in inner medulla, smoother arborisation in PLP	Responding for loom in of dark,loom out of dark and for transitions between the stimuli.

08	CMeOI	Lobula	Smoother arborizations in OLO and throughout the medulla. Punctate structures in ILO.	Exciting for transitions, natural stimuli moving from left to right but not for drifting stimuli moving from left to right.
09	DMe	Could not identify	Punctate structured arborisation in DLO, four fibres from DLO entering into the medulla.	Getting inhibited for transitions, inhibition is greater for grey to drift transition compared to drift to grey.
10	TMeIpro	Right to the midline of the brain between the antennal lobes.	Punctate arborization in the upper unit of the ILO, smoother arborizations in medulla and in AVLP.	Responded for all the stimuli except for WN.And for transitions of the stimuli.
11	TMeOpro	Posteriorly left to the midline of the brain, between the AL's.	Smooth arborizations in the contralateral posterior slope. Punctate structured arborization in contralateral OL (ALO,OLO and medulla)	Exciting for the loomin of dark and transitions between the stimuli. Inhibiting for loom out of dark.
12	OL+proco m	Could not identify	Commissural neuron, punctate structured arborization in inferior protocerebrum of the brain. Optic lobes are missing.So, can't talk about the innervation in optic lobes.	Inhibited for transitions and moving gratings and natural stimuli. Excited for stationary gratings and natural stimuli.
13	OL+pro	Could not identify	This neuron has punctate structure arborisations in the posterior slope of the protocerebrum.	It's getting inhibited for almost all the transitions.
14	pro-tri	AVLP	Smoother arborization in ipsilateral tritocerebrum	Responding for loom in of dark, loom out of dark and transitions between the stimuli.
15	pro-tri1	SIP	Smoother arborization in the medial protocerebrum, punctate arborisations in the inferior protocerebrum and major branch innervating into the tritocerebrum.	Responding to loom in of dark, loom out of dark, transitions between the stimuli,left to right moving drifting and natural stimuli.

5.2.2 Classification of neurons based on response pattern

For classifying neurons based on response pattern, only those cells are considered to which we presented visual stimuli using Samsung Tab. Using Samsung Tab, we presented synthetic stimuli like loom in of dark, loom out of dark, drifting grating and white noise stimuli. And we also presented natural stimuli like grassy fields moving in different directions, appearance of conspecific species and a predator. Overall the stimuli duration is 103 sec. Whereas for classifying cells we used loomin of dark, loom out of dark and drifting grating as synthetic stimuli (Stimulus set A) and grassy fields moving in different directions as natural stimuli set (Stimulus set B). In this experimental setup I have recorded 150 cells from the proximal optic lobe (Fig 5.16). Among 150 cells, 15 cells are filled with intracellular dyes to view the morphology. These 15 cells were classified based on response pattern for synthetic stimuli and natural stimuli.

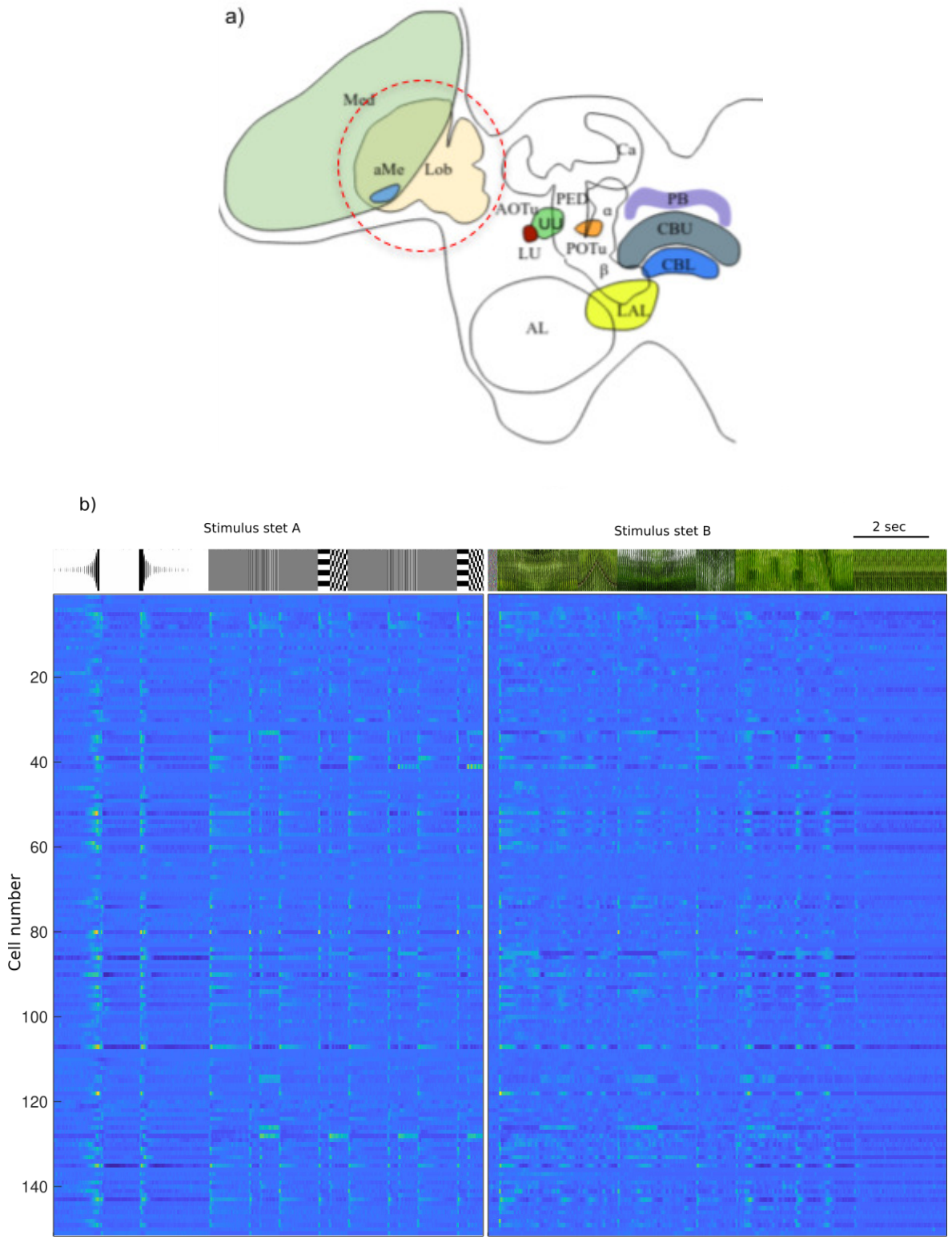

Figure 5.16: a) Dotted red circle indicates locations from which the cells were recorded b) PSTH of all the recorded cell's response to the stimuli. The time course of the video stimuli is indicated as concatenated frames above.

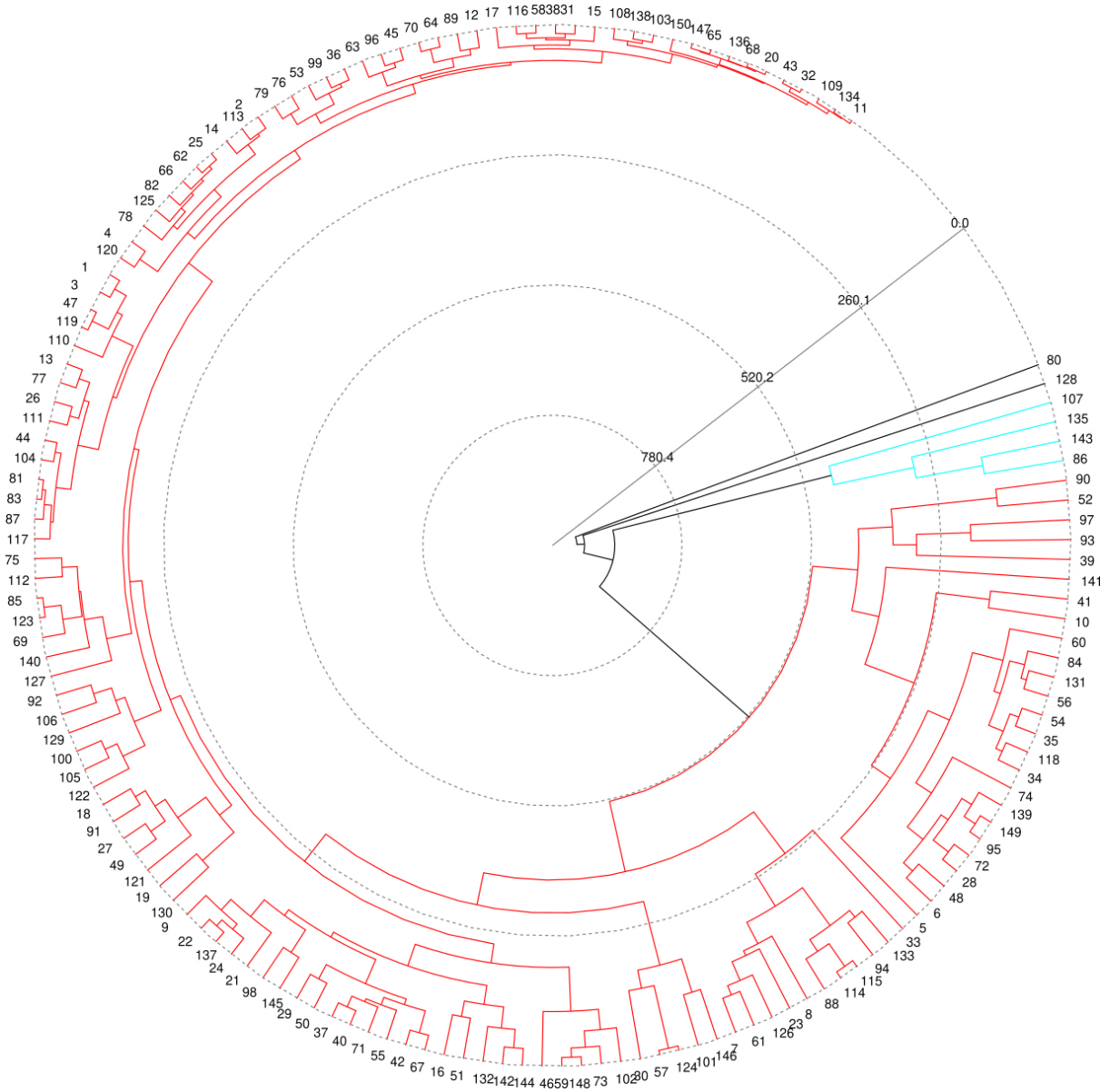

Figure 5.17: a) Polar dendrogram showing hierarchical euclidean distance relationship of the responses of all the recorded 150 neurons for stimulus set A. Cophenetic distance (0.8912)

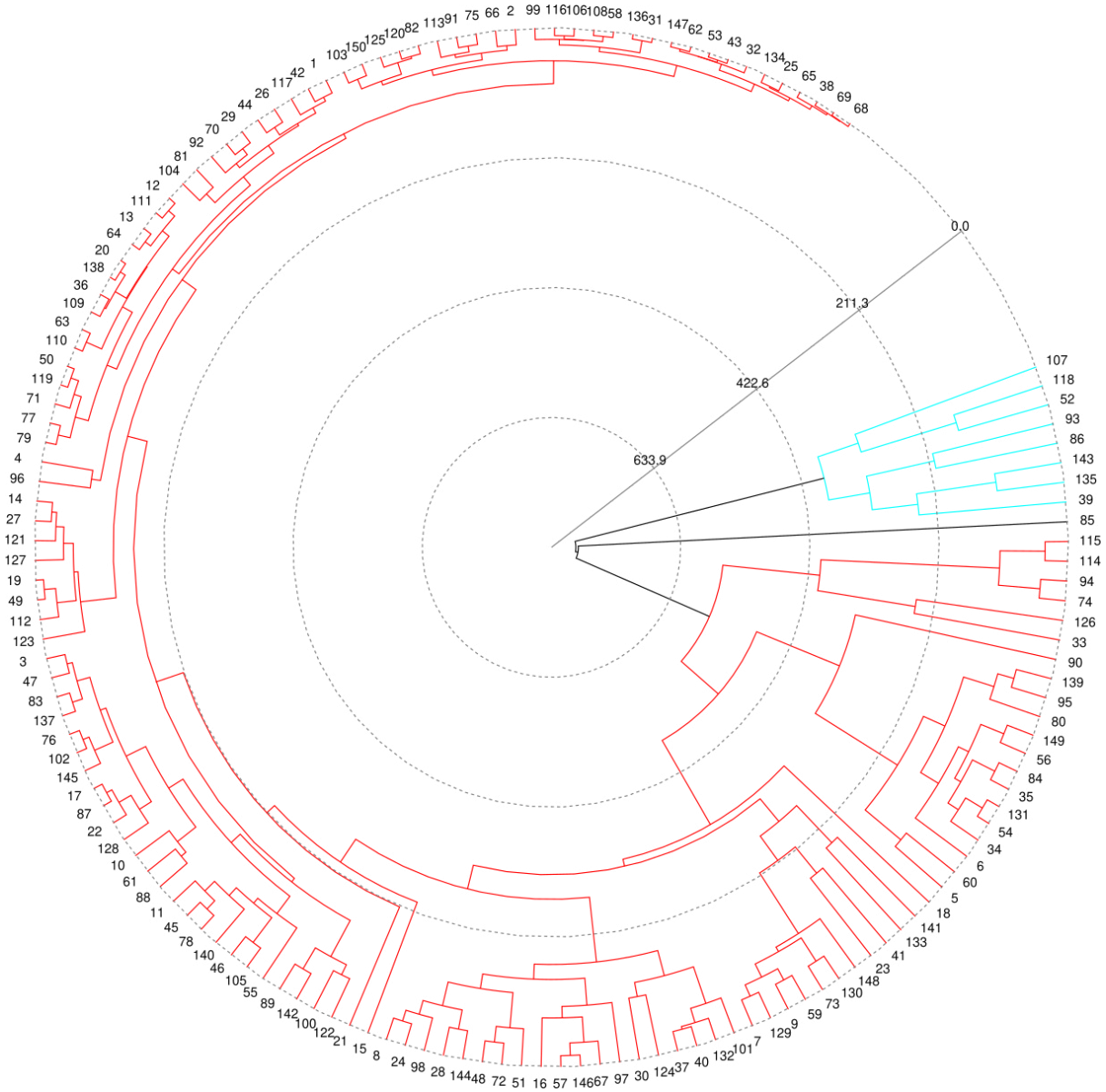

Figure 5.18: Polar tree diagram showing hierarchical euclidean distance relationship of the responses of all the recorded 150 neurons for stimulus set B. Cophenetic distance (0.8894)

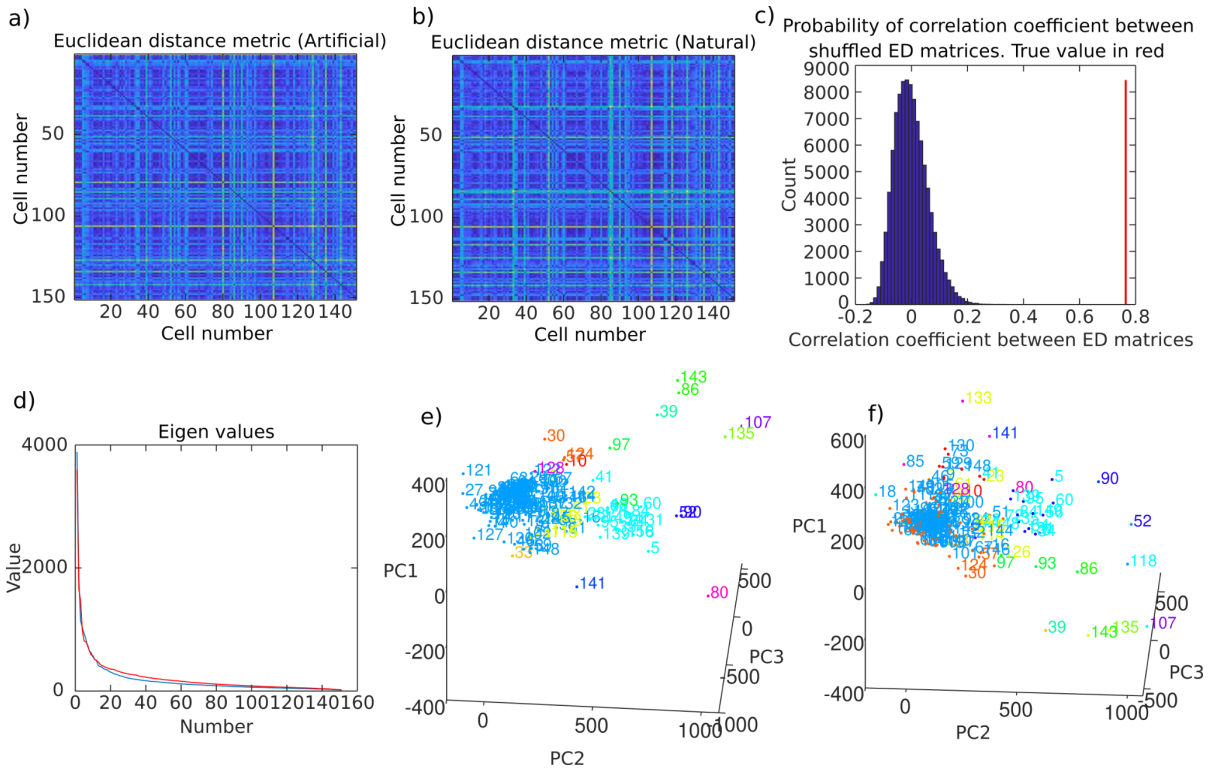

Figure 5.19: a,b) Matrix of pairwise euclidean distance metric for all the recorded cells for stimulus set A and B respectively. c) Histogram of the distance measures between permuted distance matrices for set A and set B. Area beyond the true distance was zero with 100000 permutations. d) Scree plot from svd to identify the number of important dimensions to reduce to before clustering. e) Scatter plot showing clusters from k-means clustering of their responses to stimulus set A. Cell number is given adjacent to the point in the same color as the cluster point. f) Scatter plot showing k-means clustering for stimulus set B. However the cell numbers here are coloured based on the cluster they belonged to in (e)

5.2.2.1 Classification of intracellularly recorded neurons based on response pattern

150 neurons are intracellularly recorded from the proximal optic lobe. Based on response similarities for stimulus set A and stimulus set B, a dendrogram of hierarchical clustering for 150 cells showed that most of the cells are clustered together (Fig 5.17). Cells which are clustered close by for stimulus set A have also clustered close by for stimulus set B (Fig 5.18). To check the similarity of the clustering of response pattern of 150 cells for stimulus set A and stimulus set B, we created euclidean distance matrices by taking the pairwise distances between the response of each of the cells, and then we calculated correlation coefficient of those matrices (Fig 5.19a-b). Correlation coefficient of euclidean distance matrix for stimulus set A and the euclidean distance matrix for stimulus set B is 0.78 and this is taken as the true value (Fig 5.19c, red line). To test the probability of this happening by chance, we calculated the correlation coefficient of one matrix permuted (AXA' where A is a

permutation matrix) with the other euclidean matrix fixed. None of the correlation coefficients of permutations could reach the true value in 10000 times (Fig 5.19c, blue histogram). This confirms that response similarity between the cells for stimulus set A and stimulus set B due to their intrinsic properties and not by chance. To visualise the clustering of the data, we did k-means clustering with 3 components from the PCA for stimulus set A and stimulus set B. In clustering analysis also many cells clustered together for both the stimulus (Fig 5.19e-f). And cells which are clustered together for stimulus set A have also clustered together for stimulus set B.

As I am doing blind recording from the proximal optic lobe. It might be possible that I might be recording the same cell again and again and that's why they are getting clustered together based on the responses. To find out whether it's true or not, we performed a similar classification on filled cells.

5.2.2.2 Classification of intracellularly filled neurons based on response pattern

To find out whether I am recording from the same cell repeatedly, we performed hierarchical clustering of 15 filled cells for stimulus set A and stimulus set B . Many cells clustered together for stimulus set A and stimulus set B, cells which are clustered close by for stimulus set A have also clustered close by for stimulus set B (Fig 5.20a-b). This similarity of clustering is confirmed by calculating the correlation coefficient (5.21c, red line) between the euclidean distance matrices (5.21a-b) for stimulus set A and stimulus set B. This was similar to the observations when all the cells we recorded from the optic lobe were considered together. We already saw from the earlier part of the chapter that the 15 cells are morphologically different. Thus the cells which are clustered close by response patterns in our analysis, are different morphologically (Fig 5.1-Fig 5.15 and Fig 5.20a). For example, medulla local neuron (8) and dorsal lobula neuron (3) are morphologically different and their innervation is different and yet their responses were similar to each other in our stimulus set (Fig 5.20a). This was true for stimulus set A and stimulus set B. Clustering analysis on 15 filled cells showed that most of the cells are clustered together for stimulus set A and stimulus set B despite their morphological differences.

Thus though the cells that I recorded from the proximal optic lobe are different many of them responded somewhat similarly to the stimulus set we used . There was no critical stimulus in our stimulus set which could distinguish the cell types based on their response pattern.

5.2.2.2.1 Sampling of cell types while recording from proximal optic lobe

Out of 15 filled cell types that I filled intracellularly while recording blindly using sharp electrodes, only 2 cell types were morphologically similar to that reported in literature. And within my own fills only one cell type was filled more than once, LGMD type 1. It was filled twice. And in locust, LGMD Type 1 is the most recorded cell in the literature. This shows that cell types in proximal optic lobe insect visual systems are highly undersampled in terms of morphology and physiology.

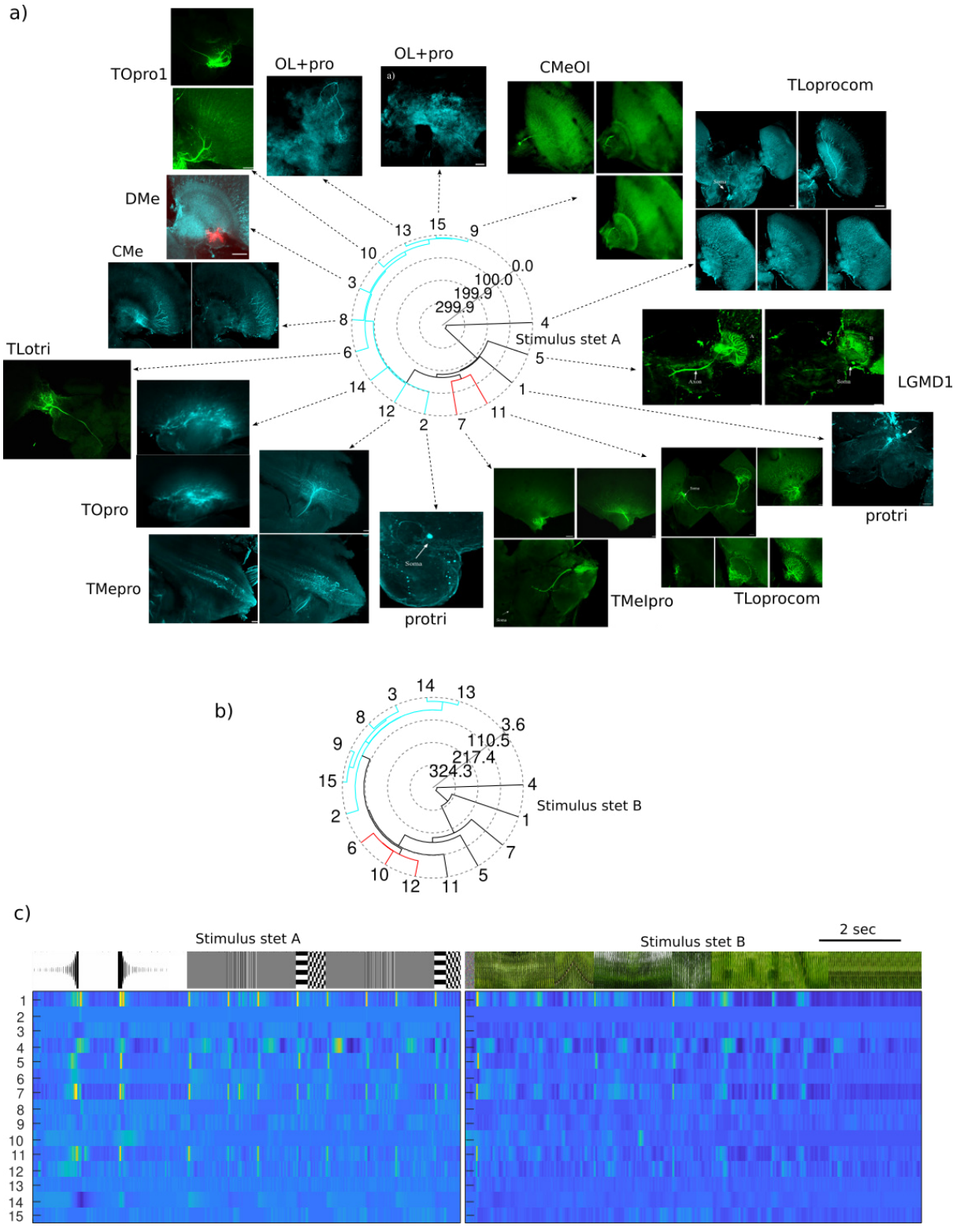

Figure 5.20: a) Polar dendrogram showing hierarchical euclidean distance relationship of the responses of the filled neurons for stimulus set A (centre), morphology of the neurons corresponding to these responses are also shown next to the cell number. Cophenetic distance (0.7688) b) Polar dendrogram showing hierarchical euclidean distance relationship of the responses of the filled neurons for stimulus set B. Cophenetic distance (0.8900) c) Image on the top, representation of subset of image sequences for stimulus set A and stimulus set B representation. Bottom, PSTH for stimulus set A and stimulus set B for the intracellularly filled neurons.

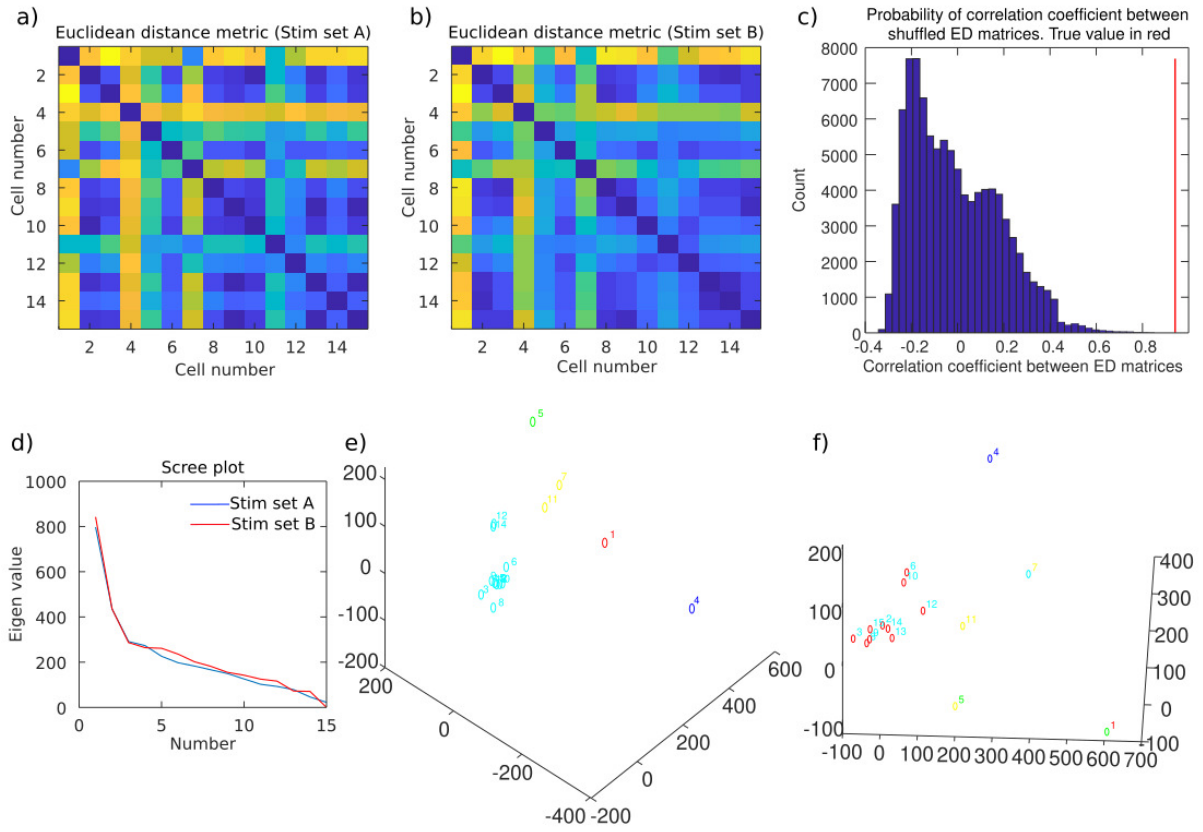

Figure 5.21: a,b) Matrix of pairwise euclidean distance metric for all the recorded cells for stimulus set A and B respectively. c) Histogram of the distance measures between permuted distance matrices for set A and set B. Area beyond the true distance was zero with 100000 permutations. d) Scree plot from svd to identify the number of important dimensions to reduce to before clustering. e) Scatter plot showing clusters from k-means clustering of their responses to stimulus set A. Cell number is given adjacent to the point in the same color as the cluster point. f) Scatter plot showing k-means clustering for stimulus set B. However the cell numbers here are coloured based on the cluster they belonged to in (e)

5.3 Discussion

Almost all the neurons recorded in this work are proximal optic lobe neurons which include 3rd (medulla) and 4th (lobula) order visual neurons. The lobula complex structure is evidently very different across the insects and equivalent compartments carrying out similar computations have not been identified. Lobula complex is present as lobula and lobula plate in the order diptera (so too in lepidoptera and coleoptera species). In many other insects, lobula complex has multiple sub neuropils and none of the compartments have been identified as equivalent to lobula or lobula plate of diptera.

According to the paper 'The lobula plate is exclusive to the insects', lobula plate is present in holometabolous insects which satisfy six defining characters (presence of inner medulla, quartets of

T4 neuron dendrites in inner medulla, quartets of T5 neuron dendrites in lobula outer stratum, precise uncrossed projections from T4 and T5 neuron axons in a retinotopic fashion into levels of large field tangential cells, T4 and T5 terminals segregating onto layered widefield tangential cells, larger diameter widefield tangential cells with layered dendritic trees) (Strausfeld, 2021). In drosophila, neurons located in the proximal optic lobe which are involved in motion detection are well studied. These are medulla intrinsic (Mi), tangential medulla (Tm), T4, T5 and lobula plate tangential neurons. Mi and Tm neurons give brightness changes inputs to the T4 and T5 neurons which are involved in ON and OFF motion detection pathways respectively. Four variants of T4 and T5 (a, b, c, and d) innervate in four layers of lobula plate and detect rightward, leftward, upward and downward motions of light and dark edges respectively.

In locusts, the lobula giant movement detector (LGMD1) is one of the well studied neuron across four species of grasshoppers (O'Shea & Williams, 1974; Peron et al., 2007; Rind, F. C.,1984). It belongs to the class of jittery movement detectors (Glantz, R. M. ,1974; Frantsevich, L., & Mokrushov, P.,1977; Wehner, R. 1981) Supra linear summation of neuronal inputs were discovered in this neuron (Gabbiani et al., 2002) In locusts it has been identified that LGMD involves in escape responses by identifying looming targets. In our recordings, only twice we could come across this neuron, we have recorded and filled this neuron. Morphologically and physiologically this neuron is similar with the reported LGMD1 neuron in four grasshopper species. Though many papers claim that LGMD-DCMD neuronal pair detects looming in targets and involves in escape response. Whereas in our recordings most of the cells also responded to looming stimulus. Knowing their morphology and their postsynaptic neurons would have helped in this discussion.

Studies in Drosophila have revealed the computation of global motion and the underlying mechanisms. This computation has been shown to be equivalent in terms of what it does and how it does it to motion computation in mammalian systems (which all have very similar circuit anatomically). However this kind of generalisation of motion computation has not happened across insect species though the general consensus is that lobula is the chief player in this computation. This conclusion has been arrived at based on recordings from neurons in the lobula in other species that

have responded to some aspect of the motion in the visual field. LGMD in locust (O'Shea & Williams, 1974), HP1 and HR1 in honeybee (Ibbotson, 1991), STMD in dragonflies (O'Carroll, 1993) are some of the well characterized in terms of their coding of motion features. Among these only LGMD has been studied to some extent in terms of the circuit underlying the computation that enables this feature coding. Thus our understanding of general motion computation in insects is largely from Drosophila, that involves clean compartmentalised processing in lobula and lobula plate. However as we saw before there are large differences between the lobula structures between insects.

From the literature, there are hardly 67 cell types which are innervating in the medulla and lobula of optic lobes in orthoptera and closely related species (Table 1). With our understanding about the olfactory system of *H. banian* cell types, which are conserved through fourth order neurons, all these cell types were well studied in *S. americana* (Singh & Joseph, 2019), no new cell type has been found that was not reported in *S. americana*. We expected at least some of the 67 cell types to be observed in our set of filled cells. We have filled fifteen cells, among them only two neurons (LGMD1/TOpro and CMe/medulla local neuron) showed morphological similarity with the available 67 cell types. Moreover in our own set only one cell type was repeatedly filled. So it is true that there are many cell types. Thus it is unlikely that not observing those cells reported in locusts in our HB recordings is due to species difference. This shows the undersampling of visual neurons in the proximal optic lobe of orthoptera and closely related species; there are many more cell types yet to be discovered.

Among 150 cells recorded and classified based on response patterns for stimulus set A and stimulus set B, many of the cells clustered together either for stimulus set A or stimulus set B. Cells clustered close by for stimulus set A also clustered close by for stimulus set B. This clustering gave us suspicion that we might be recording the same cell again and again. Whereas classifying fifteen filled cells for stimulus set A and stimulus set B based on their response pattern, confirmed us that though they are morphologically different, their response patterns clustered similarly for stimulus set A and stimulus set B. This concludes that there is no critical stimulus in our stimulus set which can distinguish the cell type based on the response pattern.

Chapter 6

Nature of models that capture the response properties of the cell types in the proximal optic lobe

6.1 Introduction

What does a neuron or a population of neurons represent is the central question of neural coding? This is also closely related to the question of what the brain knows about the outside world or state of the world given the activity (in its broadest form knowing their membrane potential, their spatial distribution and other molecularly determined internal states) of that population of neurons. The aim would be to make predictions about these states, given the state of the environment and the body. In the case of a single neuron and when the measurements we are carrying out are point measurements of membrane potentials, the aim of the model would be to predict the membrane potential or firing rates. If we assume that the neurons are coding for a narrow set or a single feature of the stimulus and the representation in the neuron is firing rate or membrane depolarization (in the case of non-spiking cells), then this question can boil down to asking what stimulus feature would make the neuron fire or depolarize strongly.

One could go about trying out some elementary stimulus based on informed guess (Where is the neuron located? What do we know about the neurons pre and post to it and so on?) and see if one could get insight into this. Quite often these findings are serendipitous. In the visual pathway of mammals, David H. Hubel and Torsten N. Wiesel accidentally discovered that neurons in the visual cortex of the cat are orientation selective due to the improper placement of the glass slide which they have used to present the stimulus (Licholai, 2021). When we are not sure what stimulus those neurons respond to, white noise stimulus (WN) based analysis is one of the options. This assumes though that the relationship between the stimulus feature being manipulated (in a spectrally white manner) and the response in the neuron can have a linear approximation. The white noise stimulus also comes with advantages like robustness to adaptation..

In the case of visual stimuli, the neuron is characterised by identifying its spatiotemporal receptive field using linear filter theory ((Chichilnisky, 2001). The receptive field of a neuron can be found by calculating the spike triggered average (STA) of a neuron's response to spatio-temporal white noise (WN) stimuli (Fig 2.6). Spike triggered average (STA) is the average of frames of the stimulus that preceded spikes (Fig 6.4). In other words, STA tells what happens in the outside world which leads to the firing of a neuron.

6.1.1 Receptive fields

Though the neurons in the visual pathway may respond to stimuli at any point in the visual field, often there are smaller regions in the visual field where the presence of the stimulus feature can cause the response. These are called receptive fields. For example some simple receptive fields may be based on whether neurons respond to light on or light off.

- On receptive field: Switching on light over this region, depolarises the neuron.
- Off receptive field: Switching off the light over this region, hyperpolarizes the neuron.

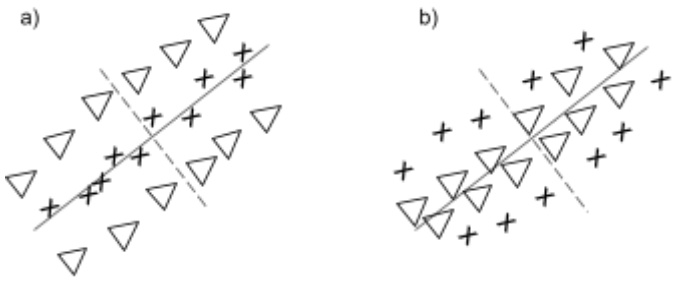

Figure 6.1: Receptive fields in the primary visual cortex of the cat. a) On centre-Off surround receptive fields. b) Off centre-On surround receptive fields.

Hubel and Wiesel were recording intracellularly from the visual cortex of the cat while presenting the light stimulus. They found that the visual cortex cell's receptive fields are the combination of On and Off receptive fields. They are On centre and Off surround (Fig 6.1a) or Off centre and On surround (Fig 6.1b) receptive fields.

Based on the properties of the receptive fields. Cells in the visual cortex are classified as simple and complex cells.

6.1.2 Simple cells

Cells whose receptive field can be distinguished as ON and OFF receptive fields are called simple cells (Fig 6.2). These cells have narrow receptive fields and are orientation sensitive. These cell's response can be captured using linear-nonlinear modelling.

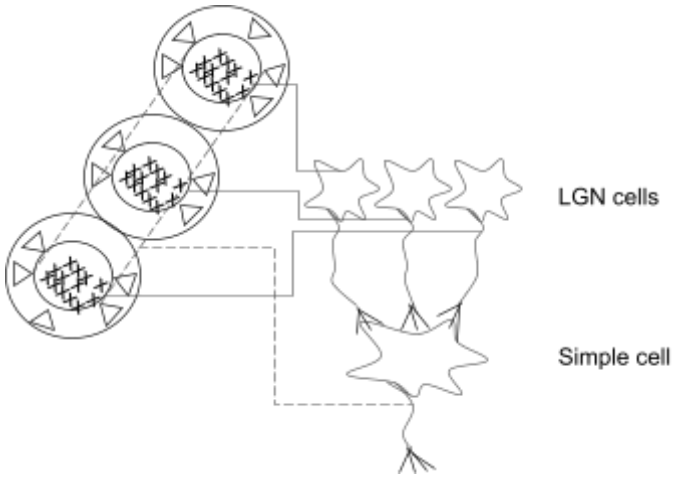

Figure 6.2: Building a simple cell from LGN input cells. In this scheme, the LGN cells will respond to ON centre, OFF surround stimuli and the simple cell will respond to white bars at the centre oriented as shown .

6.1.3 Complex cells

Complex cells have indistinguishable ON and OFF receptive fields, they have wider receptive fields (Fig 6.3). These cells (reported by Hubel and Wiesel) are also orientation sensitive. These cell's responses can not be captured by linear-nonlinear modelling, they require higher order or multilayer, nonlinear computations.

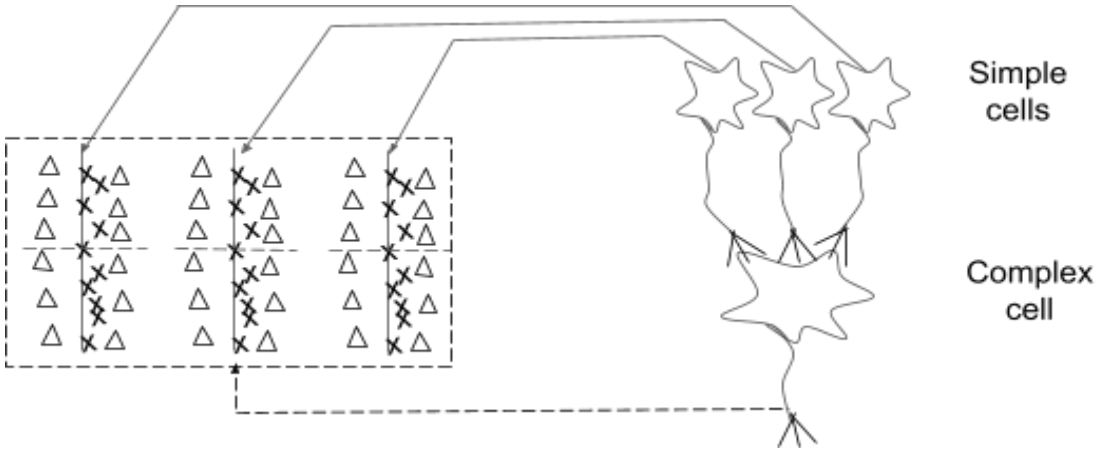

Figure 6.3: Schematic of building of a complex cell from simple cells.

6.2 Results

6.2.1 Spike triggered average (STA) for fifteen filled cells

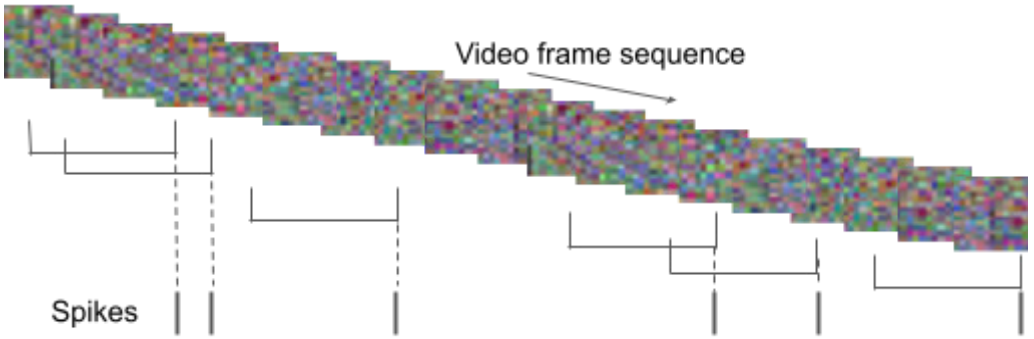

Figure 6.4: Representation of how frames are stacked triggered from the spike times for STA calculation. Though the multicolor frame is shown, in our analysis we used the red, green and blue channels separately.

For calculating the STA, average of the stimulus frames for 1500 ms before each spike were collected, like that for the ‘n’ spikes, we will get ‘n’ blocks of stimulus frames for each colour. Average over these ‘n’ blocks of frames gives the STA (Fig 6.4).

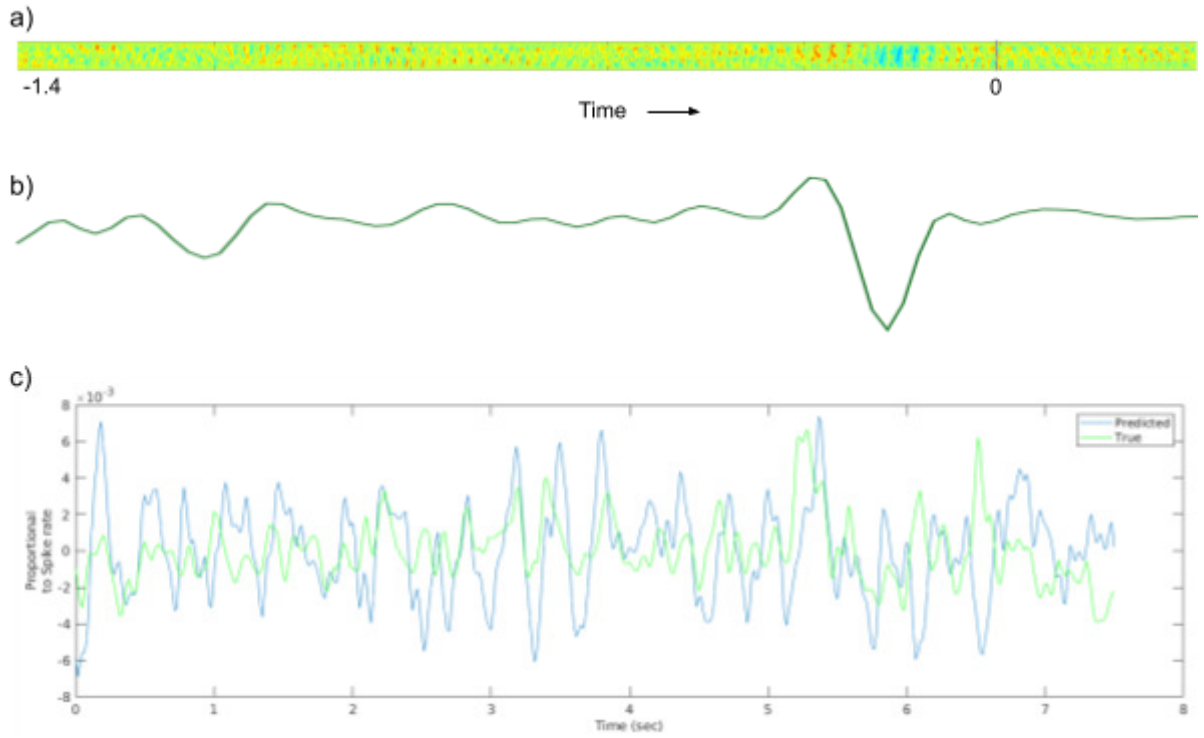

Figure 6.5: STA for green component of WN for a neuron. a) Example STA of a single cell for green colour. Dotted line at zero (0) to indicate the time of neuron spiking. b) Example STA of mean frame brightness used in prediction in (c) c) Prediction of PSTH based on STA averaged over brighteness of each frame. The prediction is for the 10% of frames not used in constructing the STA. The prediction had a correlation of 0.49 to true PSTH.

In our experiments, given the limit of stability of the intracellular recording (stimulus time and dye fill time) the white noise stimulus was limited to 1170 frames. STA is calculated using 90 % of these stimulus time (frames) for all the 15 filled cells. This STA was used to make a linear prediction of the firing rate from the stimulus by convolving the STA with the stimulus (1.11b). This prediction of the PSTH was carried out for the 10% of the stimulus that was not used in constructing the STA. To measure how good the prediction was to the true PSTH, Pearson correlation was computed between them (Fig 6.5c). We found that none of the full STA constructed for each of the colours could predict the PSTH well. This was likely given that we used only 1000 (32x32) frames.

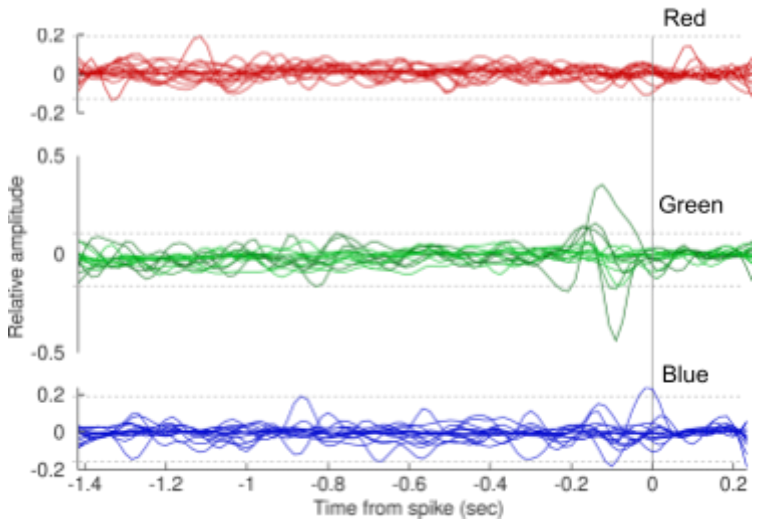

Figure 6.6: 1D-STA for Red, Blue and Green components of the WN. The dashed lines are the maximum and minimal fluctuation in the time window before 400 msec before spike. Those STAs that have amplitudes greater than these limits only in the window of time between spike and 400 msec before spike are shown in darker shades of the colour. These are present only in the green components.

We then created a one dimensional STA from these box STA by taking the mean of each frame (example in Fig 6.5b). Prediction of PSTH for the 10% kept apart was carried out using this one dimensional STA (1D-STA) (example in Fig 6.5c). These predictions were good in some cells.

Fig 6.6 shows the estimated 1D-STA from red, green and blue component frames. If we use the noise fluctuations of the baseline as cutoff then we see that red channels do not yield any prominent 1D-STA as expected given that ERG did not have a prominent response for red. Surprisingly, the blue channel which produced a strong ERG response also did not give any prominent STA by this criteria. However, the green channel gives a prominent estimate by this criteria for four of the 15 cells. They also yield reasonable predictions for PSTH as measured by correlation between prediction and true PSTH. These STAs and the correlations are presented in Fig 6.6. These likely point to the motion pathway being restricted to green spectral bands (among red, green and blue). Because we did not have UV in our stimulus, we do not know if they are involved in such processing.

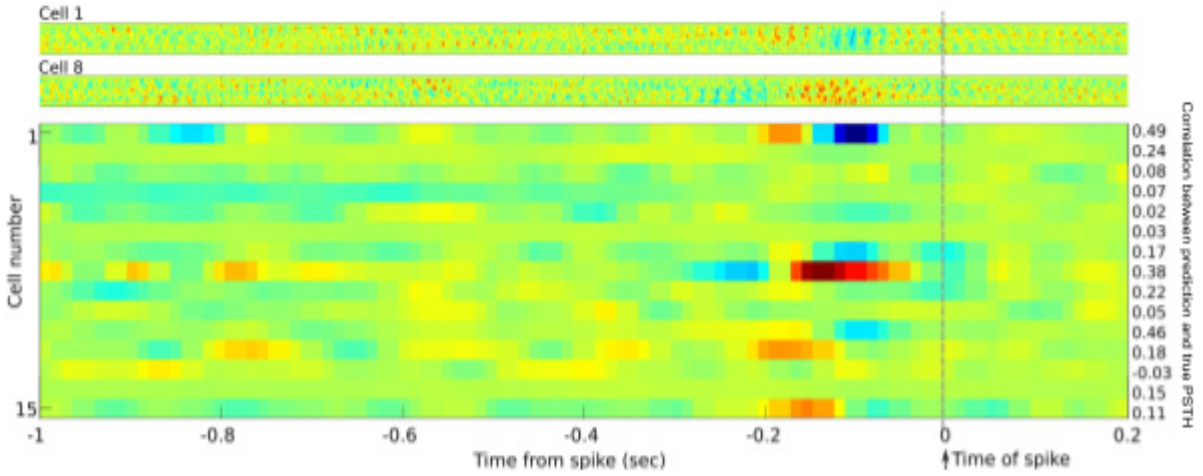

Figure 6.7: STA for fifteen filled cells. Full frame STA for cell 1 and cell 8 to show two representative STA's of different kinds (top). 1D-STA for all the 15 filled cells (bottom). Dotted line at zero (0) to indicate the neuron spiking.

If we use the criteria of a threshold of 0.2 correlation, out of 15 cells, only 5 cells could give the meaningful 1D-STA predictions. Out of 5 cells, most (four out of five) cells depolarized for a transient decrease in brightness before the depolarization or spiking. Only one cell (cell 8) responded to an increase in brightness before spiking (Fig 6.7). As in most STAs in the various cell types, in the literature, one can also see a weak opposite change in intensity prior to this main transient in intensity.

6.3 Discussion

Peaks of spectral sensitivity of *S. gregaria* are at 339 nm, 441 nm and 514 nm (Schmeling et al., 2014b) and that of *L. migratoria* is at 360 nm, 430 nm and 530 nm (Vishnevskaya et al., 1986). *H. banian* belongs to the order orthoptera, same as *S. gregaria* and *L. migratoria*. While recording *H. banian* ERG, we could see the response for blue and green stimuli because of the spectral sensitivity of the pigments. We could also see the response for red stimuli though red sensitive pigments are not present. It is likely because a small amount of red spectrum of the display overlaps with the green sensitive receptor (Fig 4.7).

Therefore, we expected meaningful STA to be estimated for blue and green components of WN stimuli while recording from proximal optic lobe neurons intracellularly. Surprisingly, we could not see the STA and use it to make predictions of the spike rate for the blue component of the white noise. Thus, it is possible that in lobula, motion detection in blue components might not be taking place or the blue spectrum may not be used for motion estimation in HB.

In the drosophila pathway, starting from R1-R6 retinula cells (and not R7 and R8) are involved in motion processing (Borst et al., 2020). R1-R6 in flies have spectral sensitivity in the green-blue (400-550nm) band and another one in the UV (250-350nm) band. The arrangement of the retinula cells in locust has been shown to be similar with six outer (analogous to R1-R6) and two inner (analogous to R7, R8) retinula cells. In locust, there are three photoreceptor types reported based on spectral sensitivity (Vishnevskaya et al., 1986). These bands are ~300-400 nm (UV), ~400-470 nm (Blue) and ~470-570 nm (Green). So, it is possible that the pathway from 400-470nm band retinulla cells are not involved in motion processing. Or they are separate from green and we did not encounter such cells in our fills.

In our experiments, the white noise was made up of red, green and blue stimulus simultaneously by linear combination forming the 32x32 coloured pixels. It is possible that processing of green components might inhibit the blue components' response and that is why we do not see responses in neurons correlated to spatiotemporal variation in blue (STA). To test this we would have to record neurons by presenting blue white noise stimuli and green white noise separately.

STA estimation has been carried out in drosophila for neurons that innervate lobula from the medulla. Even in the studies for medulla neurons in flies the colour component wise analysis has not been carried out. To the best of our knowledge, STA analysis has not been carried out from raw pixel white noise for neurons of the lobula complex and this is the first such study and it shows that there are cells at that level whose response may be approximated by linear nonlinear model. And these motion component processing may not be happening at all the wavelengths of spectrum even if the insects may perceive objects in the other colours as well.

Chapter 7

Summary

Based on immunohistochemistry techniques and neuronal innervations from tract tracings, major neuropils of *Hieroglyphus banian* were identified. Using bulk tracing techniques connections between those neuropils are established. This concludes that gross anatomy of the *Hieroglyphus banian* visual pathway is similar to that of the *Schistocerca gregaria*. However two novel structures

1. Bulb-like structures present in the posterior medial protocerebrum.
2. Another structure posterior dorsal to the protocerebral bridge.

were also found which were not reported in previous studies.

Electroretinogram (ERG) of Drosophila canton-S strain for red, blue, green, white and different intensities of white presented through mobile screen showed positive on transient, negative sustained receptor potential and negative off transient (Fig 2a). This is consistent with the Drosophila ERG recorded by presenting stimulus through LED light.

ON transients of the ERG in *H. banian* could be revealed by red and low intensity white stimuli. In *H. banian*, ON transients could be seen as a kink in the downward transient of the fast negative receptor potentials of the ERG for blue, green and white (Fig 2b). This points to a conserved mechanism of processing in the lamina.

Field potentials recorded from medulla and lobula showed positive onset, sustained potential & offset response. The onset peak response diminished in field potentials recorded from AOTu and calyx of MB. Field potentials recorded from the proximal optic lobe showed oscillations in the range of 20-40Hz and these are mediated by picrotoxin sensitive receptors, likely $GABA_A$ type (Fig 2c).

Hierarchical clustering of 150 cells recorded from the proximal optic lobe by presenting synthetic stimuli and natural stimulus set showed similar clustering for both the stimulus sets. Significant

correlation between euclidean distance matrices of both the stimulus sets showed that the similarity between hierarchical clustering is valid.

15 cell types of different morphology could be visualised among 150 recorded cells. Hierarchical clustering of these 15 cell types based on response patterns for synthetic and natural stimuli showed similarity in clustering for both the stimuli. Some of the cell types that had similar responses in our stimulus set were morphologically very different. This points to the necessity to have larger and more varied stimulus sets when we study processing from cells in the proximal optic lobe.

Among the 15 cell types, only 2 cell types were found to be similar with the existing 65 cell types present in literature so far. And only one cell type was repeatedly filled (twice) in my own recordings. Thus I have characterised 13 novel cell types in terms of morphology and responses. This also shows that the visual systems of orthoptera are highly under characterised.

Linear predictor of the responses in the neurons was estimated by spike triggered averaging of the white noise stimuli. Among red, blue and green components of white noise stimuli, only for the green component showed prominent STA and only for a small subset of the cells among 15 filled cells. For these cells, the STA filter could make linear predictions for responses to novel white noise stimuli. These cells are analogous to simple cells and the rest are likely analogous to complex cells which need multilayer nonlinear models to capture the computation. This is the first white noise analysis of the response of cells beyond medulla in insects.

References

Adrian, E. D. (1950). The electrical activity of the mammalian olfactory bulb. *Electroencephalography and Clinical Neurophysiology*, *2*(1), 377–388. https://doi.org/10.1016/0013-4694(50)90075-7

Allada, R., & Chung, B. Y. (2010). Circadian Organization of Behavior and Physiology in Drosophila. *Annual Review of Physiology*, *72*(1), 605–624. https://doi.org/10.1146/annurev-physiol-021909-135815

Autrum, H., & Hoffmann, C. (1960). Diphasic and monophasic responses in the compound eye of Calliphora. *Journal of Insect Physiology*, *4*(2), 122–127. https://doi.org/10.1016/0022-1910(60)90074-3

Barlow, H. B., Fitzhugh, R., & Kuffler, S. W. (1957). Change of organization in the receptive fields of the cat's retina during dark adaptation. *The Journal of Physiology*, *137*(3), 338–354.

Barlow, H. B., & Levick, W. R. (1965). The mechanism of directionally selective units in rabbit's retina. *The Journal of Physiology*, *178*(3), 477–504.

Borst, A. (2009). Drosophila's View on Insect Vision. *Current Biology*, *19*(1), R36–R47. https://doi.org/10.1016/j.cub.2008.11.001

Borst, A., & Egelhaaf, M. (1989). Principles of visual motion detection. *Trends in Neurosciences*, *12*(8), 297–306. https://doi.org/10.1016/0166-2236(89)90010-6

Borst, A., Haag, J., & Mauss, A. S. (2020). How fly neurons compute the direction of visual motion. *Journal of Comparative Physiology A*, *206*(2), 109–124. https://doi.org/10.1007/s00359-019-01375-9

Brunner, D., & Labhart, T. (1987). Behavioural evidence for polarization vision in crickets. *Physiological Entomology*, *12*(1), 1–10. https://doi.org/10.1111/j.1365-3032.1987.tb00718.x

Buchner, E., Buchner, S., & Bülthoff, I. (1984). Deoxyglucose mapping of nervous activity induced inDrosophila brain by visual movement. *Journal of Comparative Physiology A*, *155*(4), 471–483. https://doi.org/10.1007/BF00611912

Burkhardt, W., & Braitenberg, V. (1976). Some peculiar synaptic complexes in the first visual ganglion of the fly, Musca domestica. *Cell and Tissue Research*, *173*(3), 287–308. https://doi.org/10.1007/BF00220317

Chang, H.-W., & Lee, H.-J. (2001). Inconsistency in the expression of locomotor and ERG circadian rhythms in the German cockroach, Blattella germanica (L.). *Archives of Insect Biochemistry and Physiology*, *48*(3), 155–166. https://doi.org/10.1002/arch.1068

Chen, P.-J., Belušič, G., & Arikawa, K. (2020). Chromatic information processing in the first optic ganglion of the butterfly Papilio xuthus. *Journal of Comparative Physiology A*, *206*(2), 199–216. https://doi.org/10.1007/s00359-019-01390-w

Chichilnisky, E. J. (2001). A simple white noise analysis of neuronal light responses. *Network (Bristol, England)*, *12*(2), 199–213.

Chiou, T.-H., Kleinlogel, S., Cronin, T., Caldwell, R., Loeffler, B., Siddiqi, A., Goldizen, A., & Marshall, J. (2008). Circular Polarization Vision in a Stomatopod Crustacean. *Current Biology*, *18*(6), 429–434. https://doi.org/10.1016/j.cub.2008.02.066

Chou, W.-H., Hall, K. J., Wilson, D. B., Wideman, C. L., Townson, S. M., Chadwell, L. V., & Britt, S. G. (1996). Identification of a novel Drosophila opsin reveals specific patterning of the R7 and R8 photoreceptor cells. *Neuron*, *17*(6), 1101–1115.

Clarkson, E., Levi-Setti, R., & Horváth, G. (2006). The eyes of trilobites: The oldest preserved visual system. *Arthropod Structure & Development*, *35*(4), 247–259. https://doi.org/10.1016/j.asd.2006.08.002

Colwell, C. S., & Page, T. L. (1989). The electroretinogram of the cockroach Leucophaea maderae. *Comparative Biochemistry and Physiology Part A: Physiology*, *92*(1), 117–123. https://doi.org/10.1016/0300-9629(89)90752-4

Coombe, P. E. (1986). The large monopolar cells L1 and L2 are responsible for ERG transients inDrosophila. *Journal of Comparative Physiology A*, *159*(5), 655–665. https://doi.org/10.1007/BF00612038

Dacke, M., Nilsson, D.-E., Scholtz, C. H., Byrne, M., & Warrant, E. J. (2003). Insect orientation to polarized moonlight. *Nature*, *424*(6944), 33–33. https://doi.org/10.1038/424033a

Delaney, K. R., Gelperin, A., Fee, M. S., Flores, J. A., Gervais, R., Tank, D. W., & Kleinfeld, D. (1994). Waves and stimulus-modulated dynamics in an oscillating olfactory network. *Proceedings of the National Academy of Sciences*, *91*(2), 669–673. https://doi.org/10.1073/pnas.91.2.669

Ehmer, B., & Gronenberg, W. (2002). Segregation of visual input to the mushroom bodies in the honeybee (Apis mellifera). *Journal of Comparative Neurology*, *451*(4), 362–373. https://doi.org/10.1002/cne.10355

Feiler, R., Bjornson, R., Kirschfeld, K., Mismer, D., Rubin, G., Smith, D., Socolich, M., & Zuker, C. (1992). Ectopic expression of ultraviolet-rhodopsins in the blue photoreceptor cells of Drosophila: Visual physiology and photochemistry of transgenic animals. *The Journal of Neuroscience*, *12*(10), 3862–3868. https://doi.org/10.1523/JNEUROSCI.12-10-03862.1992

Fischbach, K.-F., & Dittrich, A. P. M. (1989a). The optic lobe of Drosophila melanogaster. I. A Golgi analysis of wild-type structure. *Cell and Tissue Research*, *258*(3). https://doi.org/10.1007/BF00218858

Fischbach, K.-F., & Dittrich, A. P. M. (1989b). The optic lobe of Drosophila melanogaster. I. A Golgi analysis of wild-type structure. *Cell and Tissue Research*, *258*(3). https://doi.org/10.1007/BF00218858

Fischbach, K.-F., & Hiesinger, P. R. (2008). Optic Lobe Development. In G. M. Technau (Ed.), *Brain Development in Drosophila melanogaster* (pp. 115–136). Springer New York. https://doi.org/10.1007/978-0-387-78261-4_8

Freeman, W. J. (1978). Spatial properties of an EEG event in the olfactory bulb and cortex. *Electroencephalography and Clinical Neurophysiology*, *44*(5), 586–605. https://doi.org/10.1016/0013-4694(78)90126-8

Frisch, K. von. (1914). *Der farbensinn und Formensinn der Biene.*

Fryxell, K. J., & Meyerowitz, E. M. (1987). An opsin gene that is expressed only in the R7 photoreceptor cell of Drosophila. *The EMBO Journal*, *6*(2), 443–451.

Gao, S., Takemura, S., Ting, C.-Y., Huang, S., Lu, Z., Luan, H., Rister, J., Thum, A. S., Yang, M., Hong, S.-T., Wang, J. W., Odenwald, W. F., White, B. H., Meinertzhagen, I. A., & Lee, C.-H.

(2008). The Neural Substrate of Spectral Preference in Drosophila. *Neuron*, *60*(2), 328–342. https://doi.org/10.1016/j.neuron.2008.08.010

Gelperin, A., & Tank, D. W. (1990). Odour-modulated collective network oscillations of olfactory interneurons in a terrestrial mollusc. *Nature*, *345*(6274), 437–440. https://doi.org/10.1038/345437a0

Goldsmith, T. H., & Bernard, G. D. (1974). Chapter 5—THE VISUAL SYSTEM OF INSECTS. In M. Rockstein (Ed.), *The Physiology of Insecta (Second Edition)* (pp. 165–272). Academic Press. https://doi.org/10.1016/B978-0-12-591602-8.50012-6

Haag, J., Arenz, A., Serbe, E., Gabbiani, F., & Borst, A. (2016). Complementary mechanisms create direction selectivity in the fly. *ELife*, *5*, e17421. https://doi.org/10.7554/eLife.17421

Habenstein, J., Amini, E., Grübel, K., el Jundi, B., & Rössler, W. (2020). The brain of Cataglyphis ants: Neuronal organization and visual projections. *Journal of Comparative Neurology*, *528*. https://doi.org/10.1002/cne.24934

Hardie, R. C. (1979). Electrophysiological analysis of fly retina. I: Comparative properties of R1-6 and R 7 and 8. *Journal of Comparative Physiology*, *129*(1), 19–33. https://doi.org/10.1007/BF00679908

Hassenstein, V., & Reichardt, W. (1956). System theoretical analysis of time, sequence and sign analysis of the motion perception of the snout-beetle Chlorophanus. *Z Naturforsch B*, *11*(9–10), 513–524.

Heinze, S. (2014). Polarized-Light Processing in Insect Brains: Recent Insights from the Desert Locust, the Monarch Butterfly, the Cricket, and the Fruit Fly. In G. Horváth (Ed.), *Polarized Light and Polarization Vision in Animal Sciences* (pp. 61–111). Springer. https://doi.org/10.1007/978-3-642-54718-8_4

Heinze, S., & Reppert, S. M. (2012). Anatomical basis of sun compass navigation I: The general layout of the monarch butterfly brain. *The Journal of Comparative Neurology*, *520*(8), 1599–1628. https://doi.org/10.1002/cne.23054

Heisenberg, M. (1971). Separation of Receptor and Lamina Potentials in the Electroretinogram of Normal and Mutant *Drosophila*. *Journal of Experimental Biology*, *55*(1), 85–100.

https://doi.org/10.1242/jeb.55.1.85

Heisenberg, M., & Buchner, E. (1977). The rôle of retinula cell types in visual behavior ofDrosophila melanogaster. *Journal of Comparative Physiology*, *117*(2), 127–162. https://doi.org/10.1007/BF00612784

Homberg, U. (2004). In search of the sky compass in the insect brain. *Naturwissenschaften*, *91*, 199–208.

Homberg, U., Hofer, S., Pfeiffer, K., & Gebhardt, S. (2003). Organization and neural connections of the anterior optic tubercle in the brain of the locust, Schistocerca gregaria. *Journal of Comparative Neurology*, *462*(4), 415–430. https://doi.org/10.1002/cne.10771

Homberg, U., & Würden, S. (1997). Movement-sensitive, polarization-sensitive, and light-sensitive neurons of the medulla and accessory medulla of the locust, Schistocerca gregaria. *Journal of Comparative Neurology*, *386*(3), 329–346. https://doi.org/10.1002/(SICI)1096-9861(19970929)386:3<329::AID-CNE1>3.0.CO;2-3

Honkanen, A., Adden, A., Freitas, J., Freitas, S., & Heinze, S. (2019). The insect central complex and the neural basis of navigational strategies. *Journal of Experimental Biology*, *222*. https://doi.org/10.1242/jeb.188854

Horridge, G. A. & others. (1966). The retina of the locust. *The Functional Organization of the Compound Eye: Proceedings of the International Symposium*.

Immonen, E.-V., Dacke, M., Heinze, S., & el Jundi, B. (2017). Anatomical organization of the brain of a diurnal and a nocturnal dung beetle. *Journal of Comparative Neurology*, *525*(8), 1879–1908. https://doi.org/10.1002/cne.24169

Jundi, B. el, Pfeiffer, K., & Homberg, U. (2011). A Distinct Layer of the Medulla Integrates Sky Compass Signals in the Brain of an Insect. *PLOS ONE*, *6*(11), e27855. https://doi.org/10.1371/journal.pone.0027855

Kelber, A. (1999). Ovipositing butterflies use a red receptor to see green. *Journal of Experimental Biology*, *202*(19), 2619–2630. https://doi.org/10.1242/jeb.202.19.2619

Kelber, A., Thunell, C., & Arikawa, K. (2001). Polarisation-dependent colour vision in Papilio butterflies. *Journal of Experimental Biology*, *204*(14), 2469–2480.

https://doi.org/10.1242/jeb.204.14.2469

Kirschfeld, K. (1992). Oscillations in the insect brain: Do they correspond to the cortical gamma-waves of vertebrates? *Proceedings of the National Academy of Sciences*, *89*(10), 4764–4768. https://doi.org/10.1073/pnas.89.10.4764

Klapoetke, N. C., Nern, A., Peek, M. Y., Rogers, E. M., Breads, P., Rubin, G. M., Reiser, M. B., & Card, G. M. (2017). Ultra-selective looming detection from radial motion opponency. *Nature*, *551*(7679), Article 7679. https://doi.org/10.1038/nature24626

Kuffler, S. W. (1953). DISCHARGE PATTERNS AND FUNCTIONAL ORGANIZATION OF MAMMALIAN RETINA. *Journal of Neurophysiology*, *16*(1), 37–68. https://doi.org/10.1152/jn.1953.16.1.37

Labhart, T., Baumann, F., & Bernard, G. D. (2009). Specialized ommatidia of the polarization-sensitive dorsal rim area in the eye of monarch butterflies have non-functional reflecting tapeta. *Cell and Tissue Research*, *338*(3), 391–400. https://doi.org/10.1007/s00441-009-0886-7

Labhart, T., & Petzold, J. (1993). *Sensory Systems of Arthropods*.

Land, M. F., & Nilsson, D. E. (2012). *Animal Eyes*. OUP Oxford. https://books.google.co.in/books?id=B4T0ZO_tKFAC

Laurent, G., & Naraghi, M. (1994). Odorant-induced oscillations in the mushroom bodies of the locust. *The Journal of Neuroscience*, *14*(5), 2993–3004. https://doi.org/10.1523/JNEUROSCI.14-05-02993.1994

Licholai, J. A. (2021, March 2). *An accidental experiment discovered new cells in cat brains and led to a Nobel Prize*. Massive Science. https://massivesci.com/notes/simple-complex-cells-neurons-cats-eyes/

Maisak, M. S., Haag, J., Ammer, G., Serbe, E., Meier, M., Leonhardt, A., Schilling, T., Bahl, A., Rubin, G. M., Nern, A., Dickson, B. J., Reiff, D. F., Hopp, E., & Borst, A. (2013a). A directional tuning map of Drosophila elementary motion detectors. *Nature*, *500*(7461), 212–216. https://doi.org/10.1038/nature12320

Maisak, M. S., Haag, J., Ammer, G., Serbe, E., Meier, M., Leonhardt, A., Schilling, T., Bahl, A.,

Rubin, G. M., Nern, A., Dickson, B. J., Reiff, D. F., Hopp, E., & Borst, A. (2013b). A directional tuning map of Drosophila elementary motion detectors. *Nature*, *500*(7461), 212–216. https://doi.org/10.1038/nature12320

Marshall, J., Cronin, T. W., Shashar, N., & Land, M. (1999). Behavioural evidence for polarisation vision in stomatopods reveals a potential channel for communication. *Current Biology*, *9*(14), 755–758. https://doi.org/10.1016/S0960-9822(99)80336-4

Martinsson, A. (Ed.). (1975). *Evolution and morphology of the Trilobita, Trilobitoidea and Merostomata: Proceedings of a NATO Advanced Study Institute held in Oslo 1st -8th July 1973*. Univ.-Forl.

Mauss, A. S., Pankova, K., Arenz, A., Nern, A., Rubin, G. M., & Borst, A. (2015a). Neural Circuit to Integrate Opposing Motions in the Visual Field. *Cell*, *162*(2), 351–362. https://doi.org/10.1016/j.cell.2015.06.035

Mauss, A. S., Pankova, K., Arenz, A., Nern, A., Rubin, G. M., & Borst, A. (2015b). Neural Circuit to Integrate Opposing Motions in the Visual Field. *Cell*, *162*(2), 351–362. https://doi.org/10.1016/j.cell.2015.06.035

Meinertzhagen, I. A., & O'Neil, S. D. (1991). Synaptic organization of columnar elements in the lamina of the wild type in Drosophila melanogaster. *Journal of Comparative Neurology*, *305*(2), 232–263. https://doi.org/10.1002/cne.903050206

Meinertzhagen, I. A., & Sorra, K. E. (2001). Chapter 3 Synaptic organization in the fly's optic lamina: Few cells, many synapses and divergent microcircuits. In *Concepts and Challenges in Retinal Biology (Progress in Brain Research)* (Vol. 131, pp. 53–69). Elsevier. https://doi.org/10.1016/S0079-6123(01)31007-5

Meinertzhagen, I., & Hanson, T. (1993). *The development of Drosophila*.

Merlin, C., Gegear, R. J., & Reppert, S. M. (2009). Antennal Circadian Clocks Coordinate Sun Compass Orientation in Migratory Monarch Butterflies. *Science*, *325*(5948), 1700–1704. https://doi.org/10.1126/science.1176221

Millard, S. S., & Pecot, M. Y. (2018). Strategies for assembling columns and layers in the Drosophila visual system. *Neural Development*, *13*(1), 11. https://doi.org/10.1186/s13064-018-0106-9

Montell, C., Jones, K., Zuker, C., & Rubin, G. (1987). A second opsin gene expressed in the ultraviolet-sensitive R7 photoreceptor cells of Drosophila melanogaster. *Journal of Neuroscience*, *7*(5), 1558–1566.

Mota, T., Kreissl, S., Carrasco Durán, A., Lefer, D., Galizia, G., & Giurfa, M. (2016). Synaptic Organization of Microglomerular Clusters in the Lateral and Medial Bulbs of the Honeybee Brain. *Frontiers in Neuroanatomy*, *10*. https://www.frontiersin.org/articles/10.3389/fnana.2016.00103

Nicol, D., & Meinertzhagen, I. A. (1982). An analysis of the number and composition of the synaptic populations formed by photoreceptors of the fly. *Journal of Comparative Neurology*, *207*(1), 29–44. https://doi.org/10.1002/cne.902070104

Nishiitsutsuji-Uwo, J., & Pittendrigh, C. S. (1968). Central nervous system control of circadian rhythmicity in the cockroach. *Zeitschrift Für Vergleichende Physiologie*, *58*(1), 14–46. https://doi.org/10.1007/BF00302434

O'Tousa, J. E., Baehr, W., Martin, R. L., Hirsh, J., Pak, W. L., & Applebury, M. L. (1985). The Drosophila ninaE gene encodes an opsin. *Cell*, *40*(4), 839–850.

Otsuna, H., & Ito, K. (2006). Systematic analysis of the visual projection neurons of Drosophila melanogaster. I. Lobula-specific pathways. *Journal of Comparative Neurology*, *497*(6), 928–958. https://doi.org/10.1002/cne.21015

Pak, W. L., Grossfield, J., & White, N. V. (1969). Nonphototactic Mutants in a Study of Vision of Drosophila. *Nature*, *222*(5191), Article 5191. https://doi.org/10.1038/222351a0

Papatsenko, D., Sheng, G., & Desplan, C. (1997). A new rhodopsin in R8 photoreceptors of Drosophila: Evidence for coordinate expression with Rh3 in R7 cells. *Development*, *124*(9), 1665–1673.

Poggio, T., & Reichardt, W. (1973). Considerations on models of movement detection. *Kybernetik*, *13*(4), 223–227. https://doi.org/10.1007/BF00274887

Potters, M., & Bialek, W. (1994). Statistical mechanics and visual signal processing. *Journal de Physique I*, *4*(11), 1755–1775. https://doi.org/10.1051/jp1:1994219

Raghu, S. V., Joesch, M., Borst, A., & Reiff, D. F. (2007). Synaptic organization of lobula plate

tangential cells in Drosophila: γ-Aminobutyric acid receptors and chemical release sites. *Journal of Comparative Neurology*, *502*(4), 598–610. https://doi.org/10.1002/cne.21319

Raghu, S. V., Joesch, M., Sigrist, S. J., Borst, A., & Reiff, D. F. (2009). Synaptic Organization of Lobula Plate Tangential Cells in *Drosophila:* Dα7 Cholinergic Receptors. *Journal of Neurogenetics*, *23*(1–2), 200–209. https://doi.org/10.1080/01677060802471684

Reppert, S. M., Zhu, H., & White, R. H. (2004). Polarized Light Helps Monarch Butterflies Navigate. *Current Biology*, *14*(2), 155–158. https://doi.org/10.1016/j.cub.2003.12.034

Rister, J., Pauls, D., Schnell, B., Ting, C.-Y., Lee, C.-H., Sinakevitch, I., Morante, J., Strausfeld, N. J., Ito, K., & Heisenberg, M. (2007). Dissection of the Peripheral Motion Channel in the Visual System of Drosophila melanogaster. *Neuron*, *56*(1), 155–170. https://doi.org/10.1016/j.neuron.2007.09.014

Rosner, R., von Hadeln, J., Salden, T., & Homberg, U. (2017). Anatomy of the lobula complex in the brain of the praying mantis compared to the lobula complexes of the locust and cockroach. *Journal of Comparative Neurology*, *525*(10), 2343–2357. https://doi.org/10.1002/cne.24208

Saifullah, A. S. M., & Tomioka, K. (2002). Serotonin sets the day state in the neurons that control coupling between the optic lobe circadian pacemakers in the cricket Gryllus bimaculatus. *Journal of Experimental Biology*, *205*(9), 1305–1314. https://doi.org/10.1242/jeb.205.9.1305

Salcedo, E., Huber, A., Henrich, S., Chadwell, L. V., Chou, W.-H., Paulsen, R., & Britt, S. G. (1999). Blue- and Green-Absorbing Visual Pigments ofDrosophila: Ectopic Expression and Physiological Characterization of the R8 Photoreceptor Cell-Specific Rh5 and Rh6 Rhodopsins. *Journal of Neuroscience*, *19*(24), 10716–10726. https://doi.org/10.1523/JNEUROSCI.19-24-10716.1999

Sanes, J. R., & Zipursky, S. L. (2010). Design Principles of Insect and Vertebrate Visual Systems. *Neuron*, *66*(1), 15–36. https://doi.org/10.1016/j.neuron.2010.01.018

Schmachtenberg, O., & Bicker, G. (1999). Nitric oxide and cyclic GMP modulate photoreceptor cell responses in the visual system of the locust. *The Journal of Experimental Biology*, *202*, 13–20. https://doi.org/10.1242/jeb.202.1.13

Schmeling, F., Wakakuwa, M., Tegtmeier, J., Kinoshita, M., Bockhorst, T., Arikawa, K., & Homberg,

U. (2014a). Opsin expression, physiological characterization and identification of photoreceptor cells in the dorsal rim area and main retina of the desert locust, Schistocerca gregaria. *Journal of Experimental Biology*, *217*(19), 3557–3568. https://doi.org/10.1242/jeb.108514

Schmeling, F., Wakakuwa, M., Tegtmeier, J., Kinoshita, M., Bockhorst, T., Arikawa, K., & Homberg, U. (2014b). Opsin expression, physiological characterization and identification of photoreceptor cells in the dorsal rim area and main retina of the desert locust, Schistocerca gregaria. *The Journal of Experimental Biology*, *217*. https://doi.org/10.1242/jeb.108514

Singh, S., & Joseph, J. (2019). Evolutionarily conserved anatomical and physiological properties of olfactory pathway through fourth-order neurons in a species of grasshopper (Hieroglyphus banian). *Journal of Comparative Physiology A*, *205*(6), 813–838. https://doi.org/10.1007/s00359-019-01369-7

Song, B.-M., & Lee, C.-H. (2018). Toward a Mechanistic Understanding of Color Vision in Insects. *Frontiers in Neural Circuits*, *12*. https://www.frontiersin.org/articles/10.3389/fncir.2018.00016

Srinivasan, M. V. (1990). Generalized gradient schemes for the measurement of two-dimensional image motion. *Biological Cybernetics*, *63*(6), 421–431. https://doi.org/10.1007/BF00199574

Stopfer, M., Bhagavan, S., Smith, B., & Laurent, G. (1997). Impaired odour discrimination on desynchronization of odour-encoding neural assemblies. *Nature*, *390*, 70–74. https://doi.org/10.1038/36335

Stopfer, M., & Laurent, G. (1999). Short-term memory in olfactory network dynamics. *Nature*, *402*(6762), 664–668. https://doi.org/10.1038/45244

Vishnevskaya, T. M., Cherkasov, A. D., & Shura-Bura, T. M. (1986). Spectral sensitivity of photoreceptors in the compound eye of the locust. *Neurophysiology*, *18*(1), 54–60. https://doi.org/10.1007/BF01052492

Vogt, K., Aso, Y., Hige, T., Knapek, S., Ichinose, T., Friedrich, A. B., Turner, G. C., Rubin, G. M., & Tanimoto, H. (2016). Direct neural pathways convey distinct visual information to Drosophila mushroom bodies. *ELife*, *5*, e14009. https://doi.org/10.7554/eLife.14009

Warrant, E., & Nilsson, D. E. (2006). *Invertebrate Vision*. Cambridge University Press. https://books.google.co.in/books?id=s0oQx7IYiO0C

Yamaguchi, S., Wolf, R., Desplan, C., & Heisenberg, M. (2008). Motion vision is independent of color in Drosophila. *Proceedings of the National Academy of Sciences*, *105*(12), 4910–4915. https://doi.org/10.1073/pnas.0711484105

Yukizane, M., Kaneko, A., & Tomioka, K. (2002). Electrophysiological and morphological characterization of the medulla bilateral neurons that connect bilateral optic lobes in the cricket, Gryllus bimaculatus. *Journal of Insect Physiology*, *48*(6), 631–641. https://doi.org/10.1016/S0022-1910(02)00091-4

Zuker, C. S., Cowman, A. F., & Rubin, G. M. (1985). Isolation and structure of a rhodopsin gene from D. melanogaster. *Cell*, *40*(4), 851–858. https://doi.org/10.1016/0092-8674(85)90344-7

Zuker, C. S., Montell, C., Jones, K., Laverty, T., & Rubin, G. M. (1987). A rhodopsin gene expressed in photoreceptor cell R7 of the Drosophila eye: Homologies with other signal-transducing molecules. *Journal of Neuroscience*, *7*(5), 1550–1557.

Appendix

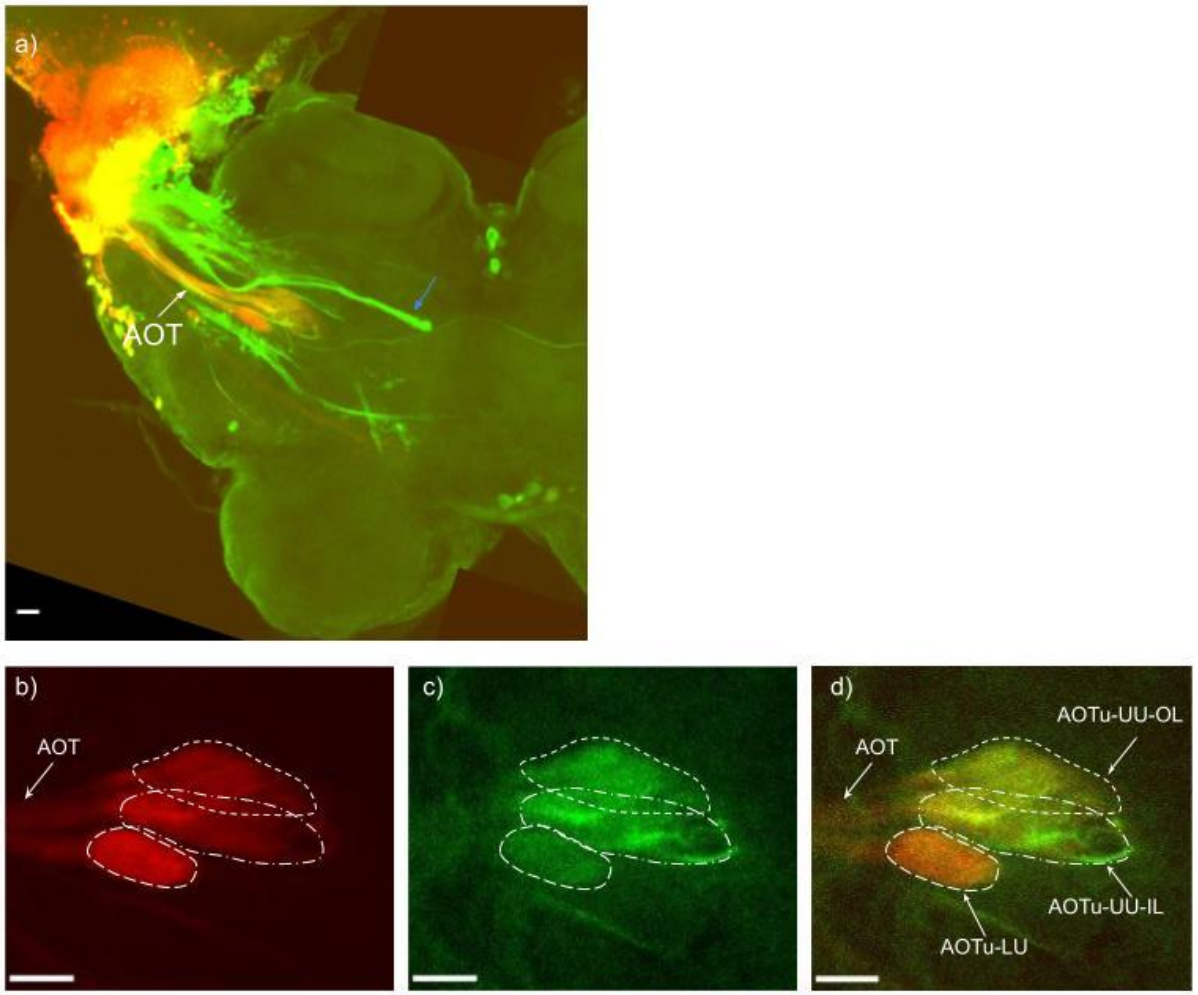

Figure A1: Dorsoventral segregation of lobula to the AOTu. a). Injecting dextran conjugated alexa fluor 488 in dorsal lobula and texas red in ventral lobula filled AOTu through AOT, and many other tracts also filled. Blue arrow indicating the novel structure filled posterior to the central complex. b). Ventral lobula has innervations into the both upper and lower units of the AOTu. c). Dorsal lobula has innervations exclusively into the upper unit of the AOTu. d). Merged picture of b and c. Scale bar : 50µm (a-d)

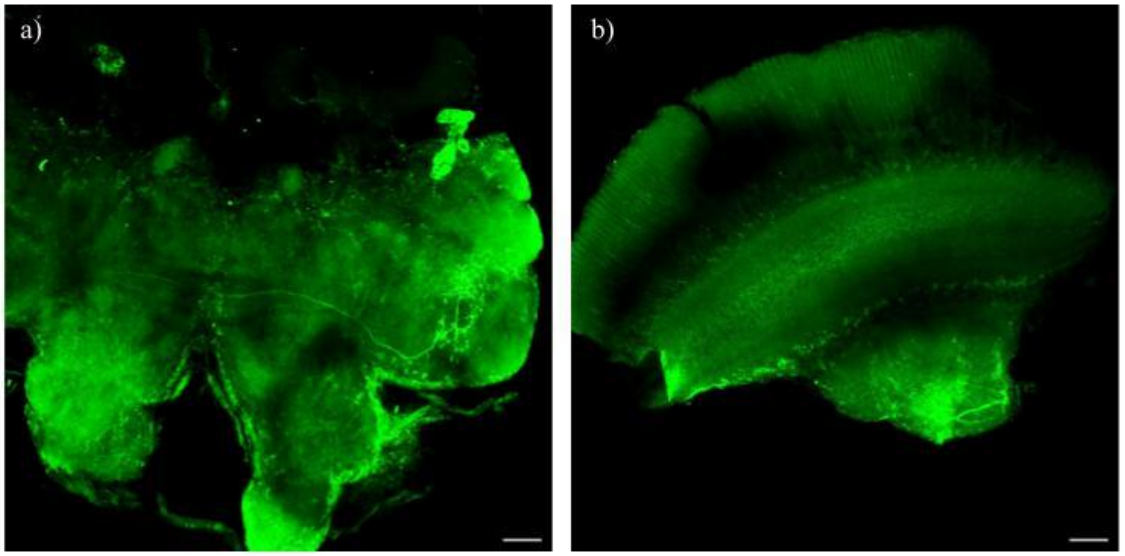

Figure A2: TIpro neuron morphology. a) TIpro neuron punctate arborisation in the ipsilateral posterior slope and an axon crossing the midline of the brain and innervating the contralateral posterior slope. b) TIpro neuron innervation in the inner lobula. Scale bars: 100µm.

This neuron is recorded from the proximal optic lobe. We could not identify the cell body of the neuron. One of the optic lobe is missing. In another optic lobe there are smoother arborizations in the inner lobula (ILO) This neuron has punctate arborisations in the posterior slope ipsilateral to the innervated optic lobe. Main branch of the neuron crossing the midline of the brain and entering the contralateral posterior slope of the brain.

This neuron has 20 spikes/sec for dark background and 10 spikes/sec for bright background. This neuron responds to loom in of dark, central quadrant, transitions from dark to bright, bright to dark,transitioning from top to bottom to bottom to top drifting, and to left to right drifting. But there is no response for loom out of dark and for white noise. Maximum response is observed for drifting from left to right.

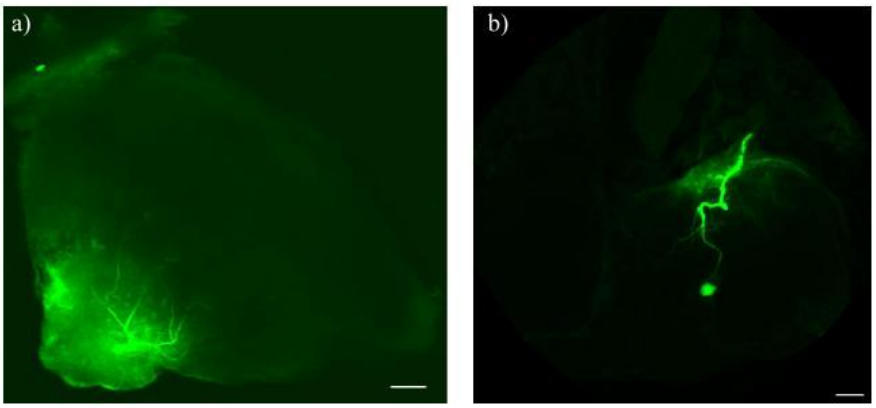

Figure A3: CMepro1 neuron morphology.. a) CMepro1 neuron arborisation in proximal medulla. b) CMepro1 neuron cell body located in the tritocerebrum. Scale bars: 100µm.

This neuron is recorded from the proximal optic lobe. Its cell body is located in the tritocerebrum. It has smoother arborizations within the tritocerebral region of the brain, restricted to the one side of the midline of the brain. Main branch of the neuron is innervating into the medulla anteriorly and arborising in the proximal medulla with smooth arborizations in a single layered manner. While travelling from tritocerebrum to optic lobe neuron has smoother dendrites. This neuron is responding for loom in of dark, loom out of dark, flash on light at lower middle quadrant, transitioning from light to dark and dark to light, and for transitioning from top to bottom to bottom to top drifting.

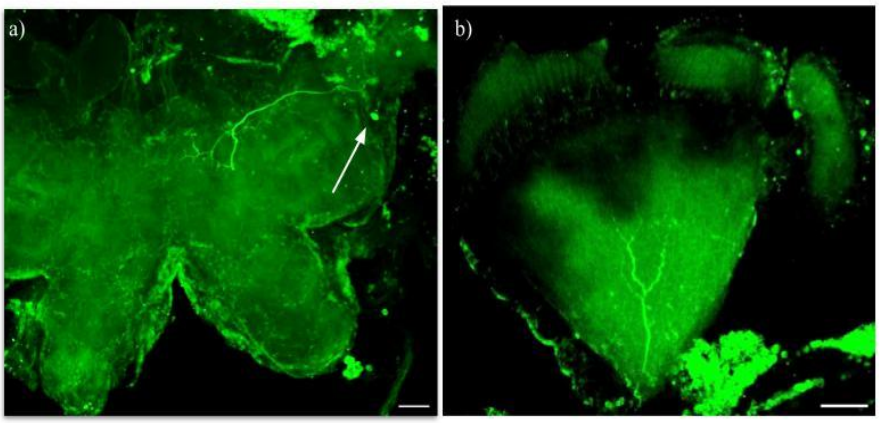

Figure A4: CMepro neuron morphology. a) CMepro neuron innervation in superior lateral protocerebrum (white arrow pointing the cell body), having punctate structures in superior medial protocerebrum. b) CMepro neuron innervation in medulla. Scale bars: 100µm.

This neuron is recorded from the proximal lobula. Its cell body is located in the superior lateral protocerebrum anteriorly. In the optic lobe,this neuron has smoother arborisations. The main branch of the neuron is divided into three sub-branches at the junction of the proximal and distal medulla. These three sub branches further subdivided and innervated throughout the distal medulla. Main branch of the neuron is also innervating in the superior medial protocerebrum posteriorly with punctate structures. Putatively inferring that, this neuron is receiving inputs from distal medulla and giving output posteriorly into the superior medial protocerebrum. This neuron is responding to loom in of dark, loom out of dark and for flash off. But not for flash on and vertical bar moving left to right or right to left.

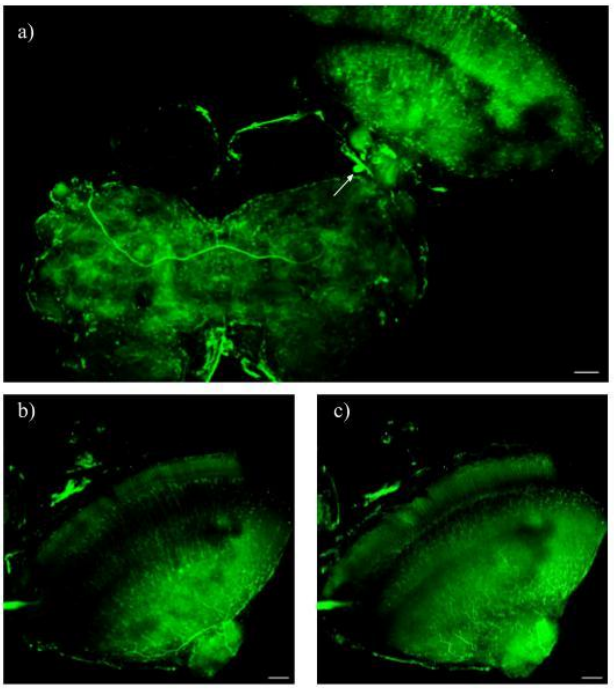

Figure A5: CMecom neuron morphology. a) CMecom neuron innervation in protocerebrum (white arrow indicates the cell body in superior lateral protocerebrum). b-c) CMecom neuron having the punctate structured arborisation throughout the medulla in the contralateral optic lobe.
Scale bars: 100µm.

This neuron is recorded from the proximal optic lobe. Cell body is located at the superior lateral protocerebrum anteriorly. This cell has arborisation in the contralateral optic lobe. Main axon from the cell body is crossing the central complex and entering the optic lobe through the dorsal lobe of the lobula and then entering the medulla anteriorly and arborising throughout the medulla. Innervations in DLO and medulla of contralateral optic lobe are having punctate structures. One of the fine branches entered the ipsilateral optic lobe but could not find the complete arborisation as it is not filled in the ipsilateral optic lobe. This neuron responds to loom in of dark, loom out of dark, transition from vertical drift to dark, flash off,flash on and lighting of top left quadrant. Maximum response is observed for looming off dark.

Table A1: Neuron's morphology and responses to the stimulus presented through LED setup.

S.No:	Neuron	Cell body	Innervation	Excitatory response to
01	CMepro	SLP	Smoother arborisations in distal medulla and punctate arborisations in superior medial protocerebrum.	Loom in of dark, loom out of dark and for flash off of LED setup but not for translating stimuli nor flash on.
02	CMepro1	Tritocerebrum	Smoother arborizations in proximal medulla and in posterior slope.	Loom in of dark, loom out of dark, flash on of light in lower middle quadrant and for transitions between translating stimuli over LED setup.
03	CMecom	SLP	Commissural neuron, Innervating in the contralateral medulla and DLO with punctate structures.	Loom in of dark, loom out of dark,flash on,flash off, transitions and lighting of top left quadrant of LED setup.
04	TIpro	Could not identify	Smoother arborization in the ILO , punctate arborization in posterior slope ipsilateral to the innervated optic lobe.	Responding for loom in of dark, transitions of stimuli and for lighting the central quadrant of the LED setup.

Anti-Plagiarism Certificate

Anatomical and physiological characterization of the optic lobe and associated pathways involved in visual processing in Hieroglyphus banian

by Chalavadi Sivaraju

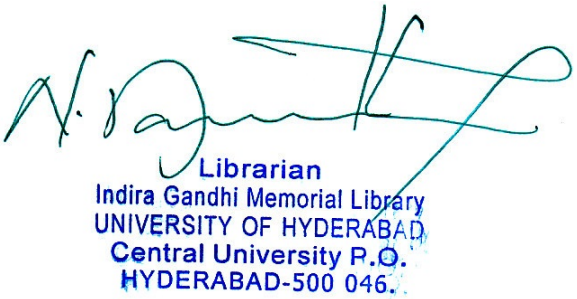

Anatomical and physiological characterization of the optic lobe and associated pathways involved in visual processing in Hieroglyphus banian

ORIGINALITY REPORT

8%	3%	7%	1%
SIMILARITY INDEX	INTERNET SOURCES	PUBLICATIONS	STUDENT PAPERS

PRIMARY SOURCES

1	Encyclopedia of Computational Neuroscience, 2015. Publication	1%
2	doi.org Internet Source	1%
3	Submitted to University of Hyderabad, Hyderabad Student Paper	<1%
4	Sanes, J.R.. "Design Principles of Insect and Vertebrate Visual Systems", Neuron, 20100415 Publication	<1%
5	onlinelibrary.wiley.com Internet Source	<1%
6	P. E. Coombe. "The large monopolar cells L1 and L2 are responsible for ERG transients inDrosophila", Journal of Comparative Physiology A, 1986 Publication	<1%

Conference certificates

BITS Pilani
K K Birla Goa Campus

DEPARTMENT OF SCIENCE & TECHNOLOGY
Ministry of Science and Technology
Government of India

CERTIFICATE OF PARTICIPATION

VI ANNUAL CONFERENCE OF COGNITIVE SCIENCE

This certifies that

C. SIVA RAJU

has delivered an oral/poster presentation at the
VI Annual Conference of Cognitive Science, 2019
held at **BITS Pilani K K Birla Goa Campus**
from the **10th to 12th of December, 2019.**

HARISH KARNICK
President, ACS - India

VEEKY BATHS
Convener, ACCS 2019

Certificate No: NEHU/IAN/2022/49

Certificate of Appreciation

THIS CERTIFICATE PROUDLY PRESENTED TO

Chalavadi Sivaraju

This is to certify that Prof./Dr./Mr./Ms. ***Chalavadi Sivaraju*** *has successfully attended/presented the research as Poster presentation/Oral talk/Symposium talk in the event of* ***XL Annual Meeting of the Indian Academy of Neurosciences (IAN-2022)*** *organized by Department of Biomedical Engineering, School of Technology, North-Eastern Hill University (NEHU), Shillong, INDIA during 7th to 10th December, 2022.*

We wish all success in life.

Prof. Ishan K. Patro
President, IAN

Dr. Sudip Paul
Organizing Secretary (IAN 2022)

IISER PUNE

Ref: Participation in NGN meeting in IISER Pune, Jan 2020.

To whomsoever it may concern,

This is to certify that C SIVA RAJU, UNIVERSITY OF HYDERABAD made a valuable contribution as a presenter at the Neuroscience meeting held IISER Pune from January 2nd, 2020 to January 4th, 2020. The presented research poster (Title: Simple and complex cells of an insect visual system) was appreciated by both experts in the field and students. We hope that we will have continued participation from C SIVA RAJU in the coming years.

Feel free to write to me or Dr. Assisi (collins@iiserpune.ac.in) if you need any other information.

Best regards
Sincerely

Nadkarni

Suhita Nadkarni
Assistant Professor
Indian Institute of Science and Education Pune
Dr. Homi Bhabha Road
Pune 411008